Three-Loop Gap Equation within Resummed 3D Yang-Mills Theory

Stefan de Boer

Master thesis

submitted to the

Faculty of Physics

at

University of Bielefeld

Supervisor and first assessor: Prof. Dr. York Schröder
Second assessor: Prof. Dr. Nicolas Borghini

September 18, 2013

Contents

1 Motivation and outline **1**

2 Basics of QCD and thermal field theory **3**
2.1 Yang-Mills theory and QCD 4
2.1.1 Path integral and QCD Feynman rules 4
2.1.2 Ultraviolet divergences and renormalization in QCD 6
2.2 Partition function and path integral 7
2.3 Weak-coupling expansion and infrared divergences 8
2.3.1 Infrared divergences and resummation in the ϕ^4 model 10

3 Resumming the non-linear SU(N) Higgs model in a nutshell **13**
3.1 Lagrangian 13
3.2 Resummation 14
3.3 BRS invariance 16

4 Review of the Laporta-algorithm **17**
4.1 Integration-by-parts identities 17
4.2 Difference equations 18
4.3 Factorial series 19
4.3.1 Example: massive zero-point five-loop sunset-integral 22

5 Framework of automated Feynman integral reduction **25**
5.1 Fire and LiteRed 25
5.2 Mincer and Matad 27
5.3 Cut-and-Tarcer technique 28
5.4 Reduze 2 30

6 Computation of the three-loop gap equation **33**
6.1 Method 35
6.2 Checks 36
6.2.1 Gauge variance of the three-loop gap equation 37
6.3 What to do next? 37

7 Calculations of the sunset-type master integrals **39**
7.1 Difference equations and recurrence relations 40
7.2 Higher order and high precision calculations 42

8 Conclusion and outlook **43**

A Three-loop self-energy diagrams and $\hat{\Pi}_{00}^{(3)}$ **45**

B D-dimensional results for $\hat{\Pi}_{12}^{(1)}$ and $\hat{\Pi}_{03}^{(1)}$ **61**

C Sunset integrals: Recurrence relations **63**

D Sunset master integrals: Numerical results around $4D$ **65**

E Sunset master integrals: Numerical results around $3D$ **69**

Bibliography **73**

Chapter 1

Motivation and outline

In recent years research in the field of elementary particles is becoming more important and popular. A fundamental building block of matter, the Higgs particle, was discovery these days [1]. Moreover, elementary particles are of interest in astrophysics and cosmology, especially in the context of the the big bang, i.e. at high temperatures. On the lower side of the temperature scale, studying the constituents of matter may give insights in cold and dense stars.
The high temperature and low chemical potential behavior is studied experimentally at e.g., the Large Hadron Collider and Relativistic Heavy Ion Collider. For such experiments theoretical predictions, in particular finite temperature gauge theory within the Standard Model of particle physics, are vital. Lattice Monte Carlo simulations solely provide controlled numerical results for chemical potentials which are, in natural units, less than the temperature.
An analytical approach to understand the properties of elementary particles is commonly stated in terms of a perturbative quantum field theory. This is formulated for weak interactions, that is high temperatures due to asymptotic freedom. Within this approach a physical event is translated into Feynman diagrams, which can be classified according to their number of loops and legs. A computation of these diagrams involves a complex algebra and multi-dimensional integrals, whereas these are becoming more involved for higher loop and leg diagrams. As a consequence, the field of performing powerful computations and designing efficient techniques evolves. The approach is to generate all relevant Feynman diagrams and symmetry factors by combinatorics, to specify the Feynman rules, to translate these diagrammatic objects in mathematical expressions and to perform the relevant algebraic manipulations. Thereafter a large set of Feynman integrals is reduced to some smaller set of integrals, called master integrals, via linear relations in the Feynman integrals. Completing, these master integrals are calculated analytically or numerically.
In this work we focus on the reduction of Feynman integrals and the numerical calculation of master integrals in the context of a three-loop gap equation. This gap equation fixes the mass of the gauge field in a three-dimensional Yang-Mills theory, whereas the mass is apparent due to a resummation at finite temperature. The work presented here, is based on [2].
In the following we outline this thesis. Chapter 2 is a sketch of the basics of Yang-Mills theory, in particular QCD, and thermal field theory, where we discuss their linking, the perturbative approach and the handling of divergences within this approach. In Chapter 3 we introduce a three-dimensional Yang-Mills theory based on the non-linear SU(N) Higgs model and its resummation. We review an algorithm by Laporta for the reduction of a set of Feynman integrals to master integrals and a technique to calculate these in Chapter 4. In Chapter 5 we present some computer systems, e.g. Reduce 2, which are designed for the purposes of automated Feynman integral reduction. The computation of the three-loop gap equation and the transverse part of the gluon self-energy up to three loop in the context of the non-linear SU(N) Higgs model is explained in Chapter 6 as well as

a further reflection on the gap equation. In Chapter 7 we apply the Laporta-algorithm to calculate the Euclidean zero-point sunset-type master integrals with one mass parameter numerically up to five loop in the dimensional regularization scheme around four and three dimensions. A conclusion and an outlook of this work is given in Chapter 8.

Chapter 2

Basics of QCD and thermal field theory

One way from a classical theory to a quantum field theory, e.g. QCD (quantum chromodynamics), is that of canonical quantization. An equivalent path is given by functional methods, that is path integrals, and the formulation of perturbations therein. We take the latter one, as it is goes hand in hand with the partition function, which is the fundamental quantity in quantum statistics, i.e. equilibrium thermodynamics. For an introduction to (perturbative) quantum field theory and to groups and symmetries in physics we refer to [3] and [4], respectively.
A quantum field theory comes along with two kinds of divergences, that are ultraviolet divergences from high momenta and infrared divergences from bare massless propagators at low momenta. The ultraviolet divergences are handled via renormalization, whereby no such a general procedure currently exists for infrared divergences. They emerge in non-Abelian gauge theories with spontaneous symmetry breaking at temperatures higher than the critical temperature and in QCD with massless gauge fields, i.e. gluons. This was first noted by A.D. Linde in 1978 [5] and is apparent in the self-energy at $\mathcal{O}(g^4)$ and the pressure at $\mathcal{O}(g^6)$ with a gauge coupling g [6]. A bare massless propagator is given a thermal mass at finite temperature T, which has the effect of an infrared cutoff and regularizes the theory. Due to the screening of color-electric and color-magnetic gauge fields, the electric and magnetic mass scales, gT and g^2T, are induced, respectively. Though the dynamically generated magnetic screening mass is of $\mathcal{O}(g^2T)$, higher orders of perturbation theory are of the same order than the lower ones and hence, it is of non-perturbative nature. A resolution of this was proposed by E. Braaten in 1994, involving the construction of effective field theories by a partial integrating of separate momentum scales [7]. However, gauge fixed lattice simulations [8] are consistent with an effectively massive gluon propagator. Moreover, a dynamically generated gauge field mass is of interest in three dimensional Yang-Mills theories [9].
In this chapter we first introduce the theory of QCD in the path integral formalism at zero temperature, where we derive its Feynman rules and renormalize it. Then, we turn to finite temperature and zero chemical potential and show that the partition function can be represented by a path integral. Concluding, we consider the perturbative expansion of the partition function in a small coupling parameter, i.e. at high temperatures. As for the Φ^4 model, we identify the infrared divergences and resum them.

2.1 Yang-Mills theory and QCD

A Yang-Mills theory is a non-Abelian SU(N) gauge theory. It is the basis for the unification of electromagnetic interactions and weak interactions, i.e. $U(1) \times SU(2)$, and of QCD, which is represented by the group $SU(3)$. The theory was formulated by C.N. Yang and R.L. Mills in 1954 [10], its renormalizable in four and less dimensions proven by G. 't Hooft and M.J.G. Veltman in 1972 [11] and its nature of asymptotic freedom shown by H.D. Politzer [12], D.J. Gross and F. Wilczek [13] in 1973. The first two and the latter three were awarded the Nobel prize in 1999 and 2004, respectively.
The QCD gauge group $SU(3)$ is acting on the color space of quarks in the fundamental representation. The gauge invariant Yang-Mills Lagrangian reads

$$\mathcal{L}_{YM} = -\frac{1}{4} F^{a\mu\nu} F^a_{\mu\nu} + \overline{\Psi}^f_i(x)[i\gamma^\mu D_\mu - m_f]_{ij}\Psi^f_j(x) \tag{2.1}$$

with the field strength tensor

$$F^a_{\mu\nu} = \partial^a_\mu A_\nu(x) - \partial^a_\nu A_\mu(x) + g f^{abc} A^b_\mu(x) A^c_\nu(x)\,, \tag{2.2}$$

where g is the coupling parameter and the covariant derivative is

$$[D_\mu]_{ij} = \delta_{ij}\partial_\mu - igA^a_\mu(x)T^a_{ij}\,. \tag{2.3}$$

The gluon fields A^a_μ carry adjoint indices $a \in \{1, ..., 8\}$, the quark fields Ψ^f_j color indices $j \in \{1, 2, 3\}$ and flavor indices f, and also their masses m_f. The generators T^a can be written as hermitian matrices with

$$[T^a, T^b] = i f^{abc} T^c\,, \tag{2.4}$$

where f^{abc} are anti-symmetric structure constants. One may e.g., consider the equations of motion, the conserved currents and approximate symmetries. However, we proceed with the quantization of the Yang-Mills theory via path integrals, see e.g. [14].

2.1.1 Path integral and QCD Feynman rules

For some Minkowskian Lagrangian $\mathcal{L}(X)$ and fields X, the vacuum-to-vacuum transition amplitude is given as the path integral[1]

$$Z = \int \mathcal{D}X \exp\left\{\frac{i}{\hbar}\int dx \mathcal{L}(X)\right\} \propto \langle 0, \infty | 0, -\infty\rangle\,. \tag{2.5}$$

Setting $\hbar = 1$ and introducing source fields J, the generating functional for the Green's functions is

$$Z[J] = \int \mathcal{D}X \exp\left\{i\int dx[\mathcal{L}(X, x) + J(x)X(x)]\right\}\,. \tag{2.6}$$

Taking functional derivatives of the generating functional we obtain the time-ordered n-point functions as

$$\langle 0|T : X(x_1) ... X(x_n) : |0\rangle = \frac{1}{Z[0]}\left(-i\delta_{J(x_1)}\right) ... \left(-i\delta_{J(x_n)}\right) Z[J]\big|_{J=0}\,. \tag{2.7}$$

Note, that the denominator in (2.7) is a sum of vacuum diagrams, which cancels disconnected diagrams in the correlation function and that the normalization in the amplitude drops. For $\mathcal{L} = \mathcal{L}_0 + \mathcal{L}_I$, where

[1] A term of the form $ig\overline{\Psi}\Psi$ for the convergence of the integral is implicit.

$\mathcal{L}_0$ is at most quadratic in the fields and $\mathcal{L}_I$ is an interaction Lagrangian of higher order, the generating functional reads

$$Z[J] = \exp\left\{ i \int dx \mathcal{L}_I(-i\delta_J) \right\} Z_0[J] \,. \tag{2.8}$$

We are going to write down the perturbative expansion of the theory, by expanding $\mathcal{L}_I$ in (2.8) in some small parameter, that is the coupling parameter here, via Feynman diagrams.
For QCD the two-quark-gluon, three-gluon and four-gluon vertices are directly read off from the interaction Lagrangian as

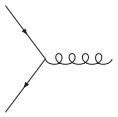

$$\equiv ig\gamma^\mu T^a \,, \tag{2.9}$$

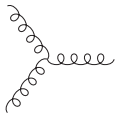

$$\equiv gf^{a_1a_2a_3}[(k_1-k_2)_{\mu_3}g_{\mu_1\mu_2} + (k_2-k_3)_{\mu_1}g_{\mu_2\mu_3} + (k_3-k_1)_{\mu_2}g_{\mu_3\mu_1}] \,, \tag{2.10}$$

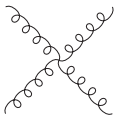

$$\begin{aligned} \equiv & -ig^2[f^{a_1a_2a_e}f^{a_ea_3a_4}(g_{\mu_1\mu_3}g_{\mu_2\mu_4} - g_{\mu_1\mu_4}g_{\mu_2\mu_3}) \\ & + f^{a_1a_3a_e}f^{a_ea_2a_4}(g_{\mu_1\mu_2}g_{\mu_3\mu_4} - g_{\mu_1\mu_4}g_{\mu_3\mu_2}) \\ & + f^{a_1a_4a_e}f^{a_ea_2a_3}(g_{\mu_1\mu_2}g_{\mu_4\mu_3} - g_{\mu_1\mu_3}g_{\mu_4\mu_2})] \,, \end{aligned} \tag{2.11}$$

where full and wiggly lines denote scalars and gluons, respectively and the color and Lorentz indices are implicitly distributed among the gluon lines. The quark propagator is given as the two-point function obtained from (2.7) with Grassmann source fields as

$$\equiv \frac{i(\gamma^\mu k_\mu + m_f)}{k^2 - m_f^2 + i\epsilon} \,. \tag{2.12}$$

The gluon propagator is in principle be read off from

$$\int dx \left(-\frac{1}{4} F^{a\mu\nu} F^a_{\mu\nu} \right) = \frac{1}{2} \int dx A^a_\mu(x) \left[\delta^{ab}(\partial^2 g^{\mu\nu} - \partial^\mu \partial^\nu) \right] A^b_\nu(x) \,, \tag{2.13}$$

where we assume, that fields vanish at the surface of the integration. However, no Green's function for the term in squared brackets exists. To resolve this, we add the covariant gauge fixing term

$$\mathcal{L}_{gf} = -\frac{1}{2\xi} \partial^\mu A^a_\mu \partial^\nu A^a_\nu \tag{2.14}$$

to the initial Lagrangian (2.1),where ξ is a gauge fixing parameter and thus, the gluon propagator reads

$$\equiv \frac{-i}{k^2 + i\epsilon} \left(g^{\mu\nu} - (1-\xi)\frac{k^\mu k^\nu}{k^2} \right) \delta^{ab} \,. \tag{2.15}$$

Note, that physics is ξ-independent. We have to mind multiple gluon fields in the functional integration, which are related by gauge transformations. This was first done by L.D. Faddeev and V.N. Popov in 1967 [15]. They separated the integration of gauge transformation related fields, inducing a

determinant, which is field-dependent in non-Abelian theories. The determinant is rewritten in terms of Grassmann fields, representing auxiliary anti-commuting scalar ghost fields. These fields cancel the unphysical longitudinal parts of the gluon fields in Feynman calculations. The ghost propagator

$$\equiv \frac{i}{k^2 + i\epsilon}\delta^{ab} \tag{2.16}$$

and the two-ghost-gluon vertex

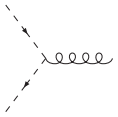
$$\equiv -gf^{abc}k_\mu \tag{2.17}$$

emerge as additional Feynman rules, where the ghost fields carry associated color indices. Merging all parts, the QCD Lagrangian reads

$$\mathcal{L}_{\mathrm{QCD}} = -\frac{1}{4}F^{a\mu\nu}F^a_{\mu\nu} + \overline{\Psi}^f_i\left[i\gamma^\mu D_\mu - m_f\right]_{ij}\Psi^f_j - \frac{1}{2\xi}\left(\partial^\mu A^a_\mu\right)^2 + \overline{c}^a\left(-\partial^\mu D^{ab}_\mu\right)c^b \tag{2.18}$$

with ghost fields c and anti-ghost fields $\overline{c}$. The residual symmetry of this gauge fixed Lagrangian is associated with BRS transformations [16]. We proceed with the schematic renormalization of QCD.

2.1.2 Ultraviolet divergences and renormalization in QCD

While performing Feynman calculations, one commonly encounters ultraviolet (UV) divergences. They emerge due to the loop integration of large momenta. The UV divergence can be estimated via the superficial degree of divergence, that is a naive counting of the momenta in a Feynman diagram e.g., within dimensional regularization,

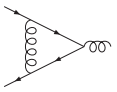
$$\begin{aligned} &= \int \frac{d^Dk}{(2\pi)^D}\left(igT^b\gamma^\nu\right)\frac{i(\gamma^\rho k_\rho + \gamma^\rho(q_2)_\rho + m)}{(k+q_2)^2 - m^2}\left(igT^a\gamma^\mu\right)\frac{i(\gamma^\rho k_\rho + \gamma^\rho(q_1)_\rho + m)}{(k+q_1)^2 - m^2} \\ &\quad \times\left(igT^b\gamma_\nu\right)\frac{-i}{k^2} \\ &\sim \int \frac{d^Dk}{k^4} \qquad k \gg 1\,, \end{aligned} \tag{2.19}$$

which is logarithmically divergent for $D = 4$. The generic procedure is to choose a regularization scheme, that is dimensional regularization in terms of ϵ here, calculate the Feynman diagrams and absorb the UV divergences in counter-terms via renormalization.
We implement the renormalization in QCD by rescaling the bare (B) fields and parameters as

$$\begin{aligned} &\Psi^f_B \equiv \Psi^f = \sqrt{Z_\Psi}\Psi^f_R\,, \quad A^{a\mu}_B \equiv A^{a\mu} = \sqrt{Z_A}A^{a\mu}_R\,, \quad c^a_B \equiv c^a = \sqrt{Z_c}c^a_R\,, \\ &m_B \equiv m = Z_m m_R\,, \quad g_B \equiv g = Z_g g_R\,, \quad \xi_B \equiv \xi = Z_\xi\xi_R\,, \end{aligned} \tag{2.20}$$

where the dimensionless renormalization constants depend on the renormalized (R) parameters and the dimension. Rewriting the bare QCD Lagrangian (2.18) in terms of the introduced renormalized quantities as

$$\mathcal{L}^B_{\mathrm{QCD}} = \mathcal{L}^R_{\mathrm{QCD}} + \mathcal{L}_{ct} \tag{2.21}$$

induces the counter term Lagrangian

$$\begin{aligned}\mathcal{L}_{ct} =&(Z_\Psi - 1)\overline{\Psi}\left(i\gamma^\mu\partial_\mu - \frac{Z_m Z_\Psi - 1}{Z_\Psi - 1}m\right)\Psi + \left(Z_m Z_\Psi Z_A^{\frac{1}{2}} - 1\right) g\overline{\Psi}\gamma^\mu A_\mu^a T^a \Psi \\ &- (Z_A - 1)\left(\frac{1}{4}(\partial^\mu A^{a\nu} - \partial^\nu A^{a\mu})^2 + \frac{Z_A Z_\xi^{-1} - 1}{Z_A - 1}\frac{1}{2\xi}(\partial^\mu A_\mu^a)^2\right) \\ &+ \left(Z_g Z_A^{\frac{3}{2}} - 1\right)\frac{1}{2}g f^{abc} A^{b\mu} A^{c\nu}(\partial_\mu A_\nu^a - \partial_\nu A_\mu^a) + \left(Z_g^2 Z_A^2 - 1\right)\left(-\frac{1}{4}g^2 f^{abc} A^{b\mu} A^{c\nu} f^{ade} A_\mu^d A_\nu^e\right) \\ &- (Z_c - 1)\overline{c}\partial^\mu\partial_\mu c - \left(Z_g Z_c Z_A^{\frac{1}{2}} - 1\right) g f^{abc}\overline{c}^a \partial^\mu A_\mu^b c^c \end{aligned} \tag{2.22}$$

dropping the indicator R. One may write down explicitly the additional Feynman rules as given by the counter term Lagrangian. We fix the renormalization constants by claiming that the sum of a type of Feynman diagrams of some loop order and its counter term is finite, that is the counter terms cancel the divergences. However, we are left with a residual fix of the renormalization constants, due to terms of $\mathcal{O}(\epsilon)$ within dimensional regularization, which are set to some value in various schemes e.g., vanish in the MS (Minimal Subtraction) scheme. The current status of the renormalization constants is given in [14] and references therein.

2.2 Partition function and path integral

The fundamental quantity in quantum statistics is the partition function

$$\mathcal{Z} = \mathrm{Tr}\left\{e^{-\beta H}\right\} \tag{2.23}$$

with $\beta = 1/(k_B T)$, the Boltzmann constant k_B, the temperature T and the Hamiltonian H. With the partition function at hand, one may compute various observables at thermodynamic equilibrium e.g., the free energy F and the thermodynamic pressure P via

$$F = -\frac{1}{\beta}\ln\mathcal{Z}\,, \quad P = \frac{1}{\beta}\partial_V \ln Z\,. \tag{2.24}$$

In the following we derive the path integral representation of the partition function for bosons. In field (ϕ) space the partition function is written as

$$\mathcal{Z} = \int d\phi \left\langle \phi \left| e^{-\beta H} \right| \phi \right\rangle = \int d\phi \left\langle \phi \left| e^{-\Delta\tau H} \ldots e^{-\Delta\tau H} \right| \phi \right\rangle\,, \tag{2.25}$$

where $\Delta\tau \equiv \beta/N$ is a small imaginary time. For each of the N terms $e^{-\Delta\tau H}$ we insert to its left a complete set of states of the canonical momentum π, i.e.

$$1 = \int \frac{d\pi_i(x)}{2\pi}|\pi_i\rangle\langle\pi_i| \qquad i \in \{1, \ldots, N\} \tag{2.26}$$

and to its right

$$1 = \int d\phi_i(x)|\phi_i\rangle\langle\phi_i|\,. \tag{2.27}$$

We have objects such as

$$\begin{aligned}\langle\phi_{i+1}|\pi_i\rangle\left\langle\pi_i\left|e^{-\Delta\tau H(\phi,\pi)}\right|\phi_i\right\rangle =& \exp\left\{i\int d^3x\pi_i(x)\phi_{i+1}(x)\right\}\langle\pi_i|\phi_i\rangle\left(1-\Delta\tau H(\phi_i,\pi_i)+\mathcal{O}\left(\Delta\tau^2\right)\right)\\ =& \exp\left\{i\int d^3x\pi_i(x)(\phi_{i+1}(x)-\phi_i(x))\right\}\\ &\times\exp\left\{-\Delta\tau\int d^3x\mathcal{H}(\phi_i(x)\pi_i(x))+\mathcal{O}\left((\Delta\tau)^2\right)\right\},\end{aligned} \tag{2.28}$$

where the operators are evaluated at a single point in time. The residual bracket $\langle\phi_1|\phi\rangle=\delta(\phi_1-\phi)$ yields $\langle\phi|=\langle\phi_1|$ when performing the ϕ-integration. For $N\to\infty$, $\mathcal{O}(\Delta\tau)\to 0$ and hence

$$\mathcal{Z}=\lim_{N\to\infty}\int\prod_{i=1}^{N}\frac{dx_i dp_i}{2\pi}\exp\left\{\Delta\tau\sum_{j=1}^{N}\int d^3x\left[i\pi_i(x)\frac{\phi_{i+1}(x)-\phi_i(x)}{\Delta\tau}-\mathcal{H}(\phi(x),\pi(x))\right]\right\}\Big|_{x_{N+1}=x_1}, \tag{2.29}$$

which in the continuum limit reads

$$\mathcal{Z}=\int\mathcal{D}\pi\int_{\phi(x,\beta)=\phi(x,0)}\mathcal{D}\phi\exp\left\{\int_0^\beta d\tau\int d^3x\left[i\pi(x,\tau)\partial_\tau\phi(x,\tau)-\mathcal{H}(\phi(x,\tau),\pi(x,\tau))\right]\right\}, \tag{2.30}$$

where the $\phi(x,\tau)$-integration is compactified and the integration measure $\mathcal{D}$ is understood as the limit of (2.29). For a Hamiltonian of the form

$$\mathcal{H}=\frac{\pi^2(x)}{2m}+V(\phi(x)) \tag{2.31}$$

with a π-independent potential V we can explicitly perform the π-integration in the discrete form of (2.29), as

$$\int\frac{d\pi_i}{2\pi}\exp\left\{-\Delta\tau\left(\frac{\pi_i^2}{2m}-i\pi_i\frac{\phi_{i+1}-\phi_i}{\Delta\tau}\right)\right\}=\left(\frac{m}{2\pi\Delta\tau}\right)^{\frac{1}{2}}\exp\left\{\frac{m(\phi_{i+1}-\phi_i)^2}{2\Delta\tau}\right\}, \tag{2.32}$$

which yields

$$\mathcal{Z}=\int_{\phi(x,\beta)=\phi(x,0)}\prod_x C\mathcal{D}\phi\exp\left\{\int_0^\beta d\tau\int d^3x[i\pi\partial_\tau\phi-\mathcal{H}]\right\},\quad C\equiv\left(\frac{mN}{2\pi\beta}\right)^{\frac{1}{2}}. \tag{2.33}$$

The Minkowskian path integral (2.5) in four dimensions is linked to the Euclidean partition function via Wick rotation, that is $t\to\tau\equiv -it$, bounding one space-time integration direction and closing one field integration in a periodic way. Thus, it is effective dimensional reduced, as common in equilibrium thermodynamics. If in addition a charge $\mathcal{N}$ is conserved, then one replaces $\mathcal{H}(\phi,\pi)\to\mathcal{H}(\phi,\pi)-\mu\mathcal{N}(\phi,\pi)$ with the chemical potential μ.

2.3 Weak-coupling expansion and infrared divergences

For a weak interaction S_I we can perform the functional integration in the partition function

$$\mathcal{Z}=N\int\mathcal{D}\phi e^{-S_E} \tag{2.34}$$

with the normalization N by expanding the Euclidean action $S_E = S_0 + S_I$, where S_0 is an unperturbed action in powers of the coupling parameter.[2] Formally, we expand (2.34) as

$$\mathcal{Z} = N \int [\mathcal{D}\phi] e^{-S_0} \sum_{l=0}^{\infty} \frac{(-S_I)^l}{l!} \,. \tag{2.35}$$

Taking the logarithm gives

$$\begin{aligned} \ln \mathcal{Z} &= \ln \mathcal{Z}_0 + \ln \mathcal{Z}_I \equiv \ln \left\{ N \int [\mathcal{D}\phi] e^{-S_0} \right\} + \ln \left\{ 1 + \sum_{l=1}^{\infty} \frac{(-1)^l}{l!} \left\langle S_I^l \right\rangle_0 \right\} , \\ \left\langle S_I^l \right\rangle_0 &\equiv \frac{\int [\mathcal{D}\phi] e^{-S_0} S_I^l}{\int [\mathcal{D}\phi] e^{-S_0}} \end{aligned} \tag{2.36}$$

with the ideal gas contribution $\ln \mathcal{Z}_0$. Expanding the logarithm in a series, yields

$$\begin{aligned} \ln \mathcal{Z}_I &= \sum_{k=0}^{\infty} \frac{(-1)^k}{k+1} \left(\sum_{l=1}^{\infty} \frac{(-1)^l}{l!} \left\langle S_I^l \right\rangle_0 \right) \\ &= \sum_{k=0}^{\infty} \frac{(-1)^k}{k+1} \left(- \left\langle S_I^1 \right\rangle_0 + \frac{1}{2} \left\langle S_I^2 \right\rangle_0 + ... \right)^{k+1} \\ &= - \left\langle S_I \right\rangle_0 + \frac{1}{2} \left(\left\langle S_I^2 \right\rangle_0 - \left\langle S_I \right\rangle_0^2 \right) + ... \,, \end{aligned} \tag{2.37}$$

where the first and the second term in the last line are of the order of the coupling parameter and the squared of the coupling parameter, respectively. However, this naive expansion is not valid after leading order, due to infrared (IR) divergences.
Before we will show this explicitly in the next section, we discretize space and time via a dimensionless Fourier transformation in the field

$$\phi(x, \tau) = \sqrt{\frac{\beta}{V}} \sum_{n=-\infty}^{+\infty} \sum_{k} e^{i(k^\mu x_\mu + \omega_n \tau)} \phi_n(k) \tag{2.38}$$

with Matsubara frequencies $\omega_n = 2n\pi\beta^{-1}$ or $\omega_n = (2n+1)\pi\beta^{-1}$ for bosons or fermions, respectively, which is a consequence of the periodicity constraint. We define the full propagator in momentum-frequency space as

$$\begin{aligned} D(k, \omega_n) &= \left[\omega_n^2 + \omega^2 + \Pi(k, \omega_n) \right]^{-1} \\ &= [1 + D_0(k, \omega_n) \Pi(k, \omega_n)]^{-1} D_0(k, \omega_n) \end{aligned} \tag{2.39}$$

with $\omega^2 = k^2 + m^2$ and the free propagator

$$D_0(k, \omega_n) = \left[\omega_n^2 + \omega^2 \right]^{-1} \,, \tag{2.40}$$

where the self-energy Π is given as

$$\Pi = -2\delta_{\mathcal{D}_0} \ln \mathcal{Z}_I \big|_{1\mathrm{PI}} \,, \tag{2.41}$$

which is evaluated for 1PI (1 Particle Irreducible) diagrams. Thus, in the momentum continuum limit the IR divergences are manifest in expressions such as

$$B(m, T) = \beta^{-1} \sum_{n=-\infty}^{+\infty} \int \frac{d^3k}{(2\pi)^3} \frac{1}{\omega_n^2 + \omega^2} \,, \tag{2.42}$$

[2] An alternative approach is to evaluate the partition function on a space-time lattice, see e.g. [6].

in the limit $m \to 0$, which are associated with bubble diagrams in the context of the computation of the logarithm of the partition function [6]. We handle the IR divergences via a resummation of an infinite number of ring diagrams such as for the ϕ^4 model.[3]

2.3.1 Infrared divergences and resummation in the ϕ^4 model

The Euclidean Lagrangian of a scalar ϕ^4 model with a coupling parameter λ reads

$$\mathcal{L}_{\phi^4} = \frac{1}{2}(\partial^\mu\phi)(\partial_\mu\phi) + \frac{1}{2}m_B^2\phi^2 + \frac{1}{4}\lambda_B\phi^4\,. \tag{2.43}$$

According to (2.37) the free energy density, which equals the negative pressure, is given as

$$f(T) \equiv \lim_{V\to\infty}\frac{F(T,V)}{V} = \lim_{V\to\infty}\left\{\frac{F_0}{V} - \frac{1}{\beta V}\left[-\langle S_I\rangle_0 + \frac{1}{2}\left(\langle S_I^2\rangle_0 - \langle S_I\rangle_0^2\right)\right] + ...\right\}. \tag{2.44}$$

In the pole mass scheme, that is m_R^2 is taken to be the physical mass squared, and the limit $m_B^2 \to 0$, the result is known as

$$f(T) = \frac{\pi^2\beta^{-4}}{90}\left[1 - \frac{15}{32}\frac{\lambda_R}{\pi^2} + \frac{15}{16}\left(\frac{\lambda_R}{\pi^2}\right)^{\frac{3}{2}}\right], \tag{2.45}$$

where $\lambda_B = \lambda_R + \mathcal{O}\left(\lambda_R^2\right)$ and $m_B^2 = m_R^2 + \mathcal{O}(\lambda_R)$ [18]. Comparing term by term of (2.45) with (2.44) we notice that a naive counting of powers in the coupling parameter as in (2.44) is not valid, i.e. a contribution of $\mathcal{O}\left(\lambda_R^{3/2}\right)$ is present in (2.45), whereby the variance in (2.44) is of $\mathcal{O}\left(\lambda_R^2\right)$. Indeed, writing $f = \sum_{n=0} f^{(n)} \sim \sum_{n=0}\mathcal{O}(\lambda_B^n)$, the contribution $f^{(2)}$ is given as

$$f^{(2)}(T) = -\frac{9}{4}\lambda_B^2\frac{\beta^{-4}}{144}\frac{\beta^{-1}}{8\pi m_B} + \mathcal{O}\left(m_B^0\right), \tag{2.46}$$

and the infrared divergence is apparent in the limit $m_B \to 0$.
In the following we sum the divergent terms to all orders, which will result in a qualitative modification of the weak-coupling expansion, due to higher order contributions, i.e. the finite half-integer term of $\mathcal{O}\left(\lambda^{3/2}\right)$ in (2.45) emerges. At order λ_B^N the dominant infrared divergent contribution is given by one zero Matsubara mode

$$B^{(0)}(T) = \beta^{-1}\int\frac{d^Dk}{(2\pi)^D}\frac{1}{(\omega^2)^N}\,, \tag{2.47}$$

which is dressed with N non-zero Matsubara modes

$$\tilde{B}(0,T) = \beta^{-1}\sum_{n\neq 0}\int\frac{d^Dk}{(2\pi)^D}\frac{1}{\omega_n^2 + k^2} \tag{2.48}$$

as

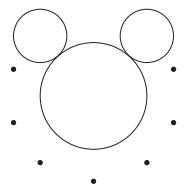

, (2.49)

[3] Alternatively, one may work with an effective field theory, which separates different scales, see e.g. [17].

where the dots denote possible $\tilde{B}(0,T)$ loops [6]. Summing the mickey-mouse diagrams (2.49) to infinite order yields a set of ring diagrams. Each ring diagram looks like[4]

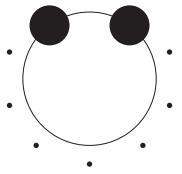

, (2.50)

whereas each full point represents a self-energy loop. A calculation of a generic mickey-mouse diagram gives

$$\begin{aligned} &= \frac{(-1)^{N+1}}{N!}\left(\frac{\lambda_B}{4}\right)^N \langle\phi\phi\phi\phi\dots\phi\phi\phi\phi\rangle_{0,\text{connected}} \\ &= \frac{(-1)^{N+1}}{N!}\left(\frac{\lambda_B}{4}\right)^N 6^N 2(N-1)2(N-1)!\dots 2\left[\tilde{B}(0,T)\right]^N \beta^{-1}\int\frac{d^Dk}{(2\pi)^D}\left(\frac{1}{k^2+m_B^2}\right)^N . \end{aligned} \tag{2.51}$$

For $D = 3 - 2\epsilon$ this reads

$$\begin{aligned} &= \frac{(-1)^{N+1}}{N!}\left(\frac{\lambda_B}{4}\right)^N 6^N 2^{N-1}(N-1)!\left[\frac{\beta^{-2}}{12}\right]^N \beta^{-1}\frac{(-1)^N}{(N-1)!}\partial^N_{m_B^2}\left(\frac{m_B^3}{6\pi}\right) \\ &= -\frac{\beta^{-1}}{2}\frac{1}{N!}\left(\frac{\lambda_B\beta^{-2}}{4}\right)^N \partial^N_{m_B^2}\left(\frac{m_B^3}{6\pi}\right) . \end{aligned} \tag{2.52}$$

We sum all orders and get

$$-\frac{\beta^{-1}}{12\pi}\sum_{N=0}^{\infty}\frac{1}{N!}\left(\frac{\lambda_B\beta^{-2}}{4}\right)^N \partial^N_{m_B^2}(m_B^3) = -\frac{\beta^{-1}}{12\pi}\left(m_B^2+\frac{\lambda_B\beta^{-2}}{4}\right)^{\frac{3}{2}} . \tag{2.53}$$

Here, the result is finite in the limit $m_B \to 0$. Moreover, (2.53) is of $\mathcal{O}\left(\lambda^{3/2}\right)$ and equals to that term in (2.45). The subsequent terms of $\mathcal{O}\left(\lambda_R^2\right)$, $\mathcal{O}\left(\lambda_R^{5/2}\ln\lambda_R\right)$ and $\mathcal{O}\left(\lambda_R^{5/2}\right)$, $\mathcal{O}\left(\lambda_R^3\ln\lambda_R\right)$ and $\mathcal{O}\left(\lambda_R^3\right)$ are calculated in [19] and references therein.
Let us conclude this section by a schematic scale separation, which is analogical for QCD.[5] The one-loop self-energy at finite temperature is given by [6] as

$$\Pi^{(1)} = 12\lambda\beta^{-1}\sum_n\int\frac{d^3k}{(2\pi)^3}\frac{1}{\omega_n^2+\omega^2} , \tag{2.54}$$

whereas the renormalized one is

$$\Pi_R^{(1)} = 12\lambda\int\frac{d^3k}{(2\pi)^3}\frac{1}{\omega}\frac{1}{e^{\beta\omega}-1} . \tag{2.55}$$

[4] One may name it frog diagram.
[5] From (2.54) and the Matsubara frequencies $\omega_n = (2n+1)\pi\beta^{-1}$ for fermions no infrared divergences emerge in the photon propagator in quantum electrodynamics.

In the high temperature limit, masses are negligible, thus $\Pi^{(1)} \to \lambda\beta^{-2}$ and hence thermal fluctuations generate an effective mass for the scalar field, that is the soft scale $m_{\rm th} = \sqrt{\lambda}\beta^{-1}$. In this limit, $\Pi_R^{(1)}$ is dominated by momenta of the order of the temperature, that is the hard scale $k \sim \beta^{-1}$ evolves. To integrate the effects of the thermal mass, we define an effective propagator

$$D_{\rm th}(k, \omega_n) = \frac{1}{\omega_n^2 + k^2 + \lambda\beta^{-2}} \,. \tag{2.56}$$

For hard momenta the self-energy correction to the propagator is of perturbative nature, whereby the thermal mass term is as large as the inverse bare propagator on the soft scale and thus, non-perturbatively.

Chapter 3

Resumming the non-linear SU(N) Higgs model in a nutshell

Historically, the term linear sigma model was introduced by M. Gell-Mann and M. Lévy in 1960 [20]. It is a renormalized maxican-hat potential inspired model for pion condensate. The $O(4)$ model consists of four scalar fields and thus, the vacuum values are on a 3-sphere. The three light field modes are the pions and the heavy one is called sigma. It was a predicted particle which was identified with the broad $\sigma(600)$ resonance, though this resonance was too broad. Consequently, the model was modified and the σ mass adjusted by slow oscillations of the potential. In the limit of fast oscillations the pion fields are restricted to a sphere. This non-renormalizable[1] effective model is called the non-linear sigma model. Actually, this is a misnomer as there is no finite energy σ left. In the context of generic SU(N) Yang-Mills theories, spontaneous symmetry breaking is described via the Higgs model. We consider a non-linear SU(N) Higgs model, that is a field $U \in \mathrm{SU}(N)$ with the constraint $U^\dagger U = \text{const.}$, by adding and subtracting a scalar field $\Phi \sim \mathrm{SU}(N)$ as e.g., treated in [2]. Thus, a gauge field mass is added, see [21].

3.1 Lagrangian

We parametrize a field $U \in \mathrm{SU}(N)$ by $N^2 - 1$ hermitian SU(N) generators T^a and real coefficients Λ^a as

$$U = e^{\Lambda(x)}\,, \quad \Lambda(x) = igT^a\Lambda^a(x)\,. \tag{3.1}$$

The pure Euclidean gauge invariant SU(N) Yang-Mills theory is

$$\mathcal{L} = -\frac{1}{2g}\mathrm{Tr}\left\{F_{\mu\nu}^2\right\}\,, \quad F_{\mu\nu} = [D_\mu, D_\nu]\,, \tag{3.2}$$

with the coupling parameter $g \sim \text{mass}^{(1/2)}$ and the covariant derivative

$$D_\mu = \partial_\mu - igT^a A_\mu^a(x)\,. \tag{3.3}$$

An additional scalar field $\Phi \sim \mathrm{SU}(N)$ with mass m in the context of the non-linear SU(N) Higgs model is parametrized as

$$\Phi = \frac{m}{g}\exp\left\{i\frac{g}{m}T^a\pi^a(x)\right\}\,. \tag{3.4}$$

[1] In two dimensions, its fields, its metric and hence, all of its coupling parameters are dimensionless, and therefore renormalizable.

The mass dimensions of the auxiliary Goldstone-like boson fields $\pi^a(x) \in \mathbb{R}$ and the gauge fields $A^a_\mu(x) \in \mathbb{R}$ are the same. The local gauge transformations of the fields read

$$\begin{aligned}
&\Psi_\Lambda \equiv U\Psi: \quad \overline{\Psi}_\Lambda = \overline{\Psi}U^\dagger\,, \quad \left(\overline{\Psi}\Psi\right)_\Lambda = \overline{\Psi}\Psi\,.\\
&(A_\mu)_\Lambda \equiv UA_\mu U^\dagger + (\partial_\mu U)U^\dagger: \quad (D_\mu\Psi)_\Lambda = UD_\mu\Psi\,, \quad \left(\overline{\Psi}D_\mu\Psi\right)_\Lambda = \overline{\Psi}UD_\mu\Psi\,.\\
&\Phi_\Lambda \equiv U\Phi: \quad (D_\mu\Phi)_\Lambda = UD_\mu\Phi\,, \quad \left((D_\mu\Phi)^\dagger(D_\mu\Phi)\right)_\Lambda = (UD_\mu\Phi)^\dagger(UD_\mu\Phi)\,.
\end{aligned} \tag{3.5}$$

Claiming gauge invariance, we write down the Lagrangian in R_ξ gauge, that is, we add a total derivative, which is zero by means of space-time integration in the action, as

$$\begin{aligned}
\mathcal{L} = \mathrm{Tr}\,\Big\{ &-\frac{1}{2g^2}([D_\mu, D_\nu])^2\\
&+ (D_\mu\Phi)^\dagger(D_\mu\Phi)\\
&+ \frac{1}{\xi}\left(\frac{1}{ig}(\partial_\mu A_\mu) + i\xi m\mathrm{Tr}\left\{\left(\Phi - \Phi^\dagger\right)T^a\right\}T^a\right)^2\\
&+ 2(\partial_\mu\overline{c})((\partial_\mu c) - [A_\mu, c]) + g\xi m\overline{c}\left(\Phi^\dagger c + c\Phi\right)\\
&-\partial_\mu\left(\frac{m}{g}\left(\Phi - \Phi^\dagger\right)A_\mu\right)\Big\}\,,
\end{aligned} \tag{3.6}$$

with a gauge fixing parameter ξ, Faddeev-Popov ghost field $c = igT^a c^a(x)$, anti-ghost field $\overline{c} = -igT^a\overline{c}^a(x)$ and the gauge term in the last line, that is to cancel explicitly the terms bilinear in πA. For the derivation of Feynman rules, we expand the Lagrangian in the field π, i.e. write $\Phi = m/g + \hat{\Phi}$ and apply $\mathrm{Tr}\left\{T^aT^b\right\} = \delta^{ab}/2$ for the gauge term, so that we rewrite the gauge fixed Lagrangian as

$$\begin{aligned}
\mathcal{L} = \mathrm{Tr}\,\Big\{ &-\frac{1}{2g^2}([D_\mu, D_\nu])^2\\
&+\left(\partial_\mu\hat{\Phi}\right)^\dagger\left(\partial_\mu\hat{\Phi}\right) + \frac{m}{g}\left(\partial_\mu\left(\hat{\Phi} - \hat{\Phi}^\dagger\right)\right)A_\mu + \left(\left(\partial_\mu\hat{\Phi}\right)\hat{\Phi}^\dagger - \hat{\Phi}\left(\partial_\mu\hat{\Phi}^\dagger\right)\right)A_\mu - \frac{m^2}{g^2}A_\mu A_\mu\\
&-\frac{1}{\xi g^2}(\partial_\mu A_\mu)^2 + \frac{m}{g}\left(\hat{\Phi} - \hat{\Phi}^\dagger\right)(\partial_\mu A_\mu) - \frac{\xi m^2}{2}\mathrm{Tr}\left\{\left(\hat{\Phi} - \hat{\Phi}^\dagger\right)T^a\right\}\left(\hat{\Phi} - \hat{\Phi}^\dagger\right)T^a\\
&+2(\partial_\mu\overline{c})((\partial_\mu c) - [A_\mu, c]) + g\xi m\overline{c}\left(\hat{\Phi}^\dagger c + c\hat{\Phi}\right) + 2\xi m^2\overline{c}c\\
&-\frac{m}{g}\left(\partial_\mu\left(\hat{\Phi} - \hat{\Phi}^\dagger\right)\right)A_\mu - \frac{m}{g}\left(\hat{\Phi} - \hat{\Phi}^\dagger\right)(\partial_\mu A_\mu)\Big\}\,,
\end{aligned} \tag{3.7}$$

where the red terms cancel and the blue highlight the Lagrangian of a pure Yang-Mills theory (2.1). To handle the infrared divergences, due to massless gauge fields, we perform a resummation of the non-linear SU(N) Higgs model.

3.2 Resummation

The way of resummation is to sum up an infinite number of higher order contributions into a given order of the perturbative expansion and to subtract these at the order they are naturally present. Formally, the rearrangement is done by subtracting contributions at one loop higher than those which are added, i.e.

$$\mathcal{L}_{\text{eff}} = \frac{1}{l}\left[\mathcal{L}\left(\sqrt{l}X\right) + \Delta\mathcal{L}\left(\sqrt{l}X\right) - l\Delta\mathcal{L}\left(\sqrt{l}X\right)\right]\,, \tag{3.8}$$

where the physical fields X are rescaled and $\Delta\mathcal{L}$ is a modified Lagrangian of the initial and possible auxiliary fields [22]. In particular, if $\Delta\mathcal{L}$ represents a mass term of the gluon, then the infrared divergences are regulated. After the expansion of the effective Lagrangian (3.8) in the counting parameter l, we set $l = 1$ and obtain the initial Lagrangian. Note, that the results in the initial and resummed theories may differ at finite order calculations and the quality of the approximation has to be estimated from the apparent convergence of the series for each observable. A resummed perturbation theory has to maintain the symmetries of the theory at every order. We choose a gauged non-linear SU(N) Higgs model, coupling a field $\Phi \sim \mathrm{SU}(N)$ as

$$\Delta\mathcal{L} \equiv \mathrm{Tr}\left\{\left[(D_\mu\Phi)^\dagger(D_\mu\Phi)\right]\right\} . \tag{3.9}$$

Thus, $\Delta\mathcal{L}$ provides a mass term for the gluon at tree-level.
Equivalently, we derive the resummation prescription by rewriting the Lagrangian (3.6) in terms of $\Phi \to V \equiv \exp\{ig/m \cdot T^a\pi^a(x)\}$ as

$$\begin{aligned}\mathcal{L} = \frac{1}{g^2}\mathrm{Tr}\Big\{ & -\frac{1}{2}([D_\mu, D_\nu])^2 \\ & + m^2(D_\mu V)^\dagger(D_\mu V) \\ & + \frac{1}{\xi}\left(\frac{1}{i}(\partial_\mu A_\mu) + i\xi m^2\mathrm{Tr}\left\{\left(V - V^\dagger\right)T^a\right\}T^a\right)^2 \\ & + 2g^2(\partial_\mu\overline{c})((\partial_\mu c) - [A_\mu, c]) + g^2\xi m^2\overline{c}\left(V^\dagger c + cV\right) \\ & - \partial_\mu\left(m^2\left(V - V^\dagger\right)A_\mu\right)\Big\} ,\end{aligned} \tag{3.10}$$

and note that the pure Yang-Mills Lagrangian (2.1) is obtained for $m^2 = 0$. Hence, the resummation prescription is to transform here $m^2 \to m^2(1-l)$ and $l \to 1$ in the end, whereby the m in V is not scaled. In addition, we rescale $g^2 \to g^2 l$ to count orders in terms of l. Thus, the ingredients are

$$\begin{aligned} & D_\mu = \partial_\mu - ig\sqrt{l}T^a A^a_\mu(x) , \\ & V(x) = \exp\left\{i\frac{g\sqrt{l}}{m}T^a\pi^a(x)\right\} , \\ & c(x) = ig\sqrt{l}T^a c^a(x) , \overline{c}(x) = -ig\sqrt{l}T^a\overline{c}^a(x) , \end{aligned} \tag{3.11}$$

with gauge transformations

$$\begin{aligned} & U = e^\Lambda , \quad U^\dagger = e^{-\Lambda} , \\ & (A_\mu)_\Lambda = UA_\mu U^\dagger + (\partial_\mu U)U^\dagger = A_\mu + \delta A_\mu[\Lambda] + \mathcal{O}\left(\Lambda^2\right) , \\ & \quad \delta A_\mu[\Lambda] = \Lambda A_\mu - A_\mu\Lambda + (\partial_\mu\Lambda) , \\ & V_\Lambda = UV = \delta V[\Lambda]V + \mathcal{O}\left(\Lambda^2\right) , \quad V^\dagger_\Lambda = V^\dagger U^\dagger = V^\dagger + \delta V[\Lambda]^\dagger + \mathcal{O}\left(\Lambda^2\right) , \\ & \quad \delta V[\Lambda] = \Lambda V , \quad \delta V[\Lambda]^\dagger = -V^\dagger\Lambda \end{aligned} \tag{3.12}$$

and the resummed Lagrangian

$$\mathcal{L}_l = -\frac{1}{g^2 l}\mathrm{Tr}\left\{\frac{1}{2}([D_\mu, D_\nu])^2 - m^2(1-l)(D_\mu V)^\dagger(D_\mu V) + \frac{1}{\xi}\mathcal{F}^2 + 2\overline{c}\delta\mathcal{F}[c]\right\} , \tag{3.13}$$

where the first two terms are left invariant by the gauge transformations. The R_ξ gauge fixing condition $\mathcal{F}$, which cancels mixed two-point functions πA reads

$$\mathcal{F} \equiv (\partial_\mu A_\mu) - \xi\mathrm{Tr}\left\{WT^a\right\}T^a , \quad W \equiv m^2(1-l)\left(V - V^\dagger\right) \tag{3.14}$$

and transforms as

$$\begin{aligned} W_\Lambda &= W + \delta W[\Lambda] + \mathcal{O}\left(\Lambda^2\right) , \\ \delta W[\Lambda] &= m^2(1-l)\left(\Lambda V + V^\dagger \Lambda\right) , \\ \mathcal{F}_\Lambda &= \mathcal{F} + \delta\mathcal{F}[\Lambda] + \mathcal{O}\left(\Lambda^2\right) , \\ \delta\mathcal{F}[\Lambda] &= \partial_\mu \delta A_\mu[\Lambda] - \xi \mathrm{Tr}\left\{\delta W[\Lambda] T^a\right\} T^a . \end{aligned} \tag{3.15}$$

The ghost term is implied in $\mathcal{F}_\Lambda$. The pure Yang-Mills Lagrangian (2.1) in covariant gauge is obtained for $l = 1$ in (3.13). We will apply the resummed non-linear SU(N) Higgs model in Chapter 6 to calculate the the transverse part of the gluon self-energy. Next, we check BRS invariance, which is the residual symmetry after gauge fixing.

3.3 BRS invariance

BRS transformations were first introduced by C. Becchi, A Rouet and R. Stora in 1975 [16] and are nilpotent of vanishing square, that is $\delta^2_{\mathrm{BRS}} = 0$. The Ward-Takahashi identities associated with BRS symmetry imply the structural stability of the action as implementing renormalization. For a broader application of BRS transformations see [23]. We introduce a global Grassmann parameter ω and derive explicitly the transformations. As gauge invariance implies BRS invariance the first two terms in (3.13) are left invariant by the particular transformation $\Lambda = \omega c$, i.e.

$$\begin{aligned} &\delta_{\mathrm{BRS}} A_\mu \equiv \delta A_\mu[\omega c] , \\ &\delta_{\mathrm{BRS}} V \equiv \delta V[\omega c] , \quad \delta_{\mathrm{BRS}} V^\dagger \equiv \delta V^\dagger[\omega c] \\ &\Rightarrow \delta_{\mathrm{BRS}} \pi = \omega \sum_{n=0}^{\infty} \frac{B_n l^{\frac{n}{2}}}{n!} \sum_{j=0}^{n} \binom{n}{j} \pi^{n-j} c \pi^j + \mathcal{O}\left(\omega^2\right) \\ &\qquad\qquad = \omega c - \frac{\omega\sqrt{l}}{2}(\pi c - c\pi) + \frac{\omega l}{12}(\pi\pi c - 2\pi c \pi + c\pi\pi) + \mathcal{O}\left(\pi^4, \omega^2\right) \end{aligned} \tag{3.16}$$

where B_n are the Bernoulli numbers. The transformations $\delta_{\mathrm{BRS}}\overline{c}$ and $\delta_{\mathrm{BRS}} c$ are given by invariance of the last two terms in (3.13). One has

$$\begin{aligned} &\delta_{\mathrm{BRS}}\mathcal{F} = \delta\mathcal{F}[\omega c] = \omega\delta\mathcal{F}[c] , \\ &0 \stackrel{!}{=} \delta_{\mathrm{BRS}}\left(\frac{1}{\xi}\mathcal{F}^2 + 2\overline{c}\delta\mathcal{F}[c]\right) = \frac{2}{\xi}\mathcal{F}\omega\delta\mathcal{F}[c] + 2\delta_{\mathrm{BRS}}\overline{c}\delta\mathcal{F}[c] + 2\overline{c}\delta_{\mathrm{BRS}}\delta\mathcal{F}[c] \end{aligned} \tag{3.17}$$

Thus, we can set

$$\delta_{\mathrm{BRS}}\overline{c} \equiv -\frac{1}{\xi}\mathcal{F}\omega \tag{3.18}$$

and are left with

$$\begin{aligned} 0 &\stackrel{!}{=} \delta_{\mathrm{BRS}}\delta\mathcal{F}[c] \\ &= \delta_{\mathrm{BRS}}(\partial_\mu \delta A_\mu[c] - \xi \mathrm{Tr}\left\{\delta W[c] T^a\right\} T^a) \\ &= \partial_\mu(\delta\delta_{\mathrm{BRS}} A_\mu[c] + \delta A_\mu[\delta_{\mathrm{BRS}} c]) - \xi \mathrm{Tr}\left\{(\delta\delta_{\mathrm{BRS}} W[c] + \delta W[\delta_{\mathrm{BRS}} c]) T^a\right\} T^a \\ &= \partial_\mu(\delta A_\mu[\delta_{\mathrm{BRS}} c] - \delta A_\mu[\omega cc]) - \xi \mathrm{Tr}\left\{(\delta W[\delta_{\mathrm{BRS}} c] - \delta W[\omega cc]) T^a\right\} T^a . \end{aligned} \tag{3.19}$$

Consequently, we deduce

$$\delta_{\mathrm{BRS}} c \equiv \omega cc . \tag{3.20}$$

Chapter 4

Review of the Laporta-algorithm

In 2000, S. Laporta described an algorithm for the reduction of a set of generic Feynman integrals to some finite set of integrals [24], henceforth called master integrals, and also the methods of their numerical solutions [25]. Here, we will give a review of the techniques applied in our computations starting with the reduction of Feynman integrals by integration-by-parts identities. Thereafter, we will present the method of difference equations[1] and their solutions by means of factorial series which allows us to calculate the master integrals numerically.

4.1 Integration-by-parts identities

The method of integration-by-parts (IBP) identities was first described by K.G. Chetyrkin and F.V. Tkachov in 1981 [26]. Once created, a system of IBP identities provides a way to reduce the number of Feynman integrals to be calculated, i.e. the master integrals. Each initial Feynman integral is expressed as a linear combination of these master integrals. To illustrate the method of IBP identities, we consider the zero-point one-loop integral in D-dimensional momentum-space

$$I(n) = \int \left[d^D k\right] \frac{1}{(k^2+1)^n}\,, \tag{4.1}$$

where $\left[d^D k\right] \equiv dk_1 \ldots dk_D/\pi^{D/2}$ and each $k_\mu \in (-\infty, +\infty)$. IBP on the level of the integrand yields

$$\int \left[d^D k\right] \partial_{k_\mu} \frac{k_\nu}{(k^2+m^2)^n} = \int \left[d^D k\right] \left[\frac{\delta_{\mu\nu}}{(k^2+1)^n} - \frac{2nk_\mu k_\nu}{(k^2+1)^{n+1}}\right]. \tag{4.2}$$

The left hand side is identically zero by Stokes' theorem. Contracting the right hand side with $\delta_{\mu\nu}$, and making use of $\delta_{\mu\mu} = D$ and $k^2/(k^2+1) = 1 - 1/(k^2+1)$, we can rewrite this for $n > 0$ as[2]

$$(D-2n)I(n) + 2nm^2 I(n+1) = 0\,. \tag{4.3}$$

Now, we have a set of recurrence relations, so that we can express any $I(n>1)$ in terms of $I(1)$, which is the irreducible master integral in this example.
Let us turn to a generic L-loop Feynman integral with N internal lines and N_e external momenta of the form

$$I(n_1, \ldots, n_N; \alpha_1, \ldots, \alpha_{N_{sp}}) = \int \left[d^D k_1\right] \ldots \left[d^D k_L\right] \frac{R_1^{\alpha_1} \ldots R_{N_{sp}}^{\alpha_{N_{sp}}}}{D_1^{n_1} \ldots D_N^{n_N}}\,, \tag{4.4}$$

[1] Alternatively, solutions of difference equations has been obtained via systems of differential equations in masses and momenta by means of Laplace's transformation, see [25].

[2] Rewriting this as $I(n+1) = (n-D/2)/(m^2 n) I(n)$ the known result $I(n+1) \propto \Gamma(n-D/2)/\Gamma(n)$ follows, recursively.

where the set $\{R_j\}$ contains all $N_{sp} = L(N_e + (L+1)/2)$ possible scalar products $k_i \cdot k_j$ and $p_i \cdot k_j$ and $D_i = q_i^2 + m_i^2$, where q_i is a linear combination of k_i and the external momenta p_i.
The next step is to write the scalar products R_j as irreducible ones, in the sense that R_j is not appearing in the numerator and denominator, in terms of D_j, simultaneously. This is done by applying the algebraic identity

$$\frac{R_j}{D_j} = \frac{1}{C_j}\left(1 - \frac{D_j - C_j R_j}{D_j}\right) \tag{4.5}$$

with C_j given as coefficients of R_j in D_j.
For these integrals with only irreducible scalar products (i.s.p.), we can write down a set of IBP identities as

$$\int \left[d^D k_1\right] ... \left[d^D k_L\right] \partial_{(k_j)_\mu} \left(\{(k_l)_\mu, (p_m)_\mu\} \left[\frac{R_1^{\alpha_1} ... R_{N_{sp}}^{\alpha_{N_{sp}}}}{D_1^{n_1} ... D_N^{n_N}} \right]_{\text{i.s.p.}} \right) = 0\,. \tag{4.6}$$

Reducible scalar products formed in the calculation of the derivative and the contraction of the index μ have to be transformed into irreducible ones via the algebraic identities (4.5).
This linear homogeneous system of equations with integrals as unknowns is infinite dimensional. Laporta suggests a Gauss algorithm for a finite subset of these identities: One IBP identity is chosen, and previously reduced integrals are substituted therein. This identity is rewritten such that one of the integrals which is not yet reduced is expressed by the residual ones. Hence, it is added to the list of reduced integrals and this procedure is repeated with another IBP identity.
The algorithm is sensible to the ordering of the identities and the integrals. The ordering of the identities does not affect the solution of the system but the computation time. A good choice is to select first the integral with the lowest number of denominators, so that the number of substitutions is minimized. The ordering of the integrals affect the form of the master integrals. Laporta's choice is a lexicographic ordering of the number of denominators, the sum of the exponents of the denominators and the sum of the exponents of the scalar products. A flow chart of the algorithm and the details on the finite sets of identities to be considered are given in [25].
Besides the IBP identities, one may make use of the Lorentz-scalar nature of Feynman integrals by constructing Lorentz-invariance (LI) identities [27]. They have the form

$$\int \left[d^D k_1\right] ... \left[d^D k_l\right] p_i^\mu p_j^\nu \left(p_{k_\nu} \partial p_{k_\mu} - p_{k_\mu} \partial p_{k_\nu}\right) \frac{1}{D_1^{n_1} ... D_N^{n_N}} = 0\,. \tag{4.7}$$

The differential operator within the round brackets is the generator of Lorentz transformations in the linear space of scalar functions depending on p_k. Though the LI identities can be represented as linear combinations of IBP identities [28], they may be useful in performing reductions.
Various computer programs have implemented the Laporta-algorithm, e.g. SYS by S. Laporta, Fire by A.V. Smirnov [29] and Reduze 2 by A. von Manteuffel and C. Studerus [30]. Next, we apply the algorithm to determine the difference equations satisfied by the master integrals.

4.2 Difference equations

In the previous section we have shown how to reduce generic Feynman integrals to master integrals. In this section we discuss how to build difference equations satisfied by the master integrals. The method to solve these, will be discussed in the next section.
Difference equations are functional equations with the parameter of the unknown function shifted by integer values. Let us recall that we have encountered an example for a linear difference equation of first order in (4.3). Linear difference equations are mathematically well understood [31]. Here, we

consider linear difference equations in one parameter. This will help us in high precision calculation of the master integrals.
We sketch the construction of difference equations by introducing an exponent x in a scalar master integral of the form,

$$U_{D_1}(x) = \int \frac{\left[d^D k_1\right] ... \left[d^D k_L\right]}{D_1^x D_2 ... D_N}\,, \tag{4.8}$$

where the master integral is given as $U_{D_1}(1)$ - diagrammatically, we place x points on the corresponding line. IBP identities yield a linear difference equation of order R of the function U_{D_1} of the form

$$\sum_{j=0}^{R} p_j(x) U_{D_1}(x+j) = F(x) \tag{4.9}$$

with polynomials $p_j(x)$. $F(x)$ is a linear combination of known integrals derived from master integrals containing D_1 but not all of the other denominators.
Next, we have a closer look at this procedure by taking into account all master integrals obtained by means of the algorithm described in the previous section. The number of denominators of the master integrals range from L to N, i.e. from the number of loops to the number of internal lines. For each $m \in \{L, ..., N\}$ we group all of the master integrals in a set which contain non of the denominators D_i with $i < m$ but the denominator D_m. In the following L_m denotes the number of elements in such a set and $1 \leq l \leq L_m$ for a given m. Different sets do not intersect, hence we treat each of them separately. We define master functions as

$$U_{ml}(x) = \int \left[d^D k_1\right] ... \left[d^D k_L\right] \left[\frac{R_1^{\alpha_1} ... R_{N_{sp}}^{\alpha_{N_{sp}}}}{D_m^{x-1+m} \Pi_{i>m} D_i}\right]_{\text{i.s.p.}}\,, \tag{4.10}$$

which are identical to the master integrals for $x = 1$. Applying a modified version of the previously described algorithm, see [25], yields a system of identities which contain solely master functions. The solution of this system of identities provides difference equations in U_{ml} with the structure

$$\sum_{i=0}^{R_h} p_{ilh}(x) U_{m,l+h}(x+i) = \sum_{k=1}^{l+h-1} \sum_{j=0}^{Q_{hlk}} q_{jkl}(x) U_{mk}(x+j)\,, \tag{4.11}$$

where h labels different master integrals with the same denominators but different numerators. This structure has a triangular form, so that we can tackle it sequentially and solve each difference equation one at a time, supposing that we know the inhomogeneity.

4.3 Factorial series

Assuming that we have worked out a triangular system of linear difference equations in the master functions $U(x)$, each linear difference equation of order R is of the form

$$\sum_{j=0}^{R} p_j(x) U_{D_1}(x+j) = F(x) \tag{4.12}$$

with known polynomials $p_j(x)$ and some function $F(x)$, which is solved by a general solution of its homogeneous equation. A particular non-homogeneous solution $U^{NH}(x)$ is given as

$$U(x) = \sum_{j=1}^{R} \omega_j(x) U_j^{HO}(x) + U^{NH}(x)\,, \tag{4.13}$$

where $\omega_j(x)$ are periodic functions of period one and $\{U_j^{HO}(x)\}$ is a fundamental system of homogeneous solutions.
We now introduce factorial series and some useful operators and describe how to use them to solve the linear difference equation 4.12. A factorial series of first kind is of the form

$$\sum_{s=0}^{\infty} \frac{a_s \Gamma(x+1)}{\Gamma(x-K+s+1)} \,. \tag{4.14}$$

This series behaves similarly to asymptotic expansions in $1/n$, but it has a better convergent behavior [32]. It converges for every point in the half-plane which is limited on the left by the abscissa of convergence $\lambda \equiv \Re x$, excluding the points $x = K - n$ with $n \in \mathbb{N}$.
For any m, the operator $\boldsymbol{\rho}$ is defined as

$$\boldsymbol{\rho}^m U(x) = \frac{\Gamma(x+1)}{\Gamma(x-m+1)} U(x-m) \tag{4.15}$$

following the identity

$$\boldsymbol{\rho}^m \boldsymbol{\rho}^n U(x) = \boldsymbol{\rho}^{m+n} U(x) \,. \tag{4.16}$$

Additionally, the operator $\boldsymbol{\pi}$ is defined as

$$\boldsymbol{\pi} U(x) = x(U(x) - U(x-1)) \,. \tag{4.17}$$

These operators obey the following identities:

$$[\boldsymbol{\rho}, \boldsymbol{\pi}] U(x) = \boldsymbol{\rho} U(x) \,, \tag{4.18}$$
$$p(\boldsymbol{\pi}) \boldsymbol{\rho}^m U(x) = \boldsymbol{\rho}^m p(\boldsymbol{\pi} + m) U(x) \,, \tag{4.19}$$
$$xU(x) = (\boldsymbol{\pi} + \boldsymbol{\rho}) U(x) \,, \tag{4.20}$$

where p is a polynomial. Applying these operators to master functions, an expansion in factorial series becomes an expansion in powers of $\boldsymbol{\rho}^{-1}$
We start with the solution of the homogeneous difference equation

$$p_0(x) U^{HO}(x+0) + ... + p_R(x) U^{HO}(x+R) = 0 \,. \tag{4.21}$$

Making the replacement $x \to x - R$ and setting $q_{R-i}(x) = p_i(x-R)$ this can be rewritten as

$$q_0(x) U^{HO}(x+0) + ... + q_R(x) U^{HO}(x-R) = 0 \,. \tag{4.22}$$

We make a change of variable $U^{HO}(x) = \mu^x V^{HO}(x)$, where μ is an unspecified parameter and obtain

$$\mu^R q_0(x) V^{HO}(x) + ... + \mu^0 q_R(x) V^{HO}(x-R) = 0 \,. \tag{4.23}$$

We now rewrite this equation in terms of $\boldsymbol{\rho}$ and $\boldsymbol{\pi}$ operators by multiplying it with $(x-0)...(x-R+1)$ and remember that $xV^{HO}(x-1) = \boldsymbol{\rho} V^{HO}(x)$ and $xV^{HO}(x) = (\boldsymbol{\pi} + \boldsymbol{\rho}) V^{HO}(x)$ to obtain the first canonical form of the difference equation

$$\left(f_0(\boldsymbol{\pi}, \mu) \boldsymbol{\rho}^0 + ... + f_{m+1}(\boldsymbol{\pi}, \mu) \boldsymbol{\rho}^{m+1} \right) V^{HO}(x) = 0 \,, \tag{4.24}$$

where f_j are polynomials. Usually, $f_{m+1}(\mu)$ is solely a function of μ. The characteristic equation

$$f_{m+1}(\mu) = 0 \tag{4.25}$$

has R non-zero solutions in powers of μ. For each distinct solution the canonical form (4.24) takes the form

$$\left(f_0(\boldsymbol{\pi})\boldsymbol{\rho}^0 + ... + f_m(\boldsymbol{\pi})\boldsymbol{\rho}^m\right) V^{HO}(x) = 0. \tag{4.26}$$

Now, we are looking for a solution of this equation in V^{HO} in terms of the factorial series

$$V^{HO}(x) = \sum_{s=0}^{\infty} \frac{a_s \Gamma(x+1)}{\Gamma(x-K+s+1)} \tag{4.27}$$

and substituting it we obtain the recurrence relations

$$\begin{aligned} &a_s f_m(K+m-s) + ... + a_0 f_{m-s}(K+m-s) = 0 \qquad 0 \leq s \leq m\,, \\ &a_s f_m(K+m-s) + ... + a_{s-m} f_0(K+m-s) = 0 \qquad s \geq m\,. \end{aligned} \tag{4.28}$$

Assuming that $a_0 \neq 0$, we first solve the indicial equation

$$f_m(K+m) = 0 \tag{4.29}$$

for K. Usually, all roots are distinct and their number is a multiple of the solution of the characteristic equation (4.25). If some roots differ by a positive integer, called congruent roots, then $f_m(K+m-s_0) = 0$ for some s_0 and the residual terms of the recurrence relations (4.28) vanish and thus, the value of a_{s_0} is undetermined and can be chosen at will.
The general solution of the homogeneous difference equation is a linear combination of λ distinct solutions of the characteristic equation (4.25) and its ν_i indicial equations (4.29), i.e.

$$U^{HO}(x) = \sum_{i=1}^{\lambda} \sum_{j=1}^{\nu_i} \omega_{ij}(x) \mu_i^x V_{ij}^{HO}(x) \tag{4.30}$$

with single-periodic functions $\omega_{ij}(x)$.
A particular solution of the non-homogeneous difference equation is obtained in a similar way, assuming that $F(x)$ can be written as a sum of factorial series. Conveniently, let us consider $F(x-R) = \mu^x T(x)$ with

$$T(x) = c_0 \boldsymbol{\rho}^{K-0} + c_1 \boldsymbol{\rho}^{K-1} + ...\,, \tag{4.31}$$

where μ, K and all c_i are known. Following the procedure for the solution of the homogeneous difference equation we obtain

$$\begin{aligned} &a_s f_m(K-s) + ... + a_0 f_{m-s}(K-s) = c_0 \qquad 0 \leq s \leq m\,, \\ &a_s f_m(K-s) + ... + a_{s-m} f_0(K-s) = c_s \qquad s \geq m\,. \end{aligned} \tag{4.32}$$

In the more general case $F(x-R) = \mu^x p(x) T(x)$, we first transform the polynomial $p(x)$ into $p(\boldsymbol{\pi}+\boldsymbol{\rho})$ and let it act on the expansion of $T(x)$.
Let us summarize what we have encountered so far and what is to be done next. We have studied how to obtain a fundamental system of the homogeneous difference equation and how to find a particular solution of the non-homogeneous difference equation based on factorial series. As we are looking for the integer values of x in the general solution, we can write it as

$$U(x) = \sum_{j=1}^{R} \eta_j U_j^{HO}(x) + U^{NH}(x) \tag{4.33}$$

with constants η_j. The next step is to determine these constants. Subsequently, we discuss the convergence of the factorial series to obtain a high precision result for the master integral.

The values of the constants can be determined in two different ways. One method is to equate the first coefficients of the expansions in factorial series of the general solution (4.33) and of the master function

$$U(x) = \int \left[d^D k_1\right] ... \left[d^D k_L\right] \left[\frac{R_1^{\alpha_1} ... R_{N_{sp}}^{\alpha_{N_{sp}}}}{D_1^x D_2 ... D_N}\right]_{\text{i.s.p.}} \tag{4.34}$$

for large x. The other one is to equate the general solution (4.33) and the master function (4.34) at x equal zero.
We now illustrate the large-x method by considering an Euclidean massive Feynman integral which we will address again in Chapter 7.

4.3.1 Example: massive zero-point five-loop sunset-integral

An Euclidean zero-point sunset-integral with one mass parameter is of the form

$$S(l, D, x) = \left[\int \frac{d^D p}{p^2+1}\right]^{-l} \int \frac{d^D k_1}{k_1^2+1} ... \frac{d^D k_l}{k_l^2+1} \frac{1}{[(k_1+...+k_l)^2+1]^x}\,, \tag{4.35}$$

where l labels the number of loops. We are interested in extracting the first two coefficients in the expansion of the factorial series for $l = 5$. Writing $S(5, D, x)$ in hyperspherical polar coordinates for k_1 yields

$$\begin{aligned} S(5, D, x) &= \frac{1}{\Gamma\left(\frac{D}{2}\right)} \int_0^\infty \frac{dk_1^2 (k_1^2)^{\frac{D}{2}-1}}{(k_1^2+1)^x} f\left(k_1^2\right)\,, \\ f(k_1^2) &\equiv \frac{1}{\Omega_D} \int d\Omega_D \hat{k_1} g(k_1)\,, \\ g(k_1) &\equiv \int \left[d^D k_2\right] ... \left[d^D k_5\right] \frac{1}{k_1^2 + 2k_1 p\cos\phi + p^2 + 1}\,, \end{aligned} \tag{4.36}$$

where $\Omega_D \equiv \frac{2\pi^{D/2}}{\Gamma(D/2)}$ and $p \equiv \sum_{i=2}^5 k_i^2$. Diagrammatically, $g(k_1)$ corresponds to the initial diagram with one line cut. In the Euclidean massive case, $f\left(k_1^2\right)$ has no singularities for $k_1^2 \geq 0$ and thus, the behavior for large x of the integral is determined by the factor $\left(k_1^2+1\right)^{-x}$, that is around $k_1^2 = 0$. Expanding the integrand of $g(k_1)$ up to second order in k_1 yields

$$g(k_1) = \int \left[d^D k_2\right] ... \left[d^D k_5\right] \left[\frac{1}{p^2+1} - \frac{2p\cos\phi}{(p^2+1)^2} k_1 + \left(\frac{-2}{(p^2+1)^2} + \frac{8p^2\cos^2\phi}{(p^2+1)^3}\right) k_1^2 + \mathcal{O}\left(k_1^3\right)\right]. \tag{4.37}$$

Integrating over the angular part and making use of the identities

$$\int_0^\pi d\phi \sin^{D-2}\phi \cos\phi = 0\,, \quad \frac{\Omega_{D-1}}{\Omega_D} \int_0^\pi d\phi \sin^{D-2}\phi \cos^2\phi = D \tag{4.38}$$

we obtain

$$\begin{aligned} f(k_1^2) =& \int \left[d^D k_2\right] ... \left[d^D k_5\right] \left[\frac{1}{(p^2+1)^2} + \left(\frac{4-D}{D}\frac{1}{(p^2+1)^2} - \frac{4}{D}\frac{1}{(p^2+1)^3}\right) k_1^2\right] \\ =& \frac{S(4, D, 1)}{\Gamma\left(2-\frac{D}{2}\right)} + \left(\frac{4-D}{D}\frac{S(4, D, 2)}{\Gamma\left(2-\frac{D}{2}\right)} - \frac{4}{D}\frac{S(4, D, 3)}{\Gamma\left(2-\frac{D}{2}\right)}\right) k_1^2 \\ \equiv& A_0 + A_1 k_1^2 \end{aligned} \tag{4.39}$$

dropping the contribution of $\mathcal{O}\left(k_1^3\right)$. Making the change of variables $k_1^2 \equiv \frac{u}{1-u}$ and expanding in powers of u we get

$$f\left(k_1^2\right) = (1-u)^{\frac{D}{2}+1}\left(A_0 + \left(\frac{2+D}{D}A_0 + A_1\right)u\right). \tag{4.40}$$

Laporta has shown [25], that the coefficients of the factorial series a_s are related to the A_s via

$$a_s = A_s \frac{\Gamma\left(s+\frac{D}{2}\right)}{\Gamma\left(\frac{D}{2}\right)}. \tag{4.41}$$

We read off

$$\begin{aligned} a_0 =& \frac{S(4,D,1)}{\Gamma\left(2-\frac{D}{2}\right)}, \\ a_1 =& \frac{D}{2\Gamma\left(2-\frac{D}{2}\right)}\left(\frac{2+D}{2}S(4,D,1) + \frac{4-D}{D}S(4,D,2) - \frac{1}{D}S(4,D,3)\right) \end{aligned} \tag{4.42}$$

and note that we have expressed the coefficients of the factorial series of the five-loop integral in terms of four-loop integrals.

It is a general feature of the large-x method, to express the coefficients of the factorial series in terms of integrals with one lower order in loop. Thus, all coefficients of the factorial series may be recursively determined. Let us now state some more common properties. For the homogeneous difference equation, the constants η_j are different from zero, if the corresponding μ_j and K_j satisfy the condition

$$\mu_j = \frac{1}{m_1^2} \quad \& \quad K_j + \frac{D}{2} \in \mathbb{Z}_- \quad \Rightarrow \quad \eta_j \neq 0, \tag{4.43}$$

where m_1 is the mass of the propagator treated separately, i.e. the propagator which is not present in $g(k_1)$ in the context of the above example. A similar equation for the non-homogeneous difference equation is usually found not to be satisfied. If no pair satisfies the condition (4.43), then the integral is completely determined by the non-homogeneous term. The non-zero constants are determined by equating the factorial series of the integral as encountered here with the factorial series of the general solution obtained previously by comparing the coefficients of the same powers of the operator $\boldsymbol{\rho}$.
For the case of non-Euclidean integrals, the radial integration has to be analytically continued to the complex plane. Thereby it may go across some singular points where the line integral has to be deformed to turn around these singularities. For such a case or for the case of non-zero masses in propagators which cause additional singularities, we refer to [25].
The zero-x method is not affected by the values of external momenta or masses but yields solely a relation between the constants, i.e.

$$U(0) - U^{NH}(0) = \sum_{j=1}^{R} U_j^{HO}(0). \tag{4.44}$$

$U(0)$ is an integral with one denominator less, which may be obtained by e.g., adding an exponent to some of the denominators and solving the corresponding difference equations.
To perform a high precision calculation of the master integral $U(1)$, we analyze the convergence of a factorial series

$$U(x) = \mu^x \sum_{s=0}^{\infty} a_s \frac{\Gamma(x+1)}{\Gamma(x+1-K+s)}. \tag{4.45}$$

The abscissa of convergence λ is finite, if none of the solutions μ_j of the characteristic equation (4.25) satisfies the condition

$$0 < \left| \frac{\mu_j}{\mu} - 1 \right| < 1 \,. \tag{4.46}$$

The convergence is logarithmic, that is

$$\left| \mu^x \sum_{s=0}^{s_{\max}} a_s \frac{\Gamma(x+1)}{\Gamma(x+1-K+s)} - U(x) \right| \sim s_{\max}^{\lambda - x} \tag{4.47}$$

for large m. Usually, $\lambda \sim 1$, hence the integral $U(x=1)$ can not be calculated directly by summing up the factorial series. The way to calculate the master integral is to calculate master functions for some large $x_{\max}$ and to apply the corresponding recurrence relations thereafter, to get the master function for all $x \in \{x_{\max}, ..., 1\}$. Here, we have to keep in mind that the recurrence relation may be unstable causing a decrease in the precision. We define a quantity $A^{-1} = \min_j |\mu_j/\mu|$. If $A > 1$, then each iteration in x increases the error of $U(x)$ by a factor A. Else, if $A = 1$ and μ is a root of the characteristic equation (4.25) of multiplicity $m > 1$, then n iterations in x increase the error of $U(x)$ by a factor n^{m-1}, which is weaker than the preceding instability. To calculate $U(1)$ with the favored number of correct digits, the parameters $s_{\max}$ and $x_{\max}$ have to be chosen appropriately. We will discuss more about this for our calculations, later on.

Chapter 5

Framework of automated Feynman integral reduction

In perturbative quantum field theories, the usual method to calculate physical observables, e.g. cross sections, involves the generation and calculation of Feynman diagrams. On the analytical level, a reduction of Feynman integrals to a set of master integrals can be implemented, which in turn can be numerically calculated, see Chapter 4. Commonly, one has to treat a large number of diagrams with a complex tensorial structure. To handle this effectively various algorithms have been implemented in computer systems.
A first attempt was made in 1967 with SCHOONSCHIP by M. Veltman written in assembler language [33]. He initially designed it to compute the quadrupole moment of the W boson as a part of his work on the renormalizability of electroweak interactions. He was awarded the Nobel prize in 1998. The next effort was made with REDUCE by A.C. Hearn in 1968 based on `Lisp`, which is yet being developed [34]. In 1982, the multi-purpose system MATHEMATICA was developed by S. Wolfram in `C` [35]. In 1989, J.A.M. Vermaseren has written the low-level symbolic manipulation system FORM in `C`, which is a successor of SCHOONSCHIP [36]. P. Nogueira has designed QGRAF in `FORTRAN77` in 1993, to automatically generate Feynman graphs by representing them in symbolic expressions [37]. The computer systems named here, excluding MATHEMATICA, are made public. We will continue with discussions on some current high-level computer programs, each covering some general or special purposes of the automated reduction of Feynman integrals.

5.1 FIRE and LITERED

The name FIRE is an abbreviation for *Feynman Integral REduction*, which refers to AIR (*Automated Integral Reduction*), developed by C. Anastasiou and A. Lazopoulos [38]. FIRE is implemented in MATHEMATICA by A.V. Smirnov [29]. It is designed to perform the reduction of dimensional regularized scalar Feynman integrals to master integrals. It provides several modes, such as the Laporta-algorithm. Further modes involve applying the s-bases-algorithm, which is based on the notion of Gröbner-bases [39], accessing QDBM [40] to store data on disc and to link FERMAT [41] for algebraic manipulations. Additionally, it makes use of the symmetries, explicit integrations by subdiagrams, ideas by R.N. Lee [28] and rules defined by hand and also the rules created with LITERED [42].
The MATHEMATICA package LITERED (*Loop InTEgrals REDuction*) is written by R.N. Lee [43]. It performs a heuristic search of the symbolic IBP reduction rules, which is not systematic and may abort but yields less redundancies with respect to the brute-force Laporta-algorithm. A reduction with the Laporta-algorithm generates large databases of IBP rules which are too large to store and

are thus re-computed in each run. Furthermore, a large number of IBP identities generated with the Laporta-algorithm are redundant. Besides, LiteRed provides tools for the search of symmetry relations, the construction of difference equations and dimensional recurrence relations [44] and for drawing graphs. The package includes various illustrative examples.
Let us return to Fire and give an example making use of IBP identities and symmetries. We reduce a subtopology of the Benz-diagram, i.e. the scalar zero-point three-loop basketball-diagram with one mass parameter and three lines with one dot, each.

```
(*declare symmetries*)
ro = Cycles[{{1, 2, 3}, {4, 5, 6}}]; (*rotation*)
re = Cycles[{{1}, {2, 3}, {4, 6}, {5}}]; (*reflection*)
de = Cycles[{{1, 4, 6}, {2, 5, 3}}]; (*deformation*)
group = PermutationGroup[{ro, re, de}];
elements = GroupElements[group];
sym = PermutationReplace[{1, 2, 3, 4, 5, 6}, elements];

Get["FIRE/FIRE_3.5.0.m"]; Get["FIRE/ibp.m"]; (*load FIRE*)

(*generate IBP identities*)
Internal = {a, b, c};
External = {};
Propagators = {a^2 + mm, b^2 + mm, c^2 + mm, (a - b)^2 + mm,
(b - c)^2 + mm, (c - a)^2 + mm};
PrepareIBP[];
startinglist = {IBP[a, a], IBP[a, b], IBP[a, c], IBP[b, a],
IBP[b, b], IBP[b, c], IBP[c, a], IBP[c, b], IBP[c, c]};

RESTRICTIONS = {}; (*define regions of vanishing integrals*)
SYMMETRIES = sym;
Prepare[]; (*transform into internal format*)
Burn[]; (*perform optimizations*)

(*reduce integral*)
F[{2, 0, 2, 2, 1, 0}]
```

This will yield some output containing various information on the evaluation and the outcome. Diagrammatically, the procedure is as follows:

↓ shrink lines and place points

$$= \frac{-3(-3+D)(-2+D)(-10+3D)(-8+3D)}{512(-4+D)[mm]^3}$$

$$- \frac{(-2+D)^3(-38+11D)}{256(-4+D)[mm]^4}$$

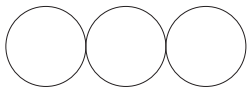

(5.1)

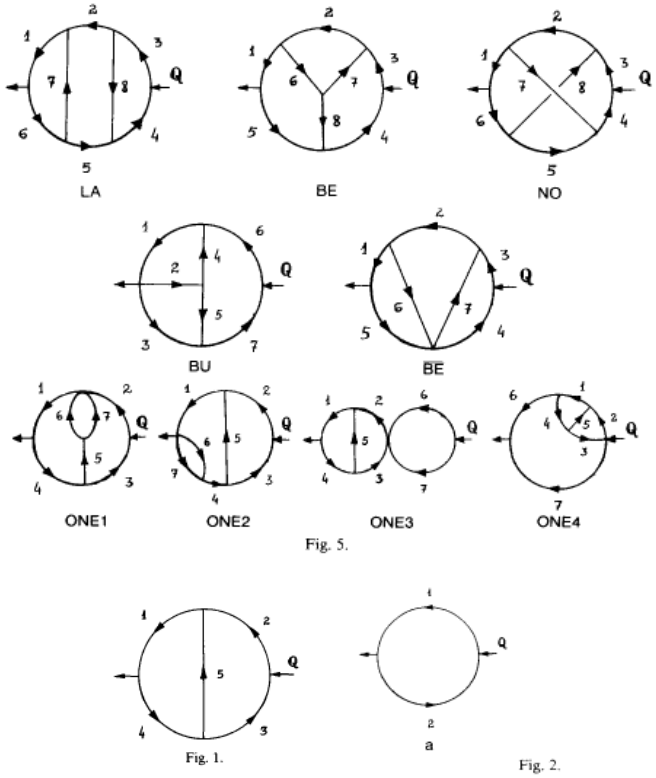

Figure 5.1: Topological graphs in MINCER (see [45])

5.2 MINCER and MATAD

The FORM package MINCER by J. Vermaseren was originally implemented by S.G. Gorishny, S.A. Larin, L.R. Surguladze and F.V. Tkachov in SCHOONSCHIP [45], based on the integration-by-parts method [26]. It performs the Laurent-expansion of scalar massless two-point Feynman integrals in terms of $\epsilon = (4 - D)/2$ up to $\mathcal{O}\left(\epsilon^{3-l}\right)$ with loops $l \leq 3$.
As there is currently no manual for the current package MINCER EXACT, we give some more details on its use. On has to disable the call to the procedure *treatqaqa.prc* in *calcdia.frm*, if no gluon currents show up in the Feynman diagram, to be calculated. Else, the trace over a single Dirac γ matrix makes the integral equal to zero. The integrals are declared in *diagram.h* by specifying the momentum carried by each line and the topology shown in Figure 5.1. **Q** labels the external momentum. Internal momenta are denoted by `p` followed by the number of the corresponding line. The names of the topologies as given in Figure 5.1 have to be written in lower case letters. Note that the topology $\overline{\textbf{be}}$ is equivalent to the topology **be** with line **8** shrunken to a point. The topologies **one1** to **one4** are called by `o1` to `o4`, respectively. The topology of the two-loop diagram (their **Fig. 1.**) and that of the one-loop diagram (their **Fig. 2.**) is named `t1` and `l1`, respectively. In the default example, a subtopology `#define SUBTOPO "12"` is stated but not applied in calculations. In addition, topologies named fa, o5, o6, y1, y2, y3, y4, y5, y6, t1, t2 and t3 are declared though not associated with diagrams. We give two more examples, hereafter.

```
Local example1=Q.Q^2/p1.p1/p2.p2/p3.p3/p4.p4/p5.p5/p6.p6/p7.p7
```

```
  /p8.p8;
#define NAME "example1"
#define TOPO "no"

Local example2=Q.Q/p1.p1/p2.p2/p3.p3/p4.p4/p5.p5/p6.p6/p7.p7;
#define NAME "example2"
#define TOPO "o1"
```

The exact result of a calculation is given in terms of rational functions in ϵ, G-scheme constants and the one- and two-loop master integrals (their **Fig. 2.** and **Fig. 1.**, respectively) and two three-loop master integrals, named BasicNOIntegral and BasicT1Integral. G-scheme constants are functions of the Euler Γ function and thus, related recursively whereas GschemeConstants(1,1) is, roughly given as the one-loop master integral. Common factors $4\pi^{-2l}$ are set to 1. The output by default is according to the $\overline{\text{MS}}$-scheme and in the G-scheme, if `#define MSBAR` is not set in *calcdia.frm*. To expand a result in powers in ϵ (`ep`) via the ζ (`z`) function, one may modify the print command in the end in *calcdia.frm*:

```
#call subvalues;
#call expansion(ep);
print;
.end
```

We give the exact and the expanded printout for our examples.

```
example1 = BasicNOIntegral * rat(1,1)
example1 = + ep * ( 50*z6 + 160*z5 + 68*z3^2 ) + 20*z5

example2 = GschemeConstants(0,0) * BasicT1Integral * rat(ep^2,1)
example2 = + ep^-1 * ( 6*z3 ) + ep * ( 102*z5 + 36*z4 + 72*z3 )
  + 9*z4 + 24*z3
```

MATAD is a FORM package written by Matthias Steinhauser [46]. Like MINCER, it is based on the method presented in [26] but approaches the opposite limit, that is the zero external momentum and massive lines. The name is an abbreviation for *MAssive TADpoles*, i.e. it is designed to expand scalar zero-point Feynman integrals with one mass scale in terms of $\epsilon = (4 - D)/2$ up to $\mathcal{O}\left(\epsilon^{3-l}\right)$ with loops $l \leq 3$. Furthermore, a user interface is provided and leg diagrams can be expanded around zero external momentum. For a representation of the master integrals in the output, see [47].

5.3 Cut-and-TARCER technique

We refer to the cut-and-TARCER technique as by cutting a three-loop vacuum bubble diagram once, reducing the residual two-loop integral with TARCER [48] and subsequently integrating the truncated line. TARCER is part of FEYNCALC [49] by R. Mertig and R. Scharf. It is an implementation of the recurrence algorithm by O.V. Tarasov [50] in MATHEMATICA for the reduction of dimensional regularized two-point two-loop Feynman integrals with arbitrary masses and tensorial structure. A

general two-loop integral is given as

$$\frac{1}{\pi^D}\int\frac{d^Dk_1d^Dk_2(\Delta k_1)^a(\Delta k_2)^b\left(k_1^2\right)^u\left(k_2^2\right)^v(pk_1)^r(pk_2)^s(k_1k_2)^t}{[k_1^2-m_1^2]^{\nu_1}[k_2^2-m_2^2]^{\nu_2}[k_3^2-m_3^2]^{\nu_3}[k_4^2-m_4^2]^{\nu_4}[k_5^2-m_5^2]^{\nu_5}}$$
$$\equiv \mathrm{TFI}\left[D,p^2,\Delta p,\{a,b\},\{u,v,r,s,t\},\{\{\nu_1,m_1\},\{\nu_2,m_2\},\{\nu_3,m_3\},\{\nu_4,m_4\},\{\nu_5,m_5\}\}\right]\,, \qquad (5.2)$$

where $k_3=k_1-p$, $k_4=k_2-p$, $k_5=k_1-k_2$ and an external light-like vector Δ. The TACRER package was designed for MATHEMATICA 3.0 but includes some pre-generated binary files *tarcer*.mx*. These files are named according to their rank limit in which all involved operators up to $\{a+b,r+s\}\leq$ \$RankLimit are constructed and the corresponding relations generated. The reduction of a defined integral is done via `TarcerRecurse[%]` which can be expanded in ϵ by means of `TarcerExpand[%,D→4-2ϵ]`. In the following, we illustrate the cut-and-TARCER technique.
We define a class of scalar zero-point three-loop Feynman integrals with one mass parameter m by

$$I_{s_1s_2s_3s_4}=\int\frac{d^Dk_1d^Dk_2d^Dk_3}{[k_1^2+m^2]^{s_1}[k_2^2+m^2]^{s_2}[k_3^2+m^2]^{s_3}[(k_1+k_2+k_3)^2+m^2]^{s_4}}\,. \qquad (5.3)$$

From mass derivatives on the respective right hand sides of (5.3), using the fact that the overall mass dimension of the integral is known and letting the mass derivatives ∂_{m^2} or $[\partial_{m^2}]^2$ explicitly act on the integrand, we get,

$$\begin{aligned}
&8m^2I_{2111}=(8-3D)I_{1111}\,,\\
&2m^2(3I_{2211}+2I_{3111})=(10-3D)I_{2111}\,,\\
&4m^2(I_{2221}+3I_{3211})=(12-3D)I_{2211}\,,\\
&24m^4(I_{2221}+3I_{3211}+I_{4111})=(10-3D)(12-3D)I_{2111}\,.
\end{aligned} \qquad (5.4)$$

Using furthermore the cut-and-TARCER technique on the specific combination

$$\begin{aligned}
&2I_{3111}-I_{2211}\,,\\
&3I_{4111}-3I_{3211}+I_{2221}\,.
\end{aligned} \qquad (5.5)$$

we deduce D-dimensional reduction relations

$$\begin{aligned}
4(4-D)I_{2211}=&\frac{1}{16m^4}(3-D)(8-3D)(10-3D)I_{1111}+I_{2220}\,,\\
8(4-D)I_{3111}=&\frac{1}{16m^4}(7-D)(8-3D)(10-3D)I_{1111}-3I_{2220}\,,\\
64(4-D)I_{4111}=&\frac{1}{16m^6}(10-3D)(8-3D)(58-17D+D^2)I_{1111}-\frac{1}{m^2}(34-7D)I_{2220}\,,\\
64(4-D)I_{3211}=&\frac{3}{16m^6}(6-D)(3-D)(10-3D)(8-3D)I_{1111}-\frac{1}{m^2}(14-5D)I_{2220}\,,\\
32(4-D)I_{2221}=&\frac{3}{16m^6}(3-D)(2-D)(10-3D)(8-3D)I_{1111}+\frac{1}{m^2}(38-11D)I_{2220}\,.
\end{aligned} \qquad (5.6)$$

Expanding both sides via MATAD we have confirmed the above relations up to $\mathcal{O}(\epsilon=(4-D)/2)$. Note, that $I_{2220}=J_2J_2J_2$ are products of one-loop tadpoles. The corresponding one-loop integral is

$$J_s\equiv\int\frac{d^Dp}{[p^2+m^2]^2}=\frac{\pi^{\frac{D}{2}}\Gamma(s-\frac{D}{2})}{|m|^{2s-D}\Gamma(s)}\,,\quad 2sm^2J_{s+1}=(2s-D)J_s\,. \qquad (5.7)$$

Thus, we have reduced some three-loop vacuum bubble diagrams by applying methods for massive two-loop propagators.

5.4 Reduze 2

We will conclude this chapter about automated reductions of Feynman integrals by presenting version 2 of Reduze, which is basically used for the computations in this thesis, see Chapter 6. Reduze is an implementation of the Laporta-algorithm in `C++`, enhanced by graph and matroid based algorithms for the identification of equivalent topologies and integrals, written by A. von Manteuffel and C. Studerus [30]. It is designed for a distributed reduction of dimensional regularized scalar Feynman diagrams with an arbitrary number of loops and legs to master integrals.
To build Reduze, the computer system GiNaC [51] or Fermat has to be provided. Both perform algebraic manipulations, whereas Fermat is more effective in polynomial greatest common divisor (GCD) computations than GiNaC, see [30]. In addition, Open MPI [52] may be linked for distributed computations. With Berkeley DB [53], the equations to be reduced are stored in a database on disc so that information which are too large for the main memory are handled and information of an aborted run are restored.
To run Reduze, some configuration files and a job file with YAML [54] syntax have to be provided. The configuration files define the integral families and kinematics, for example, the *kinematics.yaml* that we used for the computations in this thesis is:

```
kinematics :
  incoming_momenta: [kq]
  outgoing_momenta: [q]
  momentum_conservation: [kq, q]
  kinematic_invariants:
    - [xi, 2]
  scalarproduct_rules:
    - [[q,q], 1]
```

Integral families should be ordered according to their number of permutation symmetry generators to improve up on the performance. Furthermore, a *global.yaml* file configures paths e.g., the Fermat path. The job file lists all jobs, e.g. setting up sector mappings, selecting reductions, reducing identities and exporting them to e.g., Form [60] format. In addition, we can Wick rotate to Euclidean space, that is multiplying Feynman diagrams with -1 for each propagator, by setting the flag `toggle_metric_convention:true`. The metric in Minkowski space is $\mathrm{diag}(1,-1,-1,-1)$. The job `setup_sector_mappings` should be executed first to improve the performance. The jobs `select_reductions` and `reduce_files` reduce integrals listed in an input file. In the following, we introduce parameters which some of the jobs depend on.
Integrals are indexed by integral families and sectors therein. An l-loop integral family is an ordered set of n propagators which is minimal and complete, in the sense, that any scalar product of two loop momenta or one loop and one leg momentum can be uniquely expressed as a linear combination of inverse propagators and kinematic invariants. A selection of t propagators $\{D_{j_1},...,D_{j_t}\} \subseteq \{D_1,...,D_n\}$ of an integral family determines a sector of this family. Its identification number is defined as $\mathrm{ID} = \sum_{k=1}^{t} 2^{j_k-1}$. Integrals in a sector have the generic form

$$I = \int d^D k_1 ... d^D k_l D_{j_1}^{-r_1} ... D_{j_t}^{-r_t} D_{j_{t+1}}^{s_1} ... D_{j_n}^{s_{n-t}}, \tag{5.8}$$

and we define $r = \sum_{i=1}^{t} r_i \geq t$ and $s = \sum_{i=1}^{n-t} s_i \geq 0$. The integral with $r = t$ and $s = 0$ is called the corner integral of this sector.
We may set some options to control the computation. With the `t_restriction` option we may restrict the range of the parameter t. The number of jobs which run in parallel is limited via

`max_parallel_jobs`. To resume aborted runs the flag `conditional:true` may be set for jobs. Furthermore, the results of terminated runs may be called in via `alternative_input_directory`. Thus, we may first compute reductions for some parameters and in a second run extend the parameters. We choose to use REDUZE for our computations over others e.g., FIRE, as it allows parallel computations and handles effectively a large number of integrals. Indeed, the time taken by it for a sequential reduction of integrals is high compared with FIRE 3.5 and TARCER 1.97. As a benchmark we perform the reduction of massive two-point two-loop on-shell Feynman diagrams

$$I(s_1,s_2,s_3,s_4,s_5) = \int d^Dk_1 d^Dk_2 \frac{1}{[k_1^2-m^2]^{s_1}} \frac{1}{[k_2^2-m^2]^{s_2}} \frac{1}{[(k_1-p)^2-m^2]^{s_3}} \frac{1}{[(k_1-p)^2-m^2]^{s_4}} \times \frac{1}{[(k_1-k_2)^2-m^2]^{s_5}}\Bigg|_{p^2=m^2}. \tag{5.9}$$

on a 32 Bit computer system with 1000,1 MiB main memory and Intel Core Duo CPU T2350 @ 1,86GHz × 2 with MATHEMATICA 8.0. In particular, we choose the integrals $I(1,1,1,1,10)$ and $I(2,3,3,3,3)$ to be reduced. We make use of all symmetries, kinematics and IBP identities wherever possible. For REDUZE we set the range of IBP identities up to $r = 14$. The times measured in seconds are for

$$\begin{aligned} I(1,1,1,1,10): &\quad \text{REDUZE}: 1884\,, \\ &\quad \text{FIRE}: 200\,, \\ &\quad \text{TARCER}: 9\,. \end{aligned} \tag{5.10}$$

$$\begin{aligned} I(2,3,3,3,3): &\quad \text{REDUZE}: 1907\,, \\ &\quad \text{FIRE}: 124\,, \\ &\quad \text{TARCER}: 12\,. \end{aligned} \tag{5.11}$$

Chapter 6

Computation of the three-loop gap equation

In this chapter we apply the resummed non-linear SU(N) Higgs model outlined in Chapter 3, to a calculation of the gluon self-energy. The bare on-shell transverse and longitudinal self-energies Π_T and Π_L are defined as

$$\Pi^{ab}_{\mu\nu}(p) \equiv \delta^{ab}\left[\left(\delta_{\mu\nu} - \frac{p_\mu p_\nu}{p^2}\right)\Pi_T\left(p^2\right) + \frac{p_\mu p_\nu}{p^2}\Pi_L\left(p^2\right)\right]. \tag{6.1}$$

One may think of a gauge invariant pole of the transverse part of the full gauge field propagator in analog to the pole mass of a quark, which is gauge independent to all orders in perturbation theory [56]. The longitudinal part with a gauge dependent pole represents the unphysical Goldstone-like bosons, common in Higgs-like theories. These components may be set to zero in the unitary gauge. In a resummed perturbation theory, the pole of the transverse part of the bare gauge field propagator gets shifted, from $p^2 = 0$ in the original theory, to $p^2 = -m^2$, where we identify m to be the pole of the full propagator

$$D_T = \frac{1}{p^2 + m^2 - \Pi_T\left(p^2\right)} \overset{p^2=-m^2+\delta p^2}{=} \frac{\frac{1}{1-\partial_{p^2}\Pi_T(p^2)\big|_{p^2=-m^2}}}{-\frac{\Pi_T(-m^2)}{1-\partial_{p^2}\Pi_T(p^2)\big|_{p^2=-m^2}} + \delta p^2 + \mathcal{O}\left(\left(\delta p^2\right)^2\right)} \tag{6.2}$$

and have expanded the self-energy near the pole. Thus, we are left with a massive propagator with the residue $Z\left(m^2\right)$

$$D_T \propto \frac{Z\left(m^2\right)}{p^2 + m^2}, \quad Z\left(m^2\right) = \frac{1}{1 - \partial_{p^2}\Pi_T(p^2)\big|_{p^2=-m^2}}, \tag{6.3}$$

if the self-consistent gap equation

$$0 \overset{!}{=} \frac{\Pi_T(-m^2)}{1 - \partial_{p^2}\Pi_T(p^2)\big|_{p^2=-m^2}} \tag{6.4}$$

is valid. In the resummed prescription $m^2 \to m^2 - lm^2$ and $g^2 \to lg^2$ and hence, the gap equation is

$$0 = \left.\frac{\Pi_T(p^2, m^2 - lm^2, g^2 l) + lm^2}{1 - \partial_{p^2}\Pi_T(p^2, m^2, g^2 l)}\right|_{p^2=-m^2}. \tag{6.5}$$

We obtain the L-loop gap equation by truncating the equation after l^L and setting $l = 1$. We can generate the resummation mass-shift by a translation operator and subtract the on-shell condition $0 = p^2 + m^2$ in the numerator, so that the L-loop gap equation reads

$$0 = \left(e^{p^2 l \partial_{m^2}} \frac{\Pi_T(p^2, m^2, g^2 l) - p^2 - m^2}{1 - \partial p^2 \Pi_T(p^2, m^2, g^2 l)} + \mathcal{O}\left(l^{L+1}\right) \right)_{p^2 = -m^2,\, l=1} . \tag{6.6}$$

Introducing the n-loop self-energies $\Pi_T^{(n)}$ as

$$\Pi_T\left(p^2, m^2, g^2 l\right) \equiv \sum_{n \geq 1} \left(g^2 l\right)^n \Pi_T^{(n)}\left(p^2, m^2\right) \tag{6.7}$$

and the short form $\Pi_{ab}^{(n)} \equiv \partial_{p^2}^a \partial_{m^2}^b \Pi^{(n)}\left(p^2, m^2\right)\big|_{p^2=-m^2}$ the three-loop gap equation is

$$\begin{aligned}
0 =& m^2 + g^2 \left(\Pi_{00}^{(1)} - m^2 \Pi_{01}^{(1)} + \frac{1}{2} m^4 \Pi_{02}^{(1)} + m^2 \Pi_{10}^{(1)} - m^4 \Pi_{11}^{(1)} \right) \\
&+ g^4 \left(\Pi_{00}^{(1)} \Pi_{10}^{(1)} - m^2 \Pi_{00}^{(1)} \Pi_{11}^{(1)} - m^2 \Pi_{01}^{(1)} \Pi_{10}^{(1)} + m^2 \left(\Pi_{10}^{(1)}\right)^2 + \Pi_{00}^{(2)} - m^2 \Pi_{01}^{(2)} + m^2 \Pi_{10}^{(2)} \right) \\
&+ g^6 \left(\Pi_{00}^{(1)} \Pi_{10}^{(1)} + \Pi_{00}^{(1)} \Pi_{10}^{(2)} + \Pi_{10}^{(1)} \Pi_{00}^{(2)} + \Pi_{00}^{(3)} \right) \\
=& m^2 + g^2 \left(\frac{4-D}{2} \Pi_{00}^{(1)} - \frac{(4-D)m^2}{2} \Pi_{01}^{(1)} - \frac{m^4}{2} \Pi_{02}^{(1)} \right) \\
&+ g^4 \left(\frac{(4-D)(2-D)}{4m^2} \left(\Pi_{00}^{(1)}\right)^2 - m^2 \Pi_{00}^{(1)} \Pi_{02}^{(1)} + (4-D) \Pi_{00}^{(2)} \right) \\
&+ g^6 \left(\frac{(2-D)^2}{4m^4} \left(\Pi_{00}^{(1)}\right)^3 + \frac{2-D}{m^2} \left(\Pi_{00}^{(1)}\right)^2 \Pi_{01}^{(1)} + \Pi_{00}^{(1)} \left(\Pi_{01}^{(1)}\right)^2 \right. \\
&\qquad \left. + \frac{8-3D}{2m^2} \Pi_{00}^{(1)} \Pi_{00}^{(2)} + \Pi_{00}^{(1)} \Pi_{01}^{(2)} + \Pi_{01}^{(1)} \Pi_{00}^{(2)} + \Pi_{00}^{(3)} \right) ,
\end{aligned} \tag{6.8}$$

where we have rewritten the equation via

$$\left(p^2 \partial_{p^2} + m^2 \partial_{m^2} + \frac{4-D}{2} \right) \Pi_T\left(p^2, m^2 m, g^2\right) = 1 \cdot \Pi_T\left(p^2, m^2, g^2\right) \tag{6.9}$$

by means of dimensional analysis which yields $\Pi_T \sim \text{mass}^2$ and $g^2 \sim \text{mass}^{4-D}$. For the ease of computation, we rewrite the three-loop gap equation in terms of a dimensionless function $\hat{\Pi}$ with

$$\partial_{p^2}^a \partial_{p^2}^b \Pi_T\left(p^2\right) \Big|_{p^2=-m^2} \equiv \left(m^2\right)^{1-a-b} \sum_{n \geq 1} [\dim]^n \hat{\Pi}_{ab}^{(n)} \tag{6.10}$$

as

$$\begin{aligned}
0 =& \left[1 + [\dim] \frac{1}{2} \left((4-D) \hat{\Pi}_{00}^{(1)} - (4-D) \hat{\Pi}_{01}^{(1)} - \hat{\Pi}_{02}^{(1)} \right) \right. \\
&+ [\dim]^2 \left(\frac{(4-D)(2-D)}{4} \left(\hat{\Pi}_{00}^{(1)}\right)^2 - \hat{\Pi}_{00}^{(1)} \hat{\Pi}_{02}^{(1)} + (4-D) \hat{\Pi}_{00}^{(2)} \right) \\
&+ [\dim]^3 \left(\frac{(2-D)^2}{4} \left(\hat{\Pi}_{00}^{(1)}\right)^3 + (2-D) \left(\hat{\Pi}_{00}^{(1)}\right)^2 \hat{\Pi}_{01}^{(1)} + \hat{\Pi}_{00}^{(1)} \left(\hat{\Pi}_{01}^{(1)}\right)^2 \right. \\
&\qquad \left. \left. + \frac{8-3D}{2} \hat{\Pi}_{00}^{(1)} \hat{\Pi}_{00}^{(2)} + \hat{\Pi}_{00}^{(1)} \hat{\Pi}_{01}^{(2)} + \hat{\Pi}_{01}^{(1)} \hat{\Pi}_{00}^{(2)} + \hat{\Pi}_{00}^{(3)} \right) \right] m^2
\end{aligned} \tag{6.11}$$

where, in the $\overline{\text{MS}}$ scale $\overline{\mu}^2 = 4\pi e^{-\gamma_E}\mu^2$,

$$[\text{dim}] \equiv \frac{g^2 N J(D,m)}{m^2(1-D)} \overset{D=3-2\epsilon}{=} \frac{g^2\mu^{-2\epsilon}N}{8\pi m}\left(\frac{\overline{\mu}}{2m}\right)^{2\epsilon} \frac{4^\epsilon e^{\epsilon\gamma_E}\Gamma\left(\frac{1}{2}+\epsilon\right)}{(1+\epsilon)(1-2\epsilon)\Gamma\left(\frac{1}{2}\right)}$$

$$\overset{D=3-2\epsilon}{=} \frac{g^2\mu^{-2\epsilon}N}{8\pi m}\left(\frac{\overline{\mu}}{2m}\right)^{2\epsilon}\left(1-3\epsilon+\mathcal{O}\left(\epsilon^2\right)\right) \tag{6.12}$$

with the massive one-loop tadpole integral

$$J(D,m) = \int \frac{d^Dk}{(2\pi)^D}\frac{1}{k^2+m^2} = \frac{1}{m^2}\left(\frac{m^2}{4\pi}\right)^{\frac{D}{2}}\Gamma\left(1-\frac{D}{2}\right). \tag{6.13}$$

The functions $\hat{\Pi}^{(n)} = \hat{\Pi}^{(n)}(D,\xi,N)$ are calculated from n-loop Feynman diagrams. We are interested in computing $\hat{\Pi}^{(1)}_{00}$, $\hat{\Pi}^{(1)}_{01}$, $\hat{\Pi}^{(1)}_{02}$, $\hat{\Pi}^{(2)}_{00}$, $\hat{\Pi}^{(2)}_{01}$ and $\hat{\Pi}^{(3)}_{00}$ in dimensional regularization as for the three-loop gap equation.

6.1 Method

The method for the computation involves the following points.

- We automatically create a model file and Feynman rules directly from the Lagrangian (3.7). In case of three-loop self-energies we take into account vertices with up to seven legs.
- The self-energy diagrams are generated with QGRAF.[1] They are printed in Appendix A.
- We shift momenta to our conventions.
- Apply color and Lorentz projection, insert Feynman rules, perform color traces via Fierz-identity, rewrite scalar products as inverse propagators, take derivatives for $\hat{\Pi}_{ab}$ on the integrand level and set the external momentum on-shell. The crossed-ladder diagrams number 554 to 574 vanish after performing the color sum.
- We project onto the transverse part, identify symmetries and zero sectors, shift to master sectors and get an intermediate result in terms of the generic dimensionless three-loop integrals

$$\begin{aligned}\hat{I}(m_1,...,m_9;s_1,...,s_9) =& \frac{1}{J(D,1)}\int \frac{d^Dk_1}{(2\pi)^D}\frac{d^Dk_2}{(2\pi)^D}\frac{d^Dk_3}{(2\pi)^D}\frac{1}{[k_1^2+m_1]^{s_1}}\frac{1}{[k_2^2+m_2]^{s_2}}\\ &\times\frac{1}{[k_3^2+m_3]^{s_3}}\frac{1}{[(k_1-p)^2+m_4]^{s_4}}\frac{1}{[(k_2-p)^2+m_5]^{s_5}}\\ &\times\frac{1}{[(k_1-k_3)^2+m_6]^{s_6}}\frac{1}{[(k_2-k_3)^2+m_7]^{s_7}}\frac{1}{[(k_3-p)^2+m_8]^{s_8}}\\ &\times\frac{1}{[(k_1-k_2)^2+m_9]^{s_9}}\Bigg|_{p^2=-1}.\end{aligned} \tag{6.14}$$

[1] To handle vertices with seven legs set `parameter ( maxdeg=7 )` everywhere in the QGRAF source file.

The generic physical topologies are

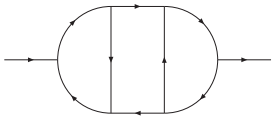

$$\equiv \hat{I}(m_1, ..., m_9; s_1, ..., s_8, s_9 = 0)\,, \tag{6.15}$$

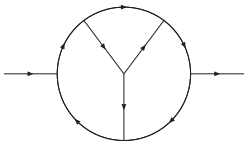

$$\equiv \hat{I}(m_1, ..., m_9; s_1, ..., s_7, s_8 = 0, s_9)\,, \tag{6.16}$$

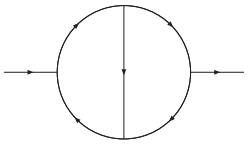

$$\equiv \hat{I}_{\rm 2loop}\,, \tag{6.17}$$

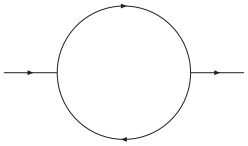

$$\equiv \hat{I}_{\rm 1loop}\,. \tag{6.18}$$

where the one- and two-loop topologies follow from the three-loop topology in various ways by contracting appropriate lines.

- After that we reduce the set of integrals to a set of master integrals via Reduze 2. We automatically create a job file and the input files containing the integral families and the integrals. As the three-loop computation is quite involved, we divide it. For the first reduction we set $s = 3$, in a second one $s = 5$ and the third reduction is subdivided via `t_restriction`.

We provide the results for $\hat{\Pi}^{(2)}_{01}$ and $\hat{\Pi}^{(3)}_{00}$ in [55]. That of $\hat{\Pi}^{(1)}_{00}$, $\hat{\Pi}^{(1)}_{01}$, $\hat{\Pi}^{(1)}_{11}$ and $\hat{\Pi}^{(2)}_{00}$ are given in [2]. The results for $\hat{\Pi}^{(1)}_{12}$ and $\hat{\Pi}^{(1)}_{03}$, which are present in the four-loop gap equation, are printed in Appendix B.

6.2 Checks

Making use of the relations [50]

$$\begin{aligned}
\hat{I}(1,1,\xi,\xi) &= \frac{1}{-3+D}\left(\hat{I}(2,0,\xi,0) - (-1+4\xi)\hat{I}(2,1,\xi,\xi)\right)\,,\\
\hat{I}(1,1,1,\xi) &= \frac{1}{-3+D}\left(2\hat{I}(2,0,\xi,0) - \hat{I}(2,0,1,0) + (-4+\xi)\hat{I}(2,1,1,\xi)\right)\,,\\
\hat{I}(a+1,0,m,0) &= \frac{1-\frac{D}{2}}{am}\hat{I}(a,0,1,0)\,,
\end{aligned} \tag{6.19}$$

we checked that the coefficients in $\hat{\Pi}^{(1)}_{12}$ and $\hat{\Pi}^{(1)}_{03}$ are not singular in ξ. We confirmed the results of the one- and two-loop computations in [2]. Additionally, we verified the dimensional relation (6.9) for $n = 1$, i.e.

$$\hat{\Pi}^{(1)}_{1,b-1} = \hat{\Pi}^{(1)}_{0,b} + \frac{2b-D}{2}\frac{\hat{\Pi}^{(1)}_{0,b-1}}{m^2} \tag{6.20}$$

up to $b = 3$. We confirmed that $\hat{\Pi}^{(1)}_{00}$ and also the combinations $\hat{\Pi}^{(1)}_{10} - \hat{\Pi}^{(1)}_{01} = -\frac{D-2}{2}\hat{\Pi}^{(1)}_{00}$ from (6.20), $\hat{\Pi}^{(2)}_{00} + \hat{\Pi}^{(1)}_{00}\hat{\Pi}^{(1)}_{10}$ and $\hat{\Pi}^{(2)}_{00} + \hat{\Pi}^{(1)}_{00}\hat{\Pi}^{(1)}_{01}$ are gauge independent. Thus, the one- and two-loop gap equations

are gauge invariant. However, we have not found any gauge invariant combinations including $\hat{\Pi}^{(3)}$. This is manifest in the three-loop gap equation.

6.2.1 Gauge variance of the three-loop gap equation

The three-loop gap equation is gauge invariant if, and only if, (6.14) is gauge invariant in each order in g^2. Investigating the g^2 part of (6.14), i.e.

$$(4-D)\hat{\Pi}^{(1)}_{00} - (4-D)\hat{\Pi}^{(1)}_{01} - \hat{\Pi}^{(1)}_{02} \tag{6.21}$$

we identify a non-vanishing ξ-dependent master integral K_1'' in $\hat{\Pi}^{(1)}_{02}$, though not in $\hat{\Pi}^{(1)}_{00}$ and $\hat{\Pi}^{(1)}_{01}$, see [2]. Hence, the g^2 part of the three-loop gap equation is not gauge invariant.
In addition, we could try to write down a generic gauge invariant combination of $\hat{\Pi}^{(1)}_{02}$ and $\hat{\Pi}^{(1)}_{03}$, as both are linear combinations of the same master integrals, such as

$$(aD+b)\hat{\Pi}^{(1)}_{02} + \hat{\Pi}^{(1)}_{03} \tag{6.22}$$

with ξ-independent constants a and b. This is motivated by the g^2 part of the four-loop gap equation

$$0 = m^2\left[1 + g^2\frac{1}{2}\left((4-D)\left(\hat{\Pi}^{(1)}_{00} - \hat{\Pi}^{(1)}_{01}\right) + \frac{4-D}{2}\hat{\Pi}^{(1)}_{02} + \frac{2}{3}\hat{\Pi}^{(1)}_{03}\right) + \mathcal{O}\left(g^4\right)\right]. \tag{6.23}$$

However, they are linearly independent in the sense that (6.22) is gauge variant for any a and b.
The potentiality to express the gap equation in terms of massive derivatives and the inevitable appearance of ξ-dependent master integrals in $\hat{\Pi}^{(1)}_{02}$ and $\hat{\Pi}^{(1)}_{03}$ in the g^2 part of the three- and four-loop gap equations implies, that the full gap equation is gauge variant. Thus, a question comes up.

6.3 What to do next?

We have checked that the resummed non-linear SU(N) Higgs model is BRS invariant, see section 3.3. Moreover, the pole mass of the quark is gauge independent to all orders in perturbation theory [56]. Thus, one may guess, that the pole of the transverse part of the full gauge field propagator (6.2) is gauge invariant order by order in perturbation theory and represents a physical mass. However, here we are left with a gauge variant gap equation at three-loop and beyond. This should be resolved before one proceeds with the computation of the three-loop gap equation, that is calculating the emerging master integrals, renormalizing the theory and solving the gap equation with respect to the mass. Moreover, the mass is of interest as for the convergence property, since no additional parameter to tune exists, since the gauge coupling drops out of the effective expansion parameter.
A possible next step is to compute the three-loop thermodynamic pressure via bubble diagrams to check the gauge dependence. If it is gauge invariant then the mass considered here is not the proper gauge invariant quantity, else the theory considered here ought to be modified. Before we will outline the calculation of master integrals in the next section, we conclude this one by collecting some remarks on the computation and the results of $\hat{\Pi}^{(2)}_{01}$ and $\hat{\Pi}^{(3)}_{00}$.
The result of $\hat{\Pi}^{(2)}_{01}$ is a sum of 30 master integrals, where each of them is multiplied with a ratio of polynomials in D and ξ. 13 of the master integrals decouple in a product of two one-loop master integrals and 2 of them have negative parameters, i.e. some momenta in the numerator. They may be transformed by specifying a file with `preferred_integrals`. One may check the number of master integrals by a method proposed by R.N. Lee and A.A. Pomeransky recently [57]. The computation of $\hat{\Pi}^{(3)}_{00}$ is quite involved due to GCD errors as a consequence of hardware limitations. Thus, we set restrictions to control the computation, that is we limit the number of parallel jobs, the number of

parallel processes and/or write the equations in a database on disc, whenever required. The result will be made available when the computation is done. One may check that no master integrals are related by a symmetry. This may happen due to an incomplete specification of the symmetries in the setup and also within the computation by REDUZE though the relevant symmetries are initially set. A possible next step is to optimize the reduction by REDUZE e.g., via a sensible tuning of the parameters `t` and `s`, as they dominate the computation time. Actually, the computation is most complex for sectors with parameters around some $\mathtt{t} = (\mathtt{t}_{\max} - \mathtt{t}_{\min})/2$ where `s` is maximal. Anyway, one should mind that the reduction is complete, as the reduction of integrals associated with some `t` and `s` may involve sectors with higher parameters.

Chapter 7

Calculations of the sunset-type master integrals

In section 4.3 we have discussed how to solve master integrals numerically with high precision by means of solving appropriate difference equations. There, we have encountered the Euclidean zero-point sunset-integrals with one mass parameter

$$S(l,D,x) = \left[\int \frac{d^Dp}{p^2+1}\right]^{-l} \int \frac{d^Dk_1}{k_1^2+1} ... \int \frac{d^Dk_l}{k_l^2+1} \frac{1}{[(k_1+...+k_l)^2+1]^x} \,. \tag{7.1}$$

Recall, that l labels the number of loops and D the dimension. The master integrals are obtained for $x = 1$. The one-loop sunset-integral is

$$S(1,D,x) = \frac{\Gamma\left(x+1-\frac{D}{2}\right)}{\Gamma(x+1)\Gamma\left(2-\frac{D}{2}\right)} \,. \tag{7.2}$$

For higher loops, the divergent parts are calculated for $D = 4-2\epsilon$ as [58] (with normalization $1/\epsilon$ for each loop in their equation (51))

$$S(2,4-2\epsilon,1) = -\frac{3}{2}\left[1+3\epsilon+\mathcal{O}\left(\epsilon^2\right)\right] \,, \tag{7.3}$$

$$S(3,4-2\epsilon,1) = +\frac{4}{2}\left[1+\frac{23}{2\cdot 3}\epsilon+\frac{5\cdot 7}{2^2}\epsilon^2+\mathcal{O}\left(\epsilon^3\right)\right] \,, \tag{7.4}$$

$$S(4,4-2\epsilon,1) = -\frac{5}{2}\left[1+\frac{2\cdot 7}{3}\epsilon+\frac{11\cdot 83}{2^3 3^2}\epsilon^2+\frac{7\cdot 1667}{2^4 3^3}\epsilon^3+\mathcal{O}\left(\epsilon^4\right)\right] \,, \tag{7.5}$$

$$S(5,4-2\epsilon,1) = +\frac{6}{2}\left[1+\frac{11}{2}\epsilon+\frac{29\cdot 43}{2^3 3^2}\epsilon^2+\frac{37\cdot 67\cdot 73}{2^5 3^3 5}\epsilon^3+\frac{197\cdot 4561}{2^7 3^4}\epsilon^4+\mathcal{O}\left(\epsilon^5\right)\right] \,. \tag{7.6}$$

Additionally, $S(5,4-2\epsilon,1)$ has been calculated with four more orders in ϵ as (their equation (85))

$$\begin{aligned} S(5,4-2\epsilon,1) =& 3+16.5\epsilon+51.95833\epsilon^2+125.6715\epsilon^3+259.9876\epsilon^4+347.3551\epsilon^5-2453.494\epsilon^6 \\ & -31545.55\epsilon^7-311303.1\epsilon^8+\mathcal{O}\left(\epsilon^9\right) \,. \end{aligned} \tag{7.7}$$

We would like to demonstrate the use of difference equations and factorial series by calculating sunset-integrals up to five loop in dimensional regularization around four and three dimensions in higher orders and with a high accuracy.[1]

[1] In one dimension the master integral is $S(l,1,1) = 2^l/(l+1)$, analytically.

7.1 Difference equations and recurrence relations

The difference equations for the sunset-integrals $S(l, D, x)$ are

$$\sum_{j=0}^{r_l} p_{l,j}(D,x)\frac{\Gamma(x+j)}{\Gamma(x+1)}\, S(l,D,x+j) = c_l\Gamma(l+1)\, S(1,D,x)\,. \tag{7.8}$$

Here, the polynomials $p_{l,j}$ and constants c_l read [59]

$$\begin{aligned}
l=1\ (r_1=1):\quad & p_{10} = x(-2+D-2x)\,,\\
& p_{11} = 2(x+1)\,,\\
& c_1 = 0\,. \qquad (7.9)\\
l=2\ (r_2=2):\quad & p_{20} = x(-2+D-x)\,,\\
& p_{21} = -3+D-2x\,,\\
& p_{22} = 3\,,\\
& c_2 = -1\,. \qquad (7.10)\\
l=3\ (r_3=2):\quad & p_{30} = x(-6+3D-2x)(-2+D-x)\,,\\
& p_{31} = 2\left(24-17D+3D^2+27x-10Dx+7x^2\right)\,,\\
& p_{32} = 16(-3+D-x)\,,\\
& c_3 = 2\,. \qquad (7.11)\\
l=4\ (r_4=4):\quad & p_{40} = x(4-2D+x)(2-D+x)(6-3D+2x)\,,\\
& p_{41} = 360-399D+147D^2-18D^3+526x-405Dx+78D^2x+234x^2-93Dx^2\\
& \qquad +32x^3\,,\\
& p_{42} = -144+129D-27D^2-2x+21Dx+20x^2\,,\\
& p_{43} = 9(-42+9D-16x)\,,\quad p_{44} = 90\,,\\
& c_4 = 2\,.\\
l=5\ (r_5=4):\quad & p_{50} = x(-6+3D-2x)(-10+5D-2x)(-2+D-x)(-4+2D-x)\,,\\
& p_{51} = 2\left(24-17D+3D^2+24x-10Dx+4x^2\right)\\
& \qquad \times\left(120-98D+20D^2+87x-36Dx+15x^2\right)\,,\\
& p_{52} = -4\left(-1248+932D-196D^2+8D^3-2130x+1180Dx-148D^2x-975x^2\right.\\
& \qquad \left.+294Dx^2-129x^3\right)\,,\\
& p_{53} = -128\left(150-83D+11D^2+85x-26Dx+11x^2\right)\,,\\
& p_{54} = -768(-6+2D-x)\,,\\
& c_5 = 4\,. \qquad (7.12)
\end{aligned}$$

To solve these difference equations we implement the approach via the $\boldsymbol{\pi}$ and $\boldsymbol{\rho}$ operators in the computer algebra system FORM 4.0 [60] as discussed in section 4.3. For the solutions of the characteristic

equation (4.25) μ_l and the indicial equation (4.29) K_l we deduce

$$l=1: \quad \mu^{(1)} \in \{1\}\,, \quad K^{(1)} \in \left\{-\frac{D}{2}\right\}\,. \tag{7.13}$$

$$l=2: \quad \mu^{(2)} \in \left\{-\frac{1}{3},1\right\}\,, \quad K^{(2)} \in \left\{-\frac{D}{2}+\frac{1}{2}\right\}\,. \tag{7.14}$$

$$l=3: \quad \mu^{(3)} \in \left\{-\frac{1}{8},1\right\}\,, \quad K^{(3)} \in \left\{-\frac{D}{2}\right\}\,. \tag{7.15}$$

$$l=4: \quad \mu^{(4)} \in \left\{-\frac{1}{15},-\frac{1}{3},1\right\}\,, \quad K^{(4)} \in \left\{-\frac{D}{2},-\frac{D}{2}+1\right\}\,. \tag{7.16}$$

$$l=5: \quad \mu^{(5)} \in \left\{-\frac{1}{24},-\frac{1}{8},1\right\}\,, \quad K^{(5)} \in \left\{-\frac{D}{2}-1,-\frac{D}{2}\right\}\,. \tag{7.17}$$

where $\mu^{(4)}=1$ and $\mu^{(5)}=1$ are roots of multiplicity two.
In section 4.3.1 we have determined the first two five-loop coefficients

$$\begin{aligned} a_0^{(5)} =& \frac{S(4,D,1)}{\Gamma\left(2-\frac{D}{2}\right)}\,, \\ a_1^{(5)} =& \frac{1}{\Gamma\left(2-\frac{D}{2}\right)}\left(\frac{D(2+D)}{4}S(4,D,1)+\frac{4-D}{2}S(4,D,2)-2S(4,D,3)\right)\,. \end{aligned} \tag{7.18}$$

The same analysis holds for the first two-, three-, and four-loop coefficient

$$a_0^{(l)} = \frac{S(l-1,D,1)}{\Gamma\left(2-\frac{D}{2}\right)} \quad l>1\,. \tag{7.19}$$

where $S(0,D,1)=1$. All further coefficients are determined by these initial ones and the recurrence relations.
We can now set the homogeneous solution to zero and solve the inhomogeneous difference equation with these coefficients. Note, that no pair $K^{(l)},\ \mu^{(l)}$ excluding $\left(\mu^{(5)}=1,\ K^{(5)}=-D/2-1\right)$ satisfies the condition (4.43) for a non-zero homogeneous solution. Here, the inhomogeneity yields $K=-D/2$ and $\mu=1$ in each order. The recurrence relations for these values are printed in Appendix C.
The abscissa of convergence is finite concerning the condition (4.46) and the factorial series diverges for $x \in \{-D/2-n, n\in\mathbb{N}\}$, which is not relevant here. As a way of illustration, let us explicitly derive the abscissa of convergence for the one-loop sunset-integral. The recurrence relation (C.1) can be rewritten as

$$a_s^{(1)} = \frac{\left[\left(s+\frac{D}{2}-1\right)!\right]^2}{s!}a_0^{(1)}\,. \tag{7.20}$$

Recalling the Stirling's approximation for large factorials

$$\Gamma(z) = \sqrt{\frac{2\pi}{z}}\left(\frac{z}{e}\right)^2\left(1+\mathcal{O}\left(\frac{1}{z}\right)\right)\,, \tag{7.21}$$

the large-s behavior of the terms in the factorial series (4.14) is

$$\frac{a_s^{(1)}}{\Gamma\left(x+\frac{D}{2}+s+1\right)} \sim s^{\frac{D}{2}-2-x} \qquad s\gg 1\,. \tag{7.22}$$

Thus, the abscissa of convergence is $\lambda = D/2+1 \sim \mathcal{O}(1)$.
Singularities in ϵ emerge in terms of the roots of the polynomials $p_{l,0}(D,x)$ of the difference equations.

This reduces the number of orders in ϵ when iterating to $x = 1$. Here, we find that $p_{n,0}(4, 2 \leq x \leq n) = 0$ and $p_{n,0}(3, 1 \leq x \leq n/2) = 0$. Recall, that each iteration in x increases the error of the master function by $\max_j \left|1/\mu_j^{(l)}\right|$.

7.2 Higher order and high precision calculations

We now compute the expansion of the factorial series (4.14) in MATHEMATICA 9.0 [61]. To appreciably accelerate the calculation time, we implement our own algorithm for the solution of the recurrence relations given in Appendix C. Additionally, we evaluate Γ-functions by hand whenever possible. Furthermore, we renormalize the coefficients $a_s \to a_s/\Gamma(x+1-K+s)$ which comes along with several improvements: Firstly, we can cancel some Γ-functions by hand before the calculation. Secondly, we readily notice the convergence of the coefficients, that is we do not have to calculate some large numerator and denominator separately and subsequently cancel them. Lastly, the master functions are summed up as $U(x) = \Gamma(x+1)\sum_s a_s$.
We estimate the accuracy of our numerical results by comparing them with the known analytical ones (7.6) and the numerical results in four dimension [62] and in three dimensions [63] for which the divergences read

$$\begin{aligned} S(2, 3-2\epsilon, 1) &= +\frac{1}{\epsilon}\,, \\ S(3, 3-2\epsilon, 1) &= -\frac{8}{\epsilon}\,, \\ S(4, 3-2\epsilon, 1) &= +\frac{45}{\epsilon}\,. \end{aligned} \tag{7.23}$$

We print the parameters used in our calculations and the numerical results around four and three dimensions in Appendices (D) and (E), respectively. For each result we present the first fifty correct digits. In principle, we may easily compute higher orders and with higher precision.
In conclusion, let us point out some empirical aspects we have encountered in our computation. As we vary $x_{\max}$ and keep $s_{\max}$ fixed, we notice that there exists a long range of values for $x_{\max}$ for which the number of correct digits is maximal and almost stable. We keep 5000 digits in each step of our calculation. However, we find that the number of correct digits can not be permanently increased by increasing the number of the correct digits of the inhomogeneity, e.g. we get about 200 correct digits in (D.2) taking into account the first 300 correct digits in (D.1). From our results we may speculate that

$$S(l, 4, 1) = (-1)^{l+1}\frac{l+1}{2}\,, \tag{7.24}$$

$$S(l \geq 2, 3-2\epsilon, 1) = (-1)^l \frac{(l-1)^2\left(3^{l-2}+1\right)}{2}\epsilon^{-1} + \mathcal{O}\left(\epsilon^0\right)\,. \tag{7.25}$$

Chapter 8

Conclusion and outlook

In this thesis we have studied the three-dimensional Yang-Mills theory based on the non-linear SU(N) Higgs model. We handled the infrared divergences encountered in the bare perturbative theory at finite temperature by adding and subtracting a covariantly coupled scalar field, which induces a gauge field mass, i.e. gluon mass. This dynamically generated pole mass regulates the infrared divergences and is self-consistently determined by a gap equation.
As an application, we computed the transverse part of the gluon self-energy from the three-loop gap equation up to three loop for the first time. This involves the reduction of a large set of Feynman diagrams to some smaller set of master integrals. We presented some computer systems for the automated Feynman integral reduction and performed the reduction in the context of the gap equation via Reduze 2, which is based on the Laporta-algorithm. We confirmed the known results for the one- and two-loop gap equation as reported in [2]. Importantly, we notice that the gap equation itself is gauge variant at three-loop and beyond. However, we could not resolve this, which indicates that either the theory ought to be modified or the gap equation does not yield a mass, which is physical. A future step is to compute the three-loop thermodynamic pressure at equilibrium via bubble diagrams to check the gauge dependence, which may rule out one of the possibilities. The pressure up to two loop in four-dimensional gauge theories has been studied in [64]. Moreover, the result of the three-loop gap equation has to be checked. In particular, a separate reduction by [65] yields a different result than ours.
In addition, we numerically calculated the Euclidean zero-point sunset-type master integrals with one mass parameter up to five loop in the dimensional regularization scheme around four and three dimensions for the first time. This was done via the difference equations approach proposed by Laporta and its solution by means of a set of recurrence relations and factorial series. Our result is correct up to more than fifty digits when compared with known integrals in the literature. The reduction of the master integrals is quite involved, whereas we notice that the evaluation of the factorial series may easily be done with higher precision and to higher orders.

Appendix A

Three-loop self-energy diagrams and $\hat{\Pi}^{(3)}_{00}$

All 895 numbered three-loop self-energy diagrams and their contribution to $\hat{\Pi}^{(3)}_{00}$, as discussed in Chapter (6): Each diagram is multiplied with its inverse symmetry factor and minus signs for each closed fermionic loop. External gluon lines are represented by fat lines, which are not yet cut in view of a compact depiction. Full, wiggly and dotted lines denote scalars, gluons and ghosts, respectively.

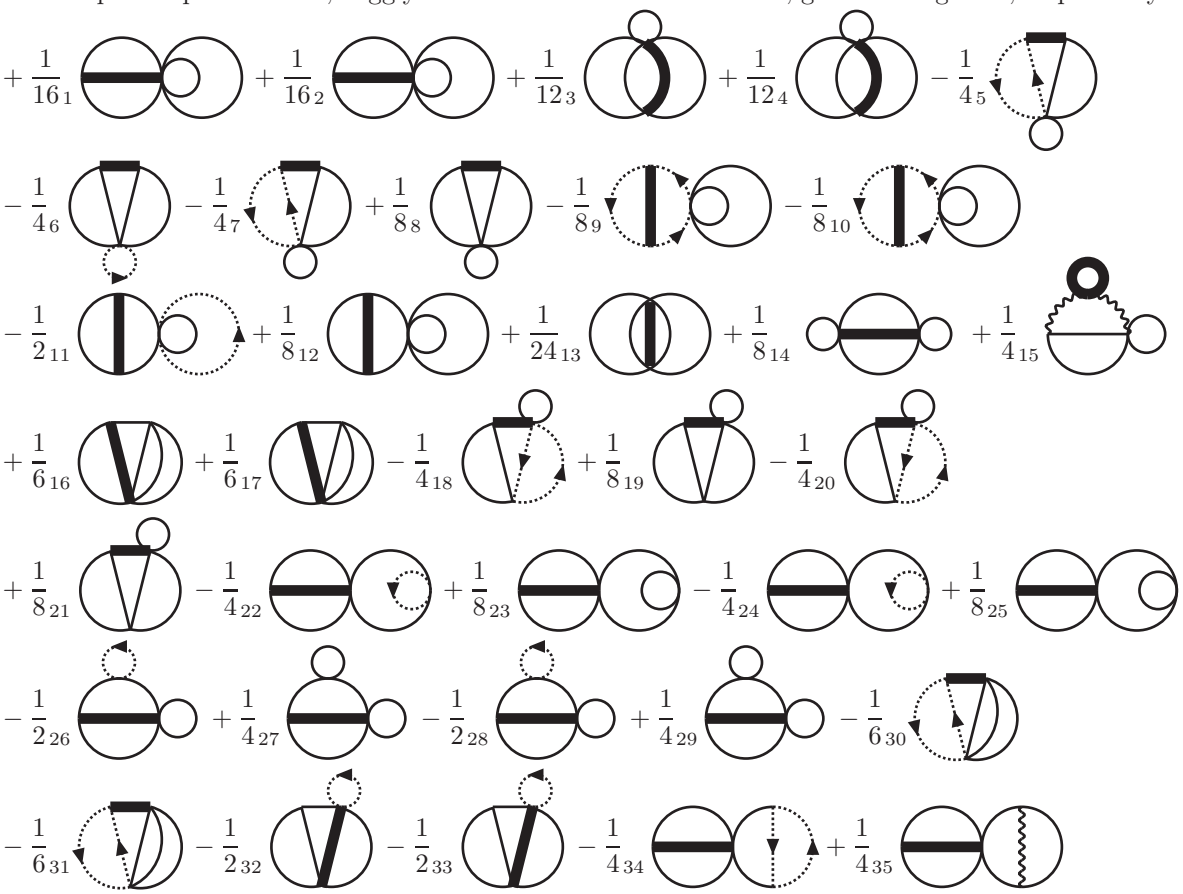

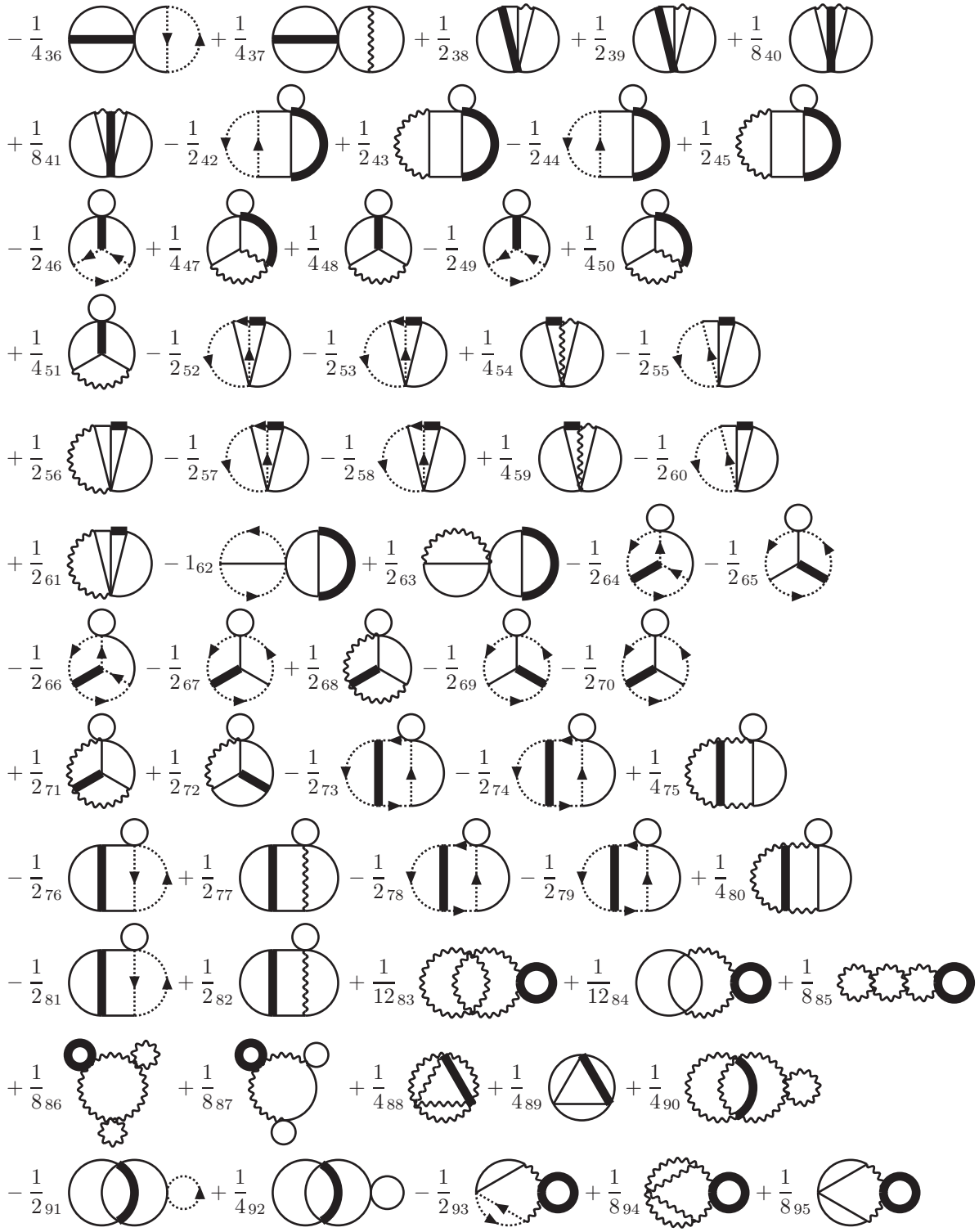
$-\frac{1}{4_{36}}$ $+\frac{1}{4_{37}}$ $+\frac{1}{2_{38}}$ $+\frac{1}{2_{39}}$ $+\frac{1}{8_{40}}$
$+\frac{1}{8_{41}}$ $-\frac{1}{2_{42}}$ $+\frac{1}{2_{43}}$ $-\frac{1}{2_{44}}$ $+\frac{1}{2_{45}}$
$-\frac{1}{2_{46}}$ $+\frac{1}{4_{47}}$ $+\frac{1}{4_{48}}$ $-\frac{1}{2_{49}}$ $+\frac{1}{4_{50}}$
$+\frac{1}{4_{51}}$ $-\frac{1}{2_{52}}$ $-\frac{1}{2_{53}}$ $+\frac{1}{4_{54}}$ $-\frac{1}{2_{55}}$
$+\frac{1}{2_{56}}$ $-\frac{1}{2_{57}}$ $-\frac{1}{2_{58}}$ $+\frac{1}{4_{59}}$ $-\frac{1}{2_{60}}$
$+\frac{1}{2_{61}}$ -1_{62} $+\frac{1}{2_{63}}$ $-\frac{1}{2_{64}}$ $-\frac{1}{2_{65}}$
$-\frac{1}{2_{66}}$ $-\frac{1}{2_{67}}$ $+\frac{1}{2_{68}}$ $-\frac{1}{2_{69}}$ $-\frac{1}{2_{70}}$
$+\frac{1}{2_{71}}$ $+\frac{1}{2_{72}}$ $-\frac{1}{2_{73}}$ $-\frac{1}{2_{74}}$ $+\frac{1}{4_{75}}$
$-\frac{1}{2_{76}}$ $+\frac{1}{2_{77}}$ $-\frac{1}{2_{78}}$ $-\frac{1}{2_{79}}$ $+\frac{1}{4_{80}}$
$-\frac{1}{2_{81}}$ $+\frac{1}{2_{82}}$ $+\frac{1}{12_{83}}$ $+\frac{1}{12_{84}}$ $+\frac{1}{8_{85}}$
$+\frac{1}{8_{86}}$ $+\frac{1}{8_{87}}$ $+\frac{1}{4_{88}}$ $+\frac{1}{4_{89}}$ $+\frac{1}{4_{90}}$
$-\frac{1}{2_{91}}$ $+\frac{1}{4_{92}}$ $-\frac{1}{2_{93}}$ $+\frac{1}{8_{94}}$ $+\frac{1}{8_{95}}$

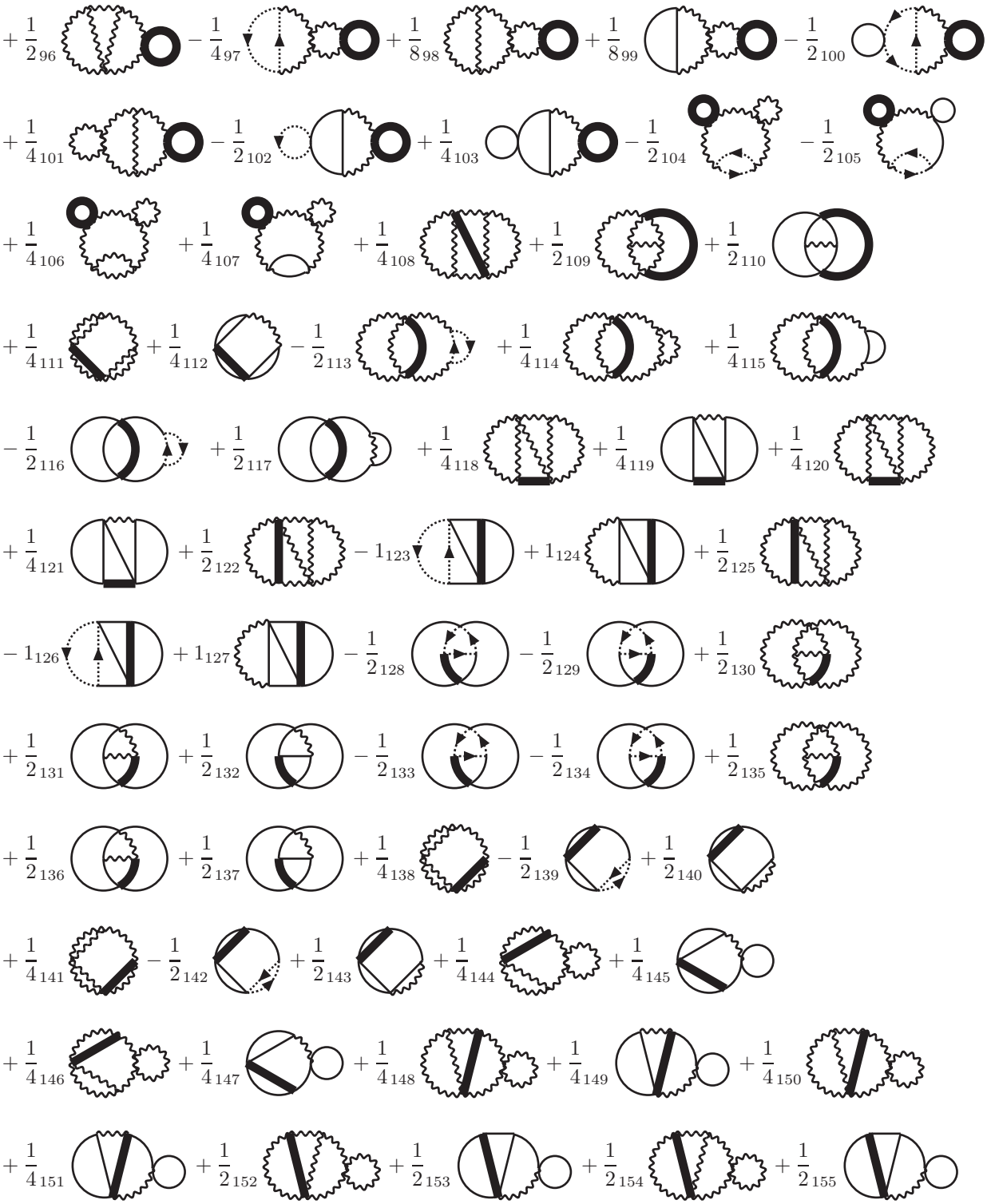

$-\frac{1}{2}_{156}$ -1_{157} 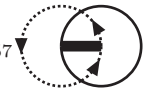 $+\frac{1}{4}_{158}$ $+\frac{1}{4}_{159}$ -1_{160}

$+\frac{1}{4}_{161}$ $-\frac{1}{2}_{162}$ 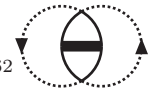 $+\frac{1}{2}_{163}$ 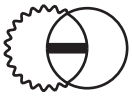 $+\frac{1}{4}_{164}$ 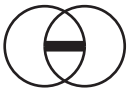 $+\frac{1}{2}_{165}$

$-\frac{1}{4}_{166}$ $+\frac{1}{8}_{167}$ $-\frac{1}{4}_{168}$ $+\frac{1}{4}_{169}$ $-\frac{1}{4}_{170}$

$+\frac{1}{8}_{171}$ $-\frac{1}{2}_{172}$ 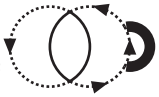 $-\frac{1}{2}_{173}$ 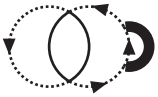 $+\frac{1}{6}_{174}$ 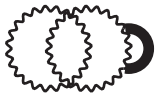 $+\frac{1}{6}_{175}$ 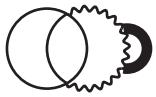

-1_{176} $+\frac{1}{2}_{177}$ 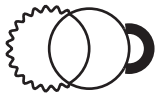 $+\frac{1}{6}_{178}$ 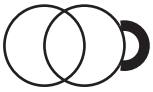 $-\frac{1}{4}_{179}$ $-\frac{1}{4}_{180}$

$+\frac{1}{4}_{181}$ 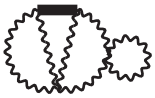 $+\frac{1}{4}_{182}$ $+1_{183}$ $-\frac{1}{2}_{184}$ $+\frac{1}{4}_{185}$ 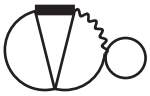

$-\frac{1}{2}_{186}$ 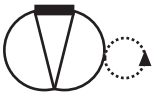 $+\frac{1}{4}_{187}$ $-\frac{1}{4}_{188}$ $-\frac{1}{4}_{189}$ $+\frac{1}{4}_{190}$ 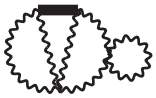

$+\frac{1}{4}_{191}$ $+1_{192}$ $-\frac{1}{2}_{193}$ $+\frac{1}{4}_{194}$ 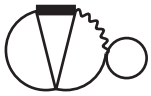 $-\frac{1}{2}_{195}$ 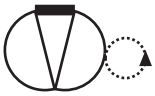

$+\frac{1}{4}_{196}$ $+\frac{1}{2}_{197}$ $-\frac{1}{4}_{198}$ $+\frac{1}{2}_{199}$ $-\frac{1}{4}_{200}$

$+\frac{1}{4}_{201}$ 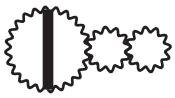 $-\frac{1}{2}_{202}$ $+\frac{1}{2}_{203}$ $-\frac{1}{2}_{204}$ $+\frac{1}{4}_{205}$

$-\frac{1}{4}_{206}$ $+\frac{1}{8}_{207}$ $+\frac{1}{8}_{208}$ $+\frac{1}{8}_{209}$ 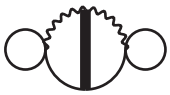 $+\frac{1}{2}_{210}$

$-\frac{1}{2}_{211}$ $+\frac{1}{8}_{212}$ $-\frac{1}{4}_{213}$ $-\frac{1}{4}_{214}$ $+\frac{1}{4}_{215}$

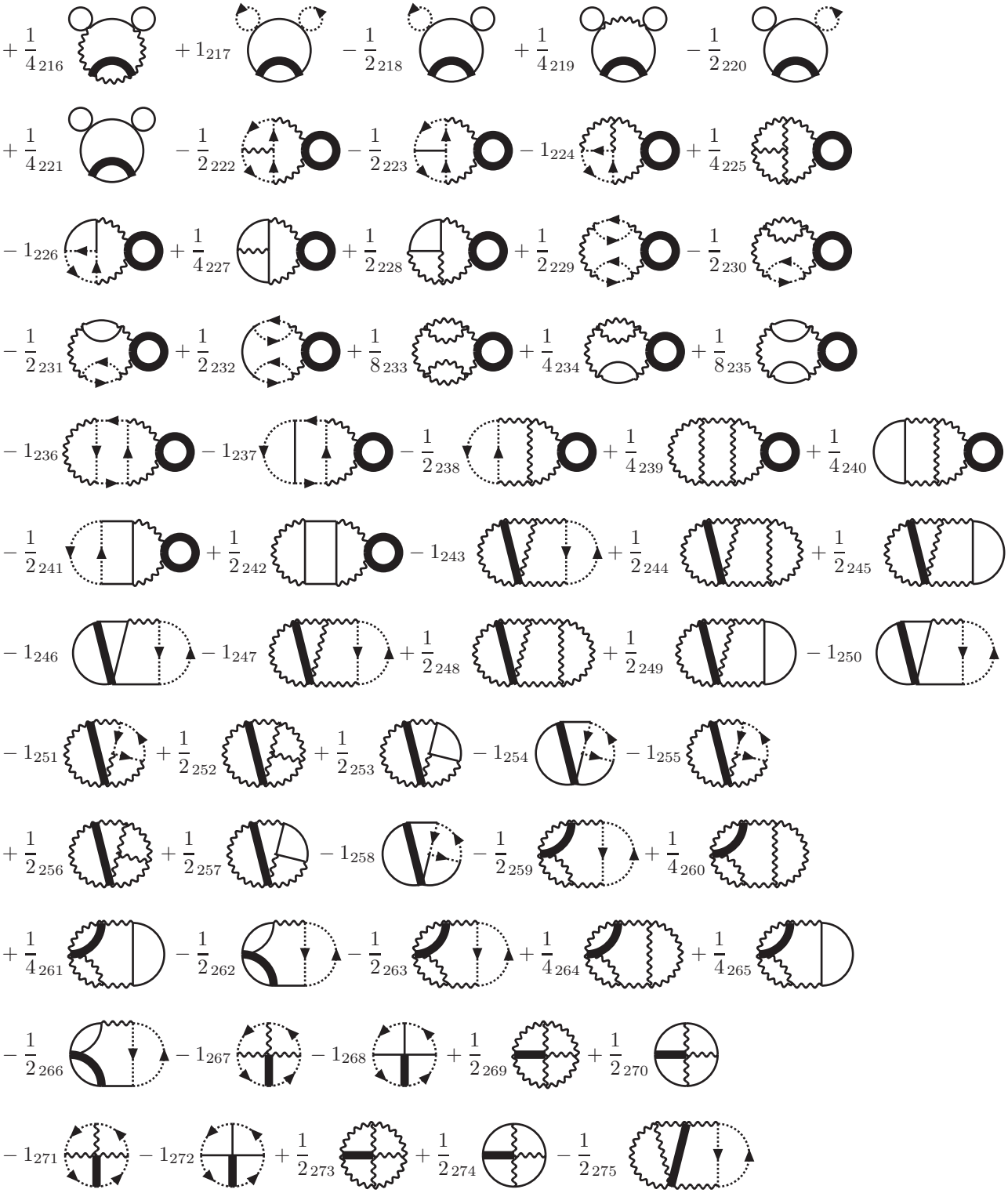
+ 1/4 216
+ 1 217
− 1/2 218
+ 1/4 219
− 1/2 220
+ 1/4 221
− 1/2 222
− 1/2 223
− 1 224
+ 1/4 225
− 1 226
+ 1/4 227
+ 1/2 228
+ 1/2 229
− 1/2 230
− 1/2 231
+ 1/2 232
+ 1/8 233
+ 1/4 234
+ 1/8 235
− 1 236
− 1 237
− 1/2 238
+ 1/4 239
+ 1/4 240
− 1/2 241
+ 1/2 242
− 1 243
+ 1/2 244
+ 1/2 245
− 1 246
− 1 247
+ 1/2 248
+ 1/2 249
− 1 250
− 1 251
+ 1/2 252
+ 1/2 253
− 1 254
− 1 255
+ 1/2 256
+ 1/2 257
− 1 258
− 1/2 259
+ 1/4 260
+ 1/4 261
− 1/2 262
− 1/2 263
+ 1/4 264
+ 1/4 265
− 1/2 266
− 1 267
− 1 268
+ 1/2 269
+ 1/2 270
− 1 271
− 1 272
+ 1/2 273
+ 1/2 274
− 1/2 275

$$-\frac{1}{2}_{276}$$
$$+\frac{1}{4}_{277}$$
$$+\frac{1}{4}_{278}$$ 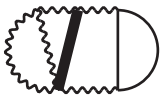
$$-\frac{1}{2}_{279}$$
$$-\frac{1}{2}_{280}$$

$$+\frac{1}{4}_{281}$$
$$+\frac{1}{4}_{282}$$ 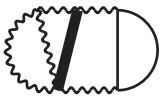
$$-\frac{1}{2}_{283}$$
$$-\frac{1}{2}_{284}$$
$$-\frac{1}{2}_{285}$$

$$-\frac{1}{2}_{286}$$
$$+\frac{1}{2}_{287}$$
$$+\frac{1}{2}_{288}$$
$$-\frac{1}{2}_{289}$$
$$-\frac{1}{2}_{290}$$

$$-\frac{1}{2}_{291}$$
$$-\frac{1}{2}_{292}$$
$$+\frac{1}{2}_{293}$$
$$+\frac{1}{2}_{294}$$
$$-\frac{1}{2}_{295}$$

$$-\frac{1}{2}_{296}$$
$$-\frac{1}{2}_{297}$$
$$-\frac{1}{2}_{298}$$
$$-\frac{1}{2}_{299}$$ 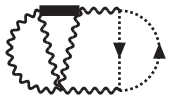
$$+\frac{1}{4}_{300}$$ 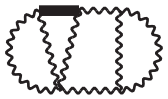

$$+\frac{1}{4}_{301}$$ 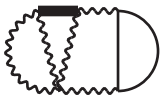
$$-\frac{1}{2}_{302}$$
$$+1_{303}$$
$$-1_{304}$$
$$-\frac{1}{2}_{305}$$ 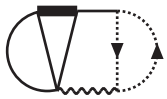

$$-\frac{1}{2}_{306}$$
$$+\frac{1}{2}_{307}$$ 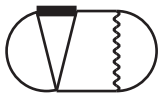
$$-\frac{1}{2}_{308}$$
$$-\frac{1}{2}_{309}$$
$$-\frac{1}{2}_{310}$$

$$-\frac{1}{2}_{311}$$
$$-\frac{1}{2}_{312}$$ 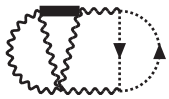
$$+\frac{1}{4}_{313}$$ 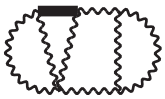
$$+\frac{1}{4}_{314}$$ 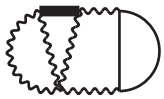
$$-\frac{1}{2}_{315}$$ 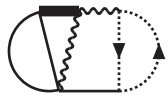

$$+1_{316}$$
$$-1_{317}$$
$$-\frac{1}{2}_{318}$$ 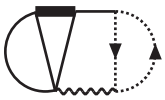
$$-\frac{1}{2}_{319}$$
$$+\frac{1}{2}_{320}$$ 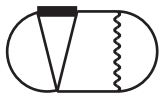

$$-1_{321}$$
$$-1_{322}$$
$$-1_{323}$$
$$-1_{324}$$
$$-1_{325}$$

$$-1_{326}$$
$$+1_{327}$$
$$-1_{328}$$
$$-1_{329}$$
$$-1_{330}$$

$$-1_{331}$$
$$-1_{332}$$
$$-1_{333}$$
$$+1_{334}$$
$$-\frac{1}{2}_{335}$$

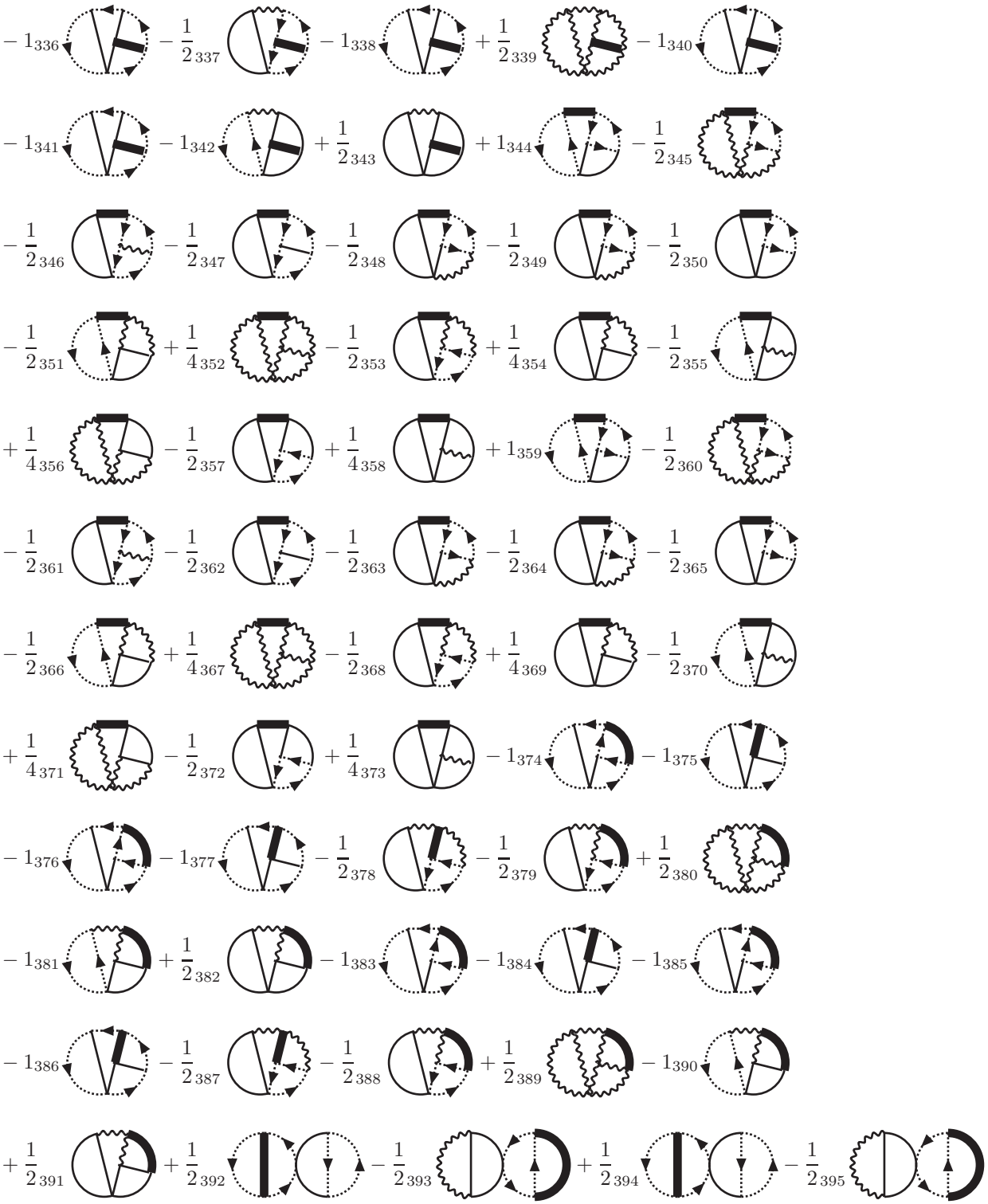

$$-\frac{1}{2}_{396}$$ 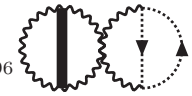 $$+\frac{1}{4}_{397}$$ 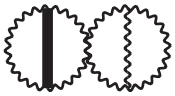 $$+\frac{1}{4}_{398}$$ 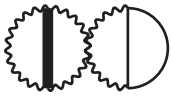 $$-1_{399}$$ $$-1_{400}$$

$$-1_{401}$$ $$-\frac{1}{2}_{402}$$ $$+\frac{1}{2}_{403}$$ $$-\frac{1}{2}_{404}$$ $$-1_{405}$$

$$-\frac{1}{2}_{406}$$ $$-1_{407}$$ $$+\frac{1}{2}_{408}$$ 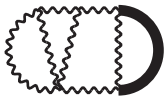 $$-1_{409}$$ $$-1_{410}$$

$$-1_{411}$$ $$+\frac{1}{2}_{412}$$ $$-\frac{1}{2}_{413}$$ $$-1_{414}$$ $$-\frac{1}{2}_{415}$$

$$-1_{416}$$ $$+\frac{1}{2}_{417}$$ 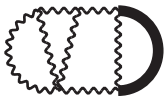 $$-1_{418}$$ $$-1_{419}$$ $$-1_{420}$$ 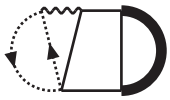

$$+\frac{1}{2}_{421}$$ $$-1_{422}$$ $$-1_{423}$$ $$-\frac{1}{2}_{424}$$ $$+\frac{1}{4}_{425}$$ 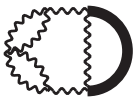

$$-\frac{1}{2}_{426}$$ $$+\frac{1}{4}_{427}$$ 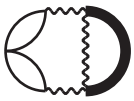 $$-\frac{1}{2}_{428}$$ $$-\frac{1}{2}_{429}$$ $$-\frac{1}{2}_{430}$$

$$-\frac{1}{2}_{431}$$ $$-\frac{1}{2}_{432}$$ 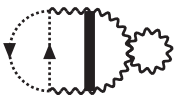 $$+\frac{1}{4}_{433}$$ 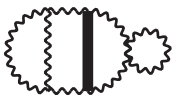 $$+\frac{1}{4}_{434}$$ 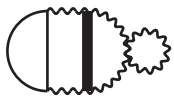 $$-\frac{1}{2}_{435}$$ 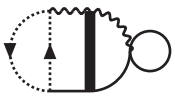

$$-\frac{1}{2}_{436}$$ $$+1_{437}$$ $$-1_{438}$$ $$-\frac{1}{2}_{439}$$ $$+\frac{1}{2}_{440}$$

$$-\frac{1}{2}_{441}$$ $$-\frac{1}{2}_{442}$$ $$-\frac{1}{2}_{443}$$ $$-\frac{1}{2}_{444}$$ 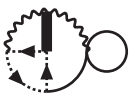 $$-\frac{1}{2}_{445}$$

$$+1_{446}$$ $$-\frac{1}{2}_{447}$$ $$-\frac{1}{2}_{448}$$ $$-\frac{1}{2}_{449}$$ $$-\frac{1}{2}_{450}$$ 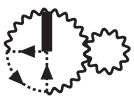

$$-\frac{1}{2}_{451}$$ 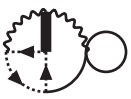 $$-\frac{1}{2}_{452}$$ $$+1_{453}$$ $$-\frac{1}{2}_{454}$$ 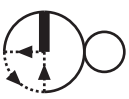 $$-\frac{1}{2}_{455}$$

$$-\frac{1}{2_{456}}$$
$$+\frac{1}{2_{457}}$$ 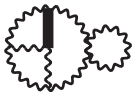
$$-1_{458}$$
$$+\frac{1}{2_{459}}$$
$$-\frac{1}{2_{460}}$$

$$-\frac{1}{2_{461}}$$
$$+\frac{1}{2_{462}}$$ 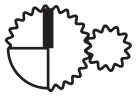
$$-1_{463}$$ 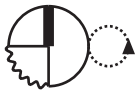
$$+\frac{1}{2_{464}}$$
$$-\frac{1}{2_{465}}$$

$$-\frac{1}{2_{466}}$$
$$-\frac{1}{2_{467}}$$ 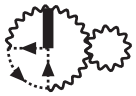
$$-\frac{1}{2_{468}}$$ 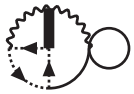
$$-\frac{1}{2_{469}}$$
$$+1_{470}$$

$$-\frac{1}{2_{471}}$$
$$-\frac{1}{2_{472}}$$
$$-\frac{1}{2_{473}}$$
$$-\frac{1}{2_{474}}$$ 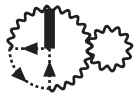
$$-\frac{1}{2_{475}}$$ 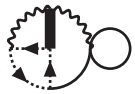

$$-\frac{1}{2_{476}}$$
$$+1_{477}$$
$$-\frac{1}{2_{478}}$$
$$-\frac{1}{2_{479}}$$
$$-\frac{1}{2_{480}}$$

$$+\frac{1}{2_{481}}$$ 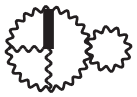
$$-1_{482}$$
$$+\frac{1}{2_{483}}$$
$$-\frac{1}{2_{484}}$$
$$-\frac{1}{2_{485}}$$

$$+\frac{1}{2_{486}}$$ 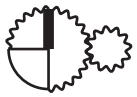
$$-1_{487}$$
$$+\frac{1}{2_{488}}$$
$$-\frac{1}{2_{489}}$$ 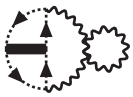
$$-\frac{1}{2_{490}}$$ 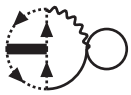

$$-\frac{1}{2_{491}}$$ 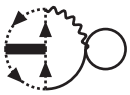
$$+1_{492}$$
$$-\frac{1}{2_{493}}$$
$$-\frac{1}{2_{494}}$$ 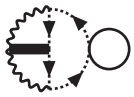
$$-\frac{1}{2_{495}}$$

$$-\frac{1}{2_{496}}$$ 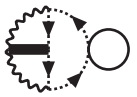
$$+\frac{1}{4_{497}}$$ 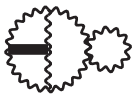
$$-\frac{1}{2_{498}}$$ 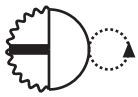
$$+\frac{1}{4_{499}}$$ 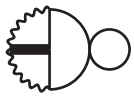
$$-\frac{1}{2_{500}}$$

$$-\frac{1}{2_{501}}$$ 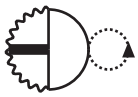
$$+\frac{1}{4_{502}}$$ 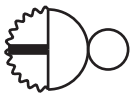
$$+\frac{1}{4_{503}}$$ 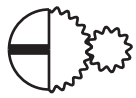
$$-\frac{1}{2_{504}}$$ 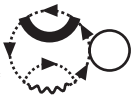
$$-\frac{1}{2_{505}}$$

$$-\frac{1}{2_{506}}$$
$$-\frac{1}{2_{507}}$$
$$-\frac{1}{2_{508}}$$
$$-\frac{1}{2_{509}}$$
$$+\frac{1}{4_{510}}$$

$$+\frac{1}{4_{511}}$$
$$-\frac{1}{2_{512}}$$
$$+1_{513}$$
$$-\frac{1}{2_{514}}$$
$$-1_{515}$$

$+\frac{1}{2}_{516}$ $-\frac{1}{2}_{517}$ 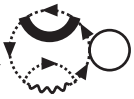 $-\frac{1}{2}_{518}$ $-\frac{1}{2}_{519}$ $-\frac{1}{2}_{520}$

$-\frac{1}{2}_{521}$ $-\frac{1}{2}_{522}$ $+\frac{1}{4}_{523}$ $+\frac{1}{4}_{524}$ $-\frac{1}{2}_{525}$ 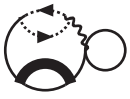

$+1_{526}$ $-\frac{1}{2}_{527}$ -1_{528} $+\frac{1}{2}_{529}$ $-\frac{1}{2}_{530}$ 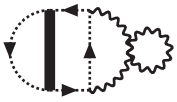

$-\frac{1}{2}_{531}$ $-\frac{1}{2}_{532}$ $+1_{533}$ $-\frac{1}{2}_{534}$ $-\frac{1}{2}_{535}$

$-\frac{1}{2}_{536}$ $-\frac{1}{2}_{537}$ 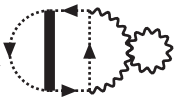 $-\frac{1}{2}_{538}$ $-\frac{1}{2}_{539}$ $+1_{540}$

$-\frac{1}{2}_{541}$ $-\frac{1}{2}_{542}$ $-\frac{1}{2}_{543}$ $-\frac{1}{2}_{544}$ $-\frac{1}{2}_{545}$

$+\frac{1}{2}_{546}$ 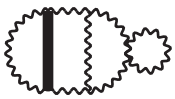 -1_{547} $+\frac{1}{2}_{548}$ $-\frac{1}{2}_{549}$ $-\frac{1}{2}_{550}$

-1_{551} $+\frac{1}{2}_{552}$ $+\frac{1}{2}_{553}$ 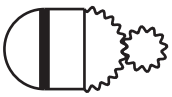 -1_{554} -1_{555}

-1_{556} -1_{557} -1_{558} -1_{559} -1_{560}

-1_{561} -1_{562} -1_{563} $-\frac{1}{2}_{564}$ $+\frac{1}{4}_{565}$

$+\frac{1}{4}_{566}$ $-\frac{1}{2}_{567}$ $+\frac{1}{2}_{568}$ -1_{569} -1_{570}

$-\frac{1}{2}_{571}$ $+\frac{1}{2}_{572}$ $-\frac{1}{2}_{573}$ $+\frac{1}{2}_{574}$ -1_{575}

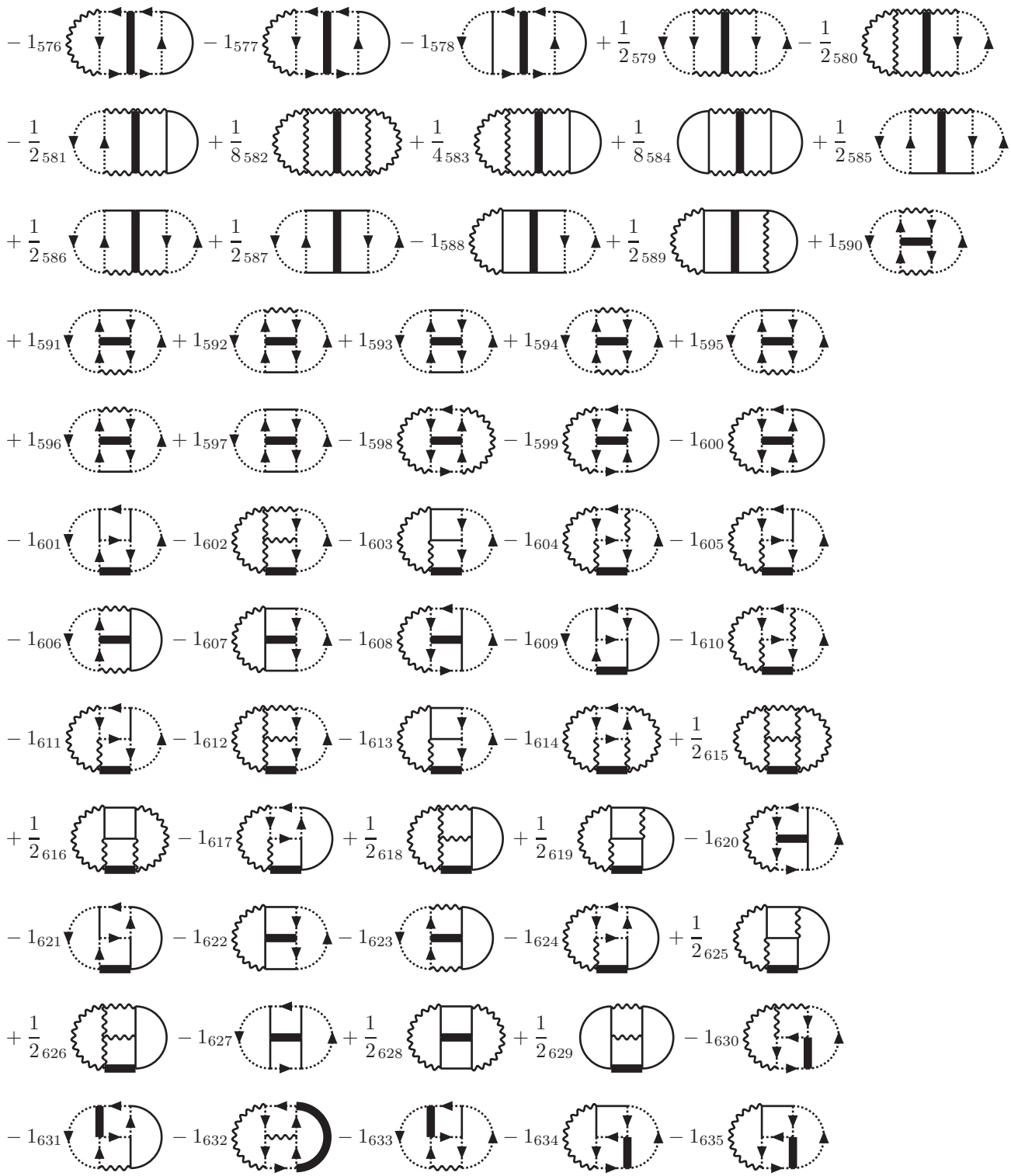
− 1576
− 1577
− 1578
+ 1/2 579
− 1/2 580
− 1/2 581
+ 1/8 582
+ 1/4 583
+ 1/8 584
+ 1/2 585
+ 1/2 586
+ 1/2 587
− 1588
+ 1/2 589
+ 1590
+ 1591
+ 1592
+ 1593
+ 1594
+ 1595
+ 1596
+ 1597
− 1598
− 1599
− 1600
− 1601
− 1602
− 1603
− 1604
− 1605
− 1606
− 1607
− 1608
− 1609
− 1610
− 1611
− 1612
− 1613
− 1614
+ 1/2 615
+ 1/2 616
− 1617
+ 1/2 618
+ 1/2 619
− 1620
− 1621
− 1622
− 1623
− 1624
+ 1/2 625
+ 1/2 626
− 1627
+ 1/2 628
+ 1/2 629
− 1630
− 1631
− 1632
− 1633
− 1634
− 1635

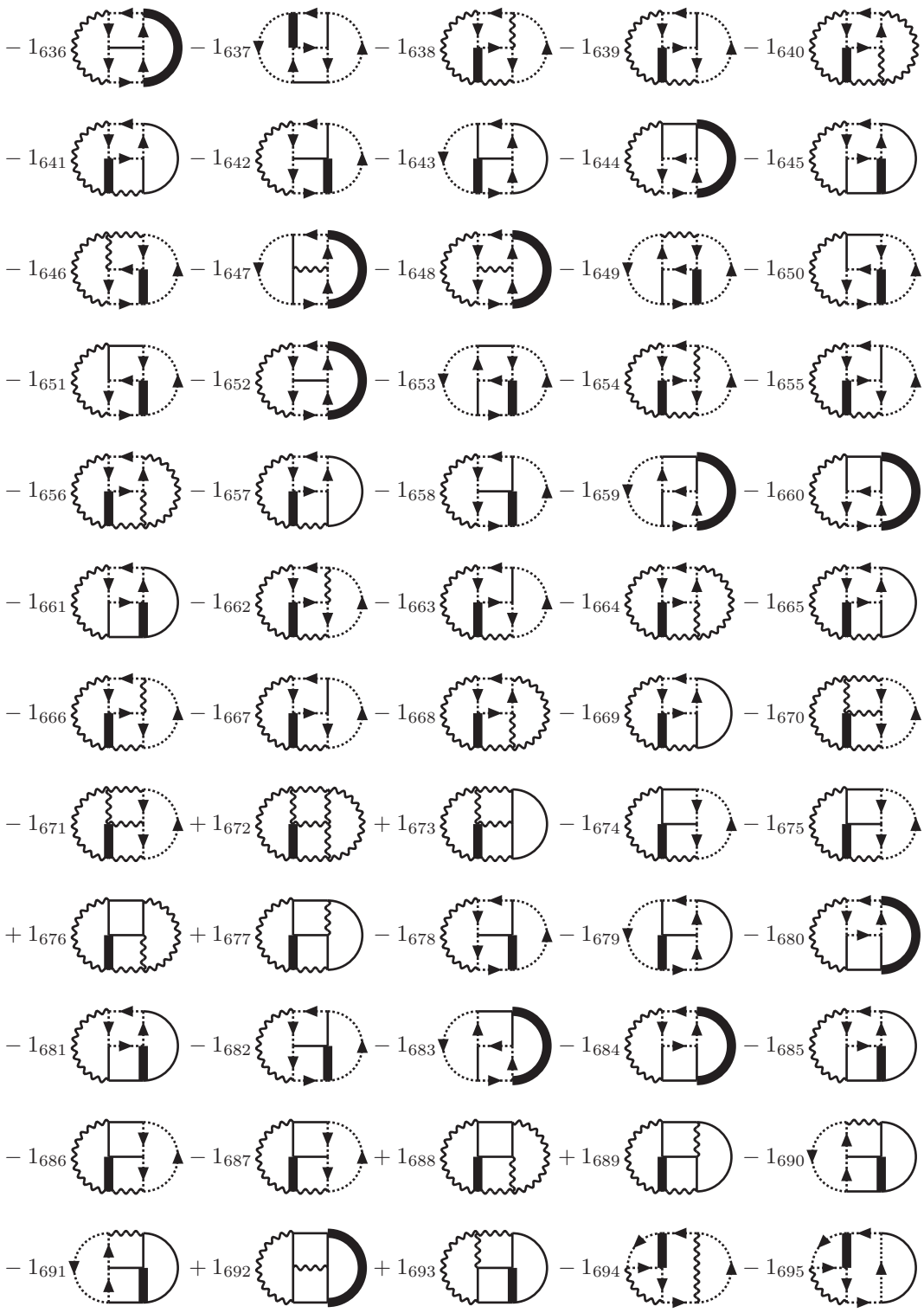
− 1636
− 1637
− 1638
− 1639
− 1640
− 1641
− 1642
− 1643
− 1644
− 1645
− 1646
− 1647
− 1648
− 1649
− 1650
− 1651
− 1652
− 1653
− 1654
− 1655
− 1656
− 1657
− 1658
− 1659
− 1660
− 1661
− 1662
− 1663
− 1664
− 1665
− 1666
− 1667
− 1668
− 1669
− 1670
− 1671
+ 1672
+ 1673
− 1674
− 1675
+ 1676
+ 1677
− 1678
− 1679
− 1680
− 1681
− 1682
− 1683
− 1684
− 1685
− 1686
− 1687
+ 1688
+ 1689
− 1690
− 1691
+ 1692
+ 1693
− 1694
− 1695

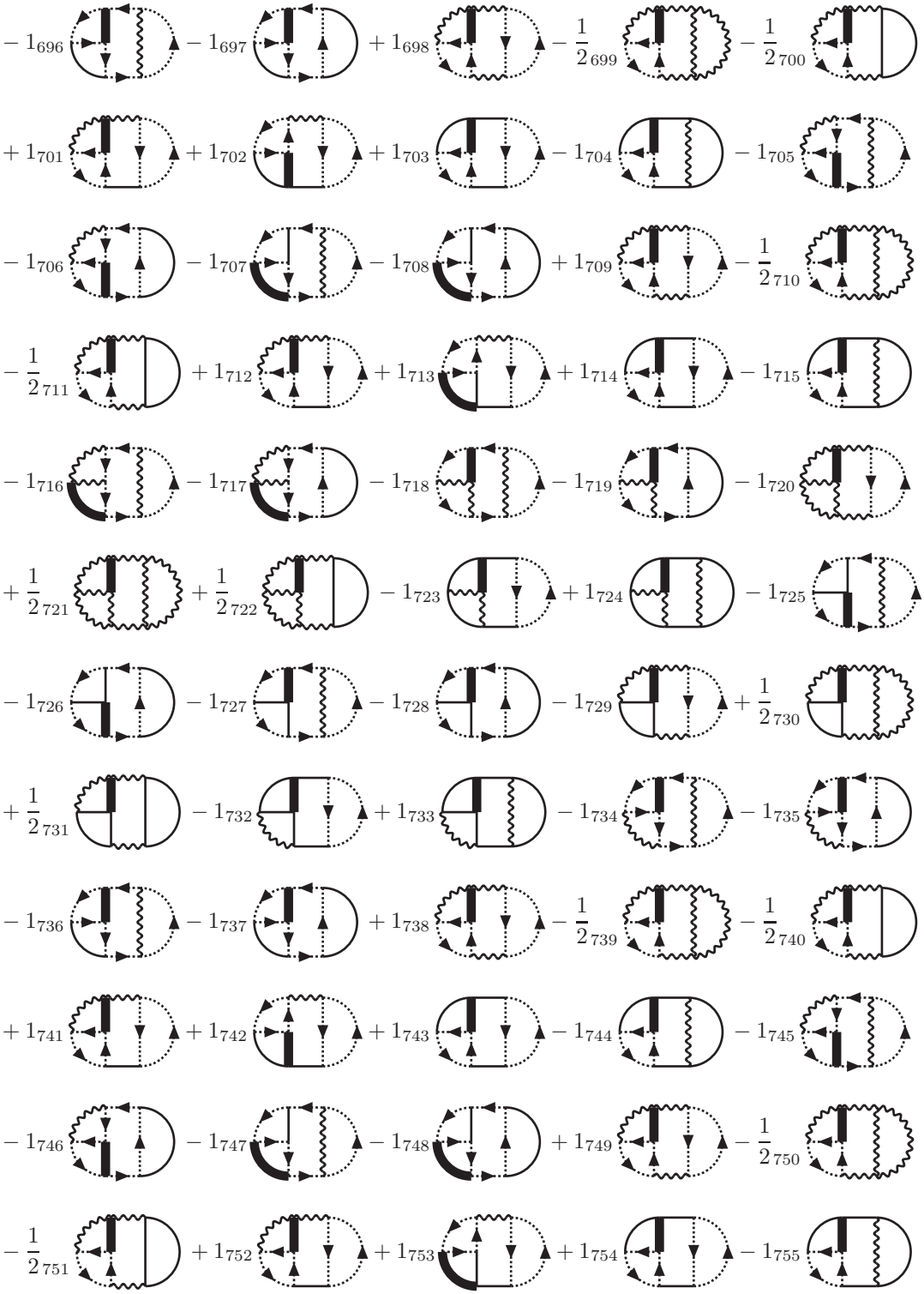
− 1696
− 1697
+ 1698
− 1/2 699
− 1/2 700
+ 1701
+ 1702
+ 1703
− 1704
− 1705
− 1706
− 1707
− 1708
+ 1709
− 1/2 710
− 1/2 711
+ 1712
+ 1713
+ 1714
− 1715
− 1716
− 1717
− 1718
− 1719
− 1720
+ 1/2 721
+ 1/2 722
− 1723
+ 1724
− 1725
− 1726
− 1727
− 1728
− 1729
+ 1/2 730
+ 1/2 731
− 1732
+ 1733
− 1734
− 1735
− 1736
− 1737
+ 1738
− 1/2 739
− 1/2 740
+ 1741
+ 1742
+ 1743
− 1744
− 1745
− 1746
− 1747
− 1748
+ 1749
− 1/2 750
− 1/2 751
+ 1752
+ 1753
+ 1754
− 1755

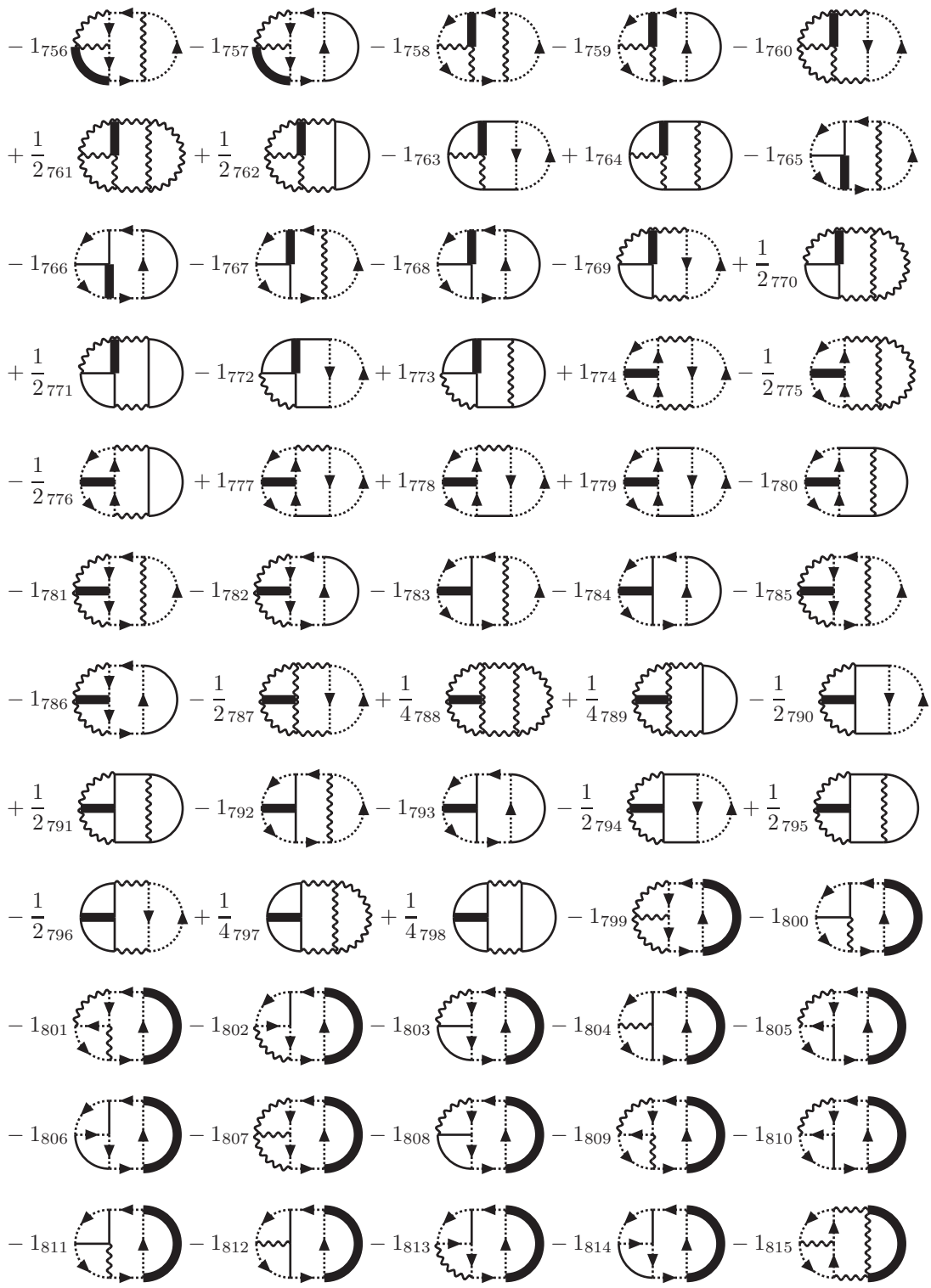
− 1756
− 1757
− 1758
− 1759
− 1760
+ 1/2 761
+ 1/2 762
− 1763
+ 1764
− 1765
− 1766
− 1767
− 1768
− 1769
+ 1/2 770
+ 1/2 771
− 1772
+ 1773
+ 1774
− 1/2 775
− 1/2 776
+ 1777
+ 1778
+ 1779
− 1780
− 1781
− 1782
− 1783
− 1784
− 1785
− 1786
− 1/2 787
+ 1/4 788
+ 1/4 789
− 1/2 790
+ 1/2 791
− 1792
− 1793
− 1/2 794
+ 1/2 795
− 1/2 796
+ 1/4 797
+ 1/4 798
− 1799
− 1800
− 1801
− 1802
− 1803
− 1804
− 1805
− 1806
− 1807
− 1808
− 1809
− 1810
− 1811
− 1812
− 1813
− 1814
− 1815

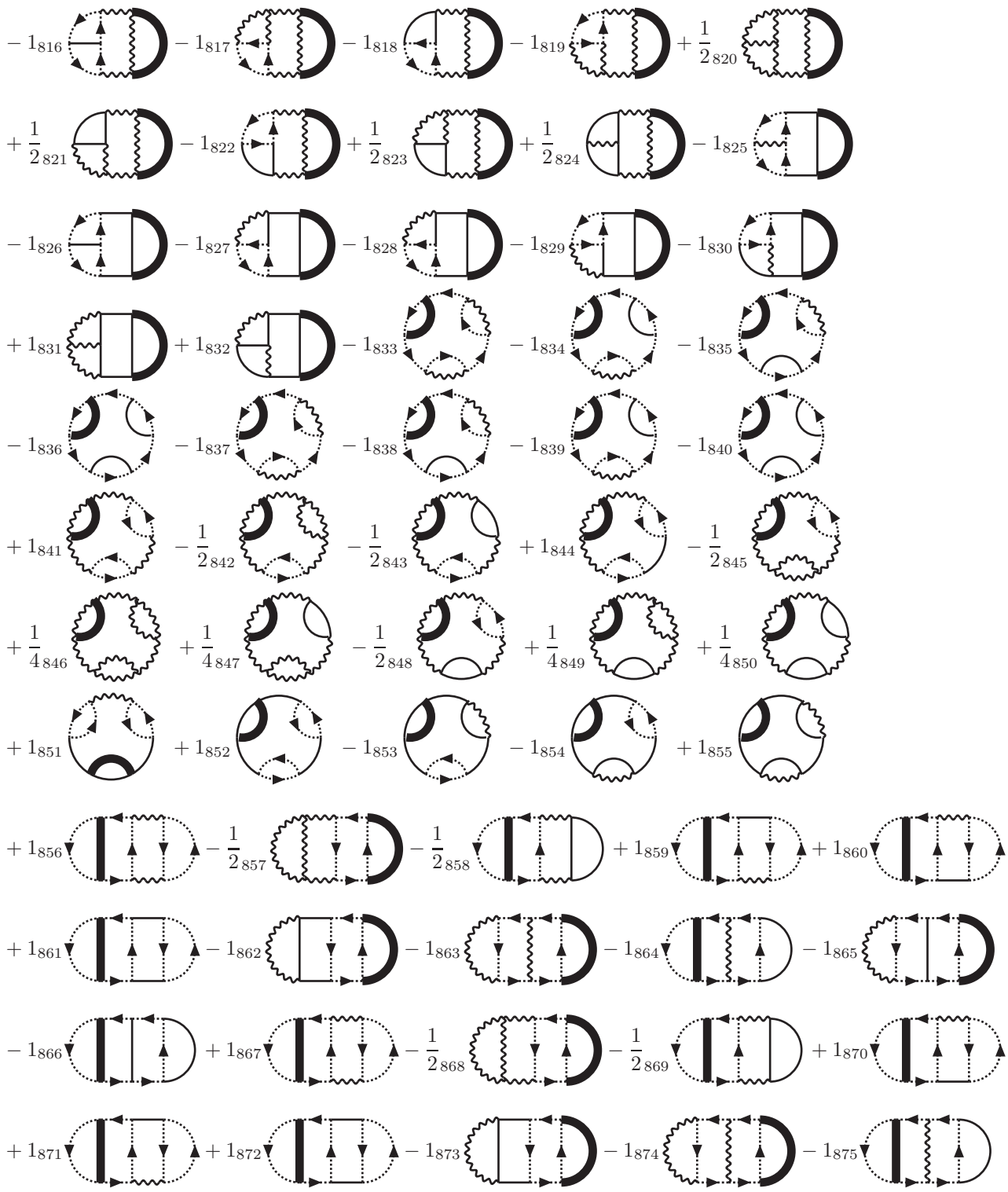
− 1816
− 1817
− 1818
− 1819
+ 1/2 820
+ 1/2 821
− 1822
+ 1/2 823
+ 1/2 824
− 1825
− 1826
− 1827
− 1828
− 1829
− 1830
+ 1831
+ 1832
− 1833
− 1834
− 1835
− 1836
− 1837
− 1838
− 1839
− 1840
+ 1841
− 1/2 842
− 1/2 843
+ 1844
− 1/2 845
+ 1/4 846
+ 1/4 847
− 1/2 848
+ 1/4 849
+ 1/4 850
+ 1851
+ 1852
− 1853
− 1854
+ 1855
+ 1856
− 1/2 857
− 1/2 858
+ 1859
+ 1860
+ 1861
− 1862
− 1863
− 1864
− 1865
− 1866
+ 1867
− 1/2 868
− 1/2 869
+ 1870
+ 1871
+ 1872
− 1873
− 1874
− 1875

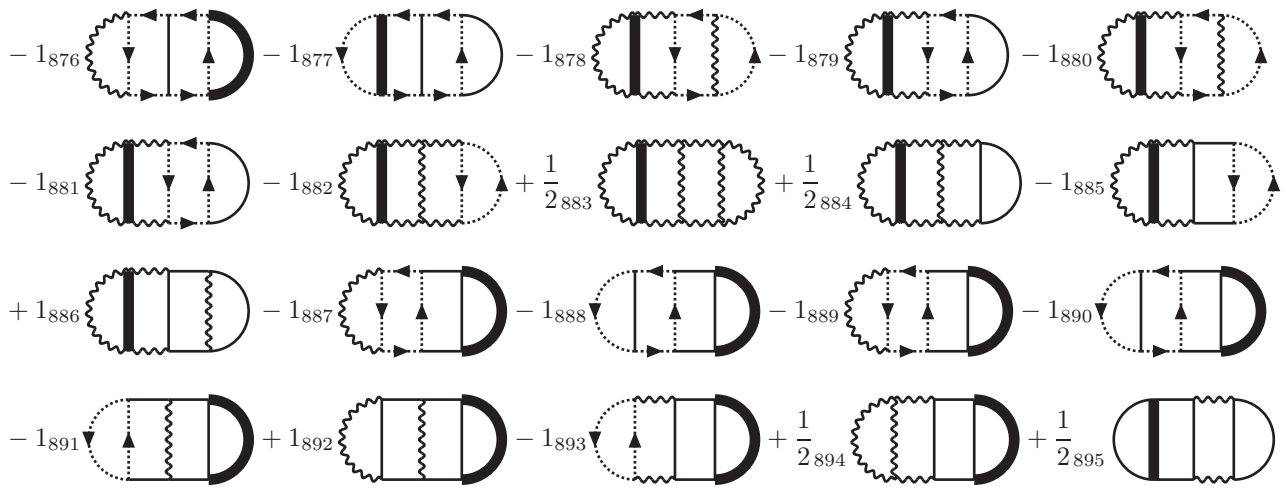
− 1876
− 1877
− 1878
− 1879
− 1880
− 1881
− 1882
+ 1/2 883
+ 1/2 884
− 1885
+ 1886
− 1887
− 1888
− 1889
− 1890
− 1891
+ 1892
− 1893
+ 1/2 894
+ 1/2 895

Appendix B

D-dimensional results for $\hat{\Pi}_{12}^{(1)}$ and $\hat{\Pi}_{03}^{(1)}$

The D-dimensional results for the derivatives of the one-loop self-energies $\hat{\Pi}_{12}^{(1)}$ and $\hat{\Pi}_{03}^{(1)}$ as given by (6.10). Th results are given in terms of master integrals K and ratios of polynomials a and b.

$$\hat{\Pi}_{12}^{(1)} = a_1 K_1 + a_2 K_1' + a_3 K_1'' + a_4 K_2 + a_5 K_2' \tag{B.1}$$

$$\hat{\Pi}_{03}^{(1)} = b_1 K_1 + b_2 K_1' + b_3 K_1'' + b_4 K_2 + b_5 K_2' \tag{B.2}$$

$$\begin{aligned}
a_1 =& \frac{1}{24}\left(330 - 749D + 472D^2 - 106D^3 + 8D^4\right) \\
a_2 =& \frac{1}{8(-1+4\xi)}\left(-6 + 60\xi - 216\xi^2 - 4D^2\xi(1+2\xi) + D\left(-3 + 16\xi + 80\xi^2\right)\right) \\
a_3 =& \frac{1}{4(-4+\xi)}\left(4D^2(-14+5\xi) - 6\left(36 + 16\xi - 15\xi^2 + 2\xi^3\right) + D\left(272 - 36\xi - 34\xi^2 + 5\xi^3\right)\right) \\
a_4 =& \frac{1}{12(-4+\xi)}\left(-736 - 89D^3(-4+\xi) + 8D^4(-4+\xi) + 22\xi + 36\xi^2 + 36D^2(-37+9\xi)\right. \\
& \left. + D\left(1852 - 376\xi - 15\xi^2\right)\right) \\
a_5 =& \frac{1}{4\xi(-4+\xi)(-1+4\xi)}\left(-D^3\xi(-4+\xi)(-1+4\xi) + D^2\left(24 - 64\xi - 115\xi^2 + 38\xi^3\right)\right. \\
& \left. -12\left(-4 + 6\xi + 43\xi^2 - 28\xi^3 + 4\xi^4\right) + D\left(-72 + 176\xi + 433\xi^2 - 215\xi^3 + 20\xi^4\right)\right)
\end{aligned} \tag{B.3}$$

$$
\begin{aligned}
b_1 =& \frac{1}{6}\left(429 - 803D + 472D^2 - 106D^3 + 8D^4\right) \\
b_2 =& \frac{-3}{2(-1+4\xi)}\left(2 + (-19+3D)\xi + 2(-5+D)^2\xi^2\right) \\
b_3 =& \frac{3}{2(-4+\xi)}\left(-52 + 4D^2(-3+\xi) - 28\xi + 23\xi^2 - 3\xi^3 + D\left(64 - 8\xi - 7\xi^2 + \xi^3\right)\right) \\
b_4 =& \frac{1}{24(-4+\xi)}\left(-145D^3(-4+\xi) - 11D^4(-4+\xi) + 3D^5(-4+\xi) + D^2(-3396 + 831\xi)\right. \\
& \left. -2D\left(-2560 + 541\xi + 18\xi^2\right) + 4\left(-440 - 7\xi + 27\xi^2\right)\right) \\
b_5 =& \frac{3}{4\xi(-4+\xi)(-1+4\xi)}\left(16 + 64\xi - 554\xi^2 + 234\xi^3 - 24\xi^4 - D^3\xi(-4+\xi)(-1+4\xi)\right. \\
& \left. +D^2\left(8 + 8\xi - 163\xi^2 + 42\xi^3\right) + 4D\left(-6 - 9\xi + 137\xi^2 - 43\xi^3 + 2\xi^4\right)\right)
\end{aligned} \tag{B.4}
$$

$$
\begin{aligned}
K_1 &= \hat{I}(1,1,1,1) \overset{D=3-2\epsilon}{=} -\frac{1}{2}\ln 3 + \mathcal{O}(\epsilon) \\
K_1' &= \hat{I}(1,1,\xi,\xi) \overset{D=3-2\epsilon}{=} -\frac{1}{2}\ln\frac{2\sqrt{\xi}+1}{2\sqrt{\xi}-1} + \mathcal{O}(\epsilon) \\
K_1'' &= \hat{I}(1,1,1,\xi) \overset{D=3-2\epsilon}{=} -\frac{1}{2}\ln\frac{\sqrt{\xi}+2}{\sqrt{\xi}} + \mathcal{O}(\epsilon) \\
K_2 &= \hat{I}(1,0,1,0) = 1 \\
K_2' &= \hat{I}(1,0,\xi,0) = \xi^{\frac{D-2}{2}}
\end{aligned} \tag{B.5}
$$

Appendix C

Sunset integrals: Recurrence relations

The recurrence relations for the sunset-type integrals (7.1) up to five loop as for the coefficients of the factorial series (4.14), see Chapter (4). They are deduced from the difference equations (7.8).

$$
\begin{aligned}
&+ a_{s-1}^{(1)} \frac{-1}{4}(-2+D+2s)^2 \\
&+ a_s^{(1)} s = 0
\end{aligned}
\tag{C.1}
$$

$$
\begin{aligned}
&+ a_{s-2}^{(2)} \frac{3}{16}(-4+D+2s)(-2+D+2s)^2 \\
&+ a_{s-1}^{(2)} \frac{-1}{8}(-2+D+2s)(-6+5D+14s) \\
&+ a_s^{(2)}(1+2s) = a_s^{(1)}
\end{aligned}
\tag{C.2}
$$

$$
\begin{aligned}
&+ a_{s-3}^{(3)} \frac{-1}{12}(-6+D+2s)(-4+D+2s)^2(-8+3D+2s) \\
&+ a_{s-2}^{(3)} \frac{1}{48}(-4+D+2s)\left(440+41D^2+4s(-111+25s)+2D(-137+78s)\right) \\
&+ a_{s-1}^{(3)} \frac{1}{24}\left(-11D^2+D(90-110s)-8(-2+s)(-10+13s)\right) \\
&+ a_s^{(3)} \frac{3}{2} = a_{s-1}^{(1)}
\end{aligned}
\tag{C.3}
$$

$$
\begin{aligned}
&+ a^{(4)}_{s-5}\frac{-15}{1024}\left(D+2(-5+s)\right)(-8+D+2s)^2(-6+D+2s)^2(-4+D+2s)^2\big) \\
&+ a^{(4)}_{s-4}\frac{9}{256}(-8+D+2s)(-6+D+2s)^2(-4+D+2s)^2(-22+3D+9s) \\
&+ a^{(4)}_{s-3}\frac{-1}{768}(-6+D+2s)(-4+D+2s)^2\left(7416+43D^2+4D(-461+310s)+4s(-1963+523s)\right) \\
&+ a^{(4)}_{s-2}\frac{-1}{64}(-4+D+2s)\big(29D^3-D^2(123+25s)-4D(92+s(-277+147s)) \\
&\qquad +4(396+s(-952+11(67-17s)s))\big) \\
&+ a^{(4)}_{s-1}\frac{1}{48}\big(19D^3+D^2(-153+110s)-2D(-151+2s(47+63s)) \\
&\qquad -12(2+s(45+s(-101+50s)))\big) \\
&+ a^{(4)}_{s}\frac{4}{3}s(2-D+2s) = a^{(1)}_{s-1}
\end{aligned}
\tag{C.4}
$$

$$
\begin{aligned}
&+ a^{(5)}_{s-6}\frac{1}{160}(5D+2(-8+s))(D+2(-6+s))(D+2(-5+s))^2(-8+D+2s)^2(-6+D+2s)^2 \\
&+ a^{(5)}_{s-5}\frac{-1}{480}(D+2(-5+s))(-8+D+2s)^2(-6+D+2s)^2 \\
&\qquad \times\left(109D^2+38D(-39+10s)+4(908+s(-387+37s))\right) \\
&+ a^{(5)}_{s-4}\frac{1}{7680}(-8+D+2s)(-6+D+2s)^2\left(3389D^3+D^2(-94874+32278s)\right. \\
&\qquad \left.+D(679432+12s(-34694+5285s))+8(-164552+s(135322+s(-36085+3041s)))\right) \\
&+ a^{(5)}_{s-3}\frac{-1}{1920}(-6+D+2s)\big(240D^4+D^3(-24779+12058s)+D^2(347814+16s(-17988+3713s)) \\
&\qquad +4D(-415954+s(468347+s(-175529+21810s))) \\
&\qquad +96(26596+s(-36758+s(18882+s(-4241+347s))))\big) \\
&+ a^{(5)}_{s-2}\frac{1}{1920}\big(-261D^4+6D^3(-921+850s)+4D^2(38523+s(-46134+13699s)) \\
&\qquad +8D(-109878+s(165645+s(-82619+13494s))) \\
&\qquad +32(45192+s(-80384+s(53045+7s(-2182+229s))))\big) \\
&+ a^{(5)}_{s-1}\frac{-1}{240}(-1+s)\left(8256+18D^2+56s(-178+47s)+3D(-883+934s)\right) \\
&+ a^{(5)}_{s}\frac{15}{8}(-1+s)s = a^{(1)}_{s-2}
\end{aligned}
\tag{C.5}
$$

Appendix D

Sunset master integrals: Numerical results around $4D$

The numerical results for the sunset-type master integrals (7.1) up to five loop for $D = 4 - 2\epsilon$ deduced from the recurrence relations given in Appendix C by means of factorial series (4.14). For each result we present the first fifty correct digits and several orders in ϵ. See Chapter (7) for more details.

$$
\begin{aligned}
&S(2, 4-2\epsilon, 1;\ s_{\max}=5000, x_{\max}=2000;\ \gtrsim 810 \text{ correct digits}) = \\
&- 1.50000000000000000000000000000000000000000000000000 \\
&- 4.49999999999999999999999999999999999999999999999999\epsilon \\
&- 6.98413914196581166409765656669158439635689548554 62\epsilon^2 \\
&- 18.00878162354616799999520813117528556508120482287 0\epsilon^3 \\
&- 27.99422356367517870595476226725654916799106141515 0\epsilon^4 \\
&- 72.00378659798856817398208683209757725736966397977 1\epsilon^5 \\
&- 111.99749833554743962025539910121146396234513990701\epsilon^6 \\
&- 288.00165889594361462413210083202734513521610523660\epsilon^7 \\
&- 447.99889753939191138684622763845184953766743107074\epsilon^8 \\
&- 1152.00073360719583600028501236690998504076090814 84\epsilon^9 \\
&- 1791.99951146920052229980019160100572633844339300 59\epsilon^{10} \\
&- 4608.00032547258921091608694992955467668239342278 57\epsilon^{11} \\
&- 7167.99978310365451034206788038510756333890526003 10\epsilon^{12} \\
&- 18432.00014456354180991323208348820581104992831451 5\epsilon^{13} \\
&- 28671.99990363787737681163929365734702609764258572 7\epsilon^{14} \\
&- 73728.00006423599674148116192732797816913926494359 6\epsilon^{15} \\
&- 114687.99995717816655041457799393757664324527054306\epsilon^{16} \\
&- 294912.00002854702405583264265294205219377138601124\epsilon^{17} \\
&- 458751.99998096899635447027799732378155117699074281\epsilon^{18} \\
&- 1.17964800001268719754179989538919607452927490318 87 \cdot 10^6 \epsilon^{19} \\
&+ \mathcal{O}\left(\epsilon^{20}\right)
\end{aligned}
\tag{D.1}
$$

$$
\begin{aligned}
&S(3, 4-2\epsilon, 1;\ s_{\max} = 5000, x_{\max} = 1000;\ \gtrsim 220 \text{ correct digits}) = \\
&+ 1.99999999999999999999999999999999999999999999999999 \\
&+ 7.66666666666666666666666666666666666666666666666666\epsilon \\
&+ 17.49999999999999999999999999999999999999999999999999\epsilon^2 \\
&+ 22.91666666666666666666666666666666666666666666666666\epsilon^3 \\
&+ 21.25179105129151998825689136309413298855948824737 8\epsilon^4 \\
&- 184.23000510529848342108563128392064450073752779056\epsilon^5 \\
&- 661.11058615335383325470884105246026525585456567192\epsilon^6 \\
&- 3685.05477938169880569422657784370448521380019292 37\epsilon^7 \\
&- 10050.97540393838058754054554200191871045970459169 9\epsilon^8 \\
&- 42319.97454641326180936066371926177196522190945693 1\epsilon^9 \\
&- 108418.43440062975771692491717556958327646321159009\epsilon^{10} \\
&- 419852.46289091247862674300972973441506701524599367\epsilon^{11} \\
&- 1.05110491348373562236783648367978159770404807421 34 \cdot 10^6\epsilon^{12} \\
&- 3.93986116781671614923566977456092080300647596029 41 \cdot 10^6\epsilon^{13} \\
&- 9.76917609028068254893175780867479036671516694595 52 \cdot 10^6\epsilon^{14} \\
&- 3.61154275432617485247938700037442295728846983886 56 \cdot 10^7\epsilon^{15} \\
&- 8.91772329609682418955343175720837636007066773078 60 \cdot 10^7\epsilon^{16} \\
&- 3.27692378325517539270854151793007263307384683406 16 \cdot 10^8\epsilon^{17} \\
&+ \mathcal{O}\left(\epsilon^{18}\right)
\end{aligned}
\tag{D.2}
$$

$$
\begin{aligned}
&S(4, 4-2\epsilon, 1;\ s_{\max} = 5000, x_{\max} = 400;\ \gtrsim 100 \text{ correct digits}) = \\
&- 2.50000000000000000000000000000000000000000000000000 \\
&- 11.66666666666666666666666666666666666666666666666666\epsilon \\
&- 31.70138888888888888888888888888888888888888888888888\epsilon^2 \\
&- 67.52893518518518518518518518518518518518518518518518\epsilon^3 \\
&- 140.22054328754050776933771050005766373065616848378\epsilon^4 \\
&- 573.53470046065660579886343669973365466645294764018\epsilon^5 \\
&- 2756.21982203281444579061754076564737855440199311 95\epsilon^6 \\
&- 18239.92567459385823754749754950468803805679931518 8\epsilon^7 \\
&- 86167.47858000922568382128165100058902481973500663 3\epsilon^8 \\
&- 468163.76600358235076045808377411086825064850857429\epsilon^9 \\
&- 1.97661111224497547116753862679308932701939242927 11 \cdot 10^6\epsilon^{10} \\
&- 9.57323683728658266329080404208830875763342677316 34 \cdot 10^6\epsilon^{11} \\
&- 3.80756289275219274330026803877424966767254301943 34 \cdot 10^7\epsilon^{12} \\
&- 1.74207033998896280957740569089500965921260677441 81 \cdot 10^8\epsilon^{13} \\
&+ \mathcal{O}\left(\epsilon^{14}\right)
\end{aligned}
\tag{D.3}
$$

$$
\begin{aligned}
&S(5, 4-2\epsilon, 1;\ s_{\max}=5000, x_{\max}=300;\ \gtrsim 50 \text{ correct digits}) = \\
&+ 2.999999999999999999999999999999999999999999999999 \\
&+ 16.500000000000000000000000000000000000000000000000\epsilon \\
&+ 51.958333333333333333333333333333333333333333333333\epsilon^2 \\
&+ 125.671527777777777777777777777777777777777777777777\epsilon^3 \\
&+ 259.987557870370370370370370370370370370370370370370\epsilon^4 \\
&+ 347.355116219478692787842480070385221658427477871 56\epsilon^5 \\
&- 2453.494245425829710333331455898075292235751716 3385\epsilon^6 \\
&- 31545.548328529725289178386528451320539035565109951\epsilon^7 \\
&- 311303.085463217401967301187671527442884718571745 71\epsilon^8 \\
&- 2.132877859660525601463014564924534770569624934 1140 \cdot 10^6\epsilon^9 \\
&+ \mathcal{O}\left(\epsilon^{10}\right)
\end{aligned}
\tag{D.4}
$$

Appendix E

Sunset master integrals: Numerical results around $3D$

The numerical results for the sunset-type master integrals (7.1) up to five loop for $D = 3 - 2\epsilon$ deduced from the recurrence relations given in Appendix (C) by means of factorial series (4.14). For each result we present the first fifty correct digits and several orders in ϵ. See Chapter (7) for more details.

$$
\begin{aligned}
&S(2, 3-2\epsilon, 1;\ s_{\max}=4000, x_{\max}=1600;\ \gtrsim 650 \text{ correct digits}) = \\
&+ 1.0000000000000000000000000000000000000000000000000000\epsilon^{-1} \\
&+ 0.37813956756734247208794753814260345371203830615 00 \\
&- 0.11368274138813551309172028630355577131165759329 86\epsilon^{1} \\
&+ 0.13321341968942982259786385115980280241438910364 97\epsilon^{2} \\
&- 0.12779035812817962009824156716106024852967979331 57\epsilon^{3} \\
&+ 0.12641420542638899537955871501240528407491654983 97\epsilon^{4} \\
&- 0.12568749496694921673643475175069451238231565382 80\epsilon^{5} \\
&+ 0.12533888155183737287735312774255364205216226081 06\epsilon^{6} \\
&- 0.12516782762429754341896297701654464734261138634 22\epsilon^{7} \\
&+ 0.12508339407668708000759613924134960536814652830 44\epsilon^{8} \\
&- 0.12504152745098479376717183514219943358104097027 19\epsilon^{9} \\
&+ 0.12502070809233529337085419838575442384710944040 37\epsilon^{10} \\
&- 0.12501033571785724039045247129078288798515981428 47\epsilon^{11} \\
&+ 0.12500516180214109469793260351155421489271776484 33\epsilon^{12} \\
&- 0.12500257889503786625361625036117284025675321674 78\epsilon^{13} \\
&+ 0.12500128878201425953528611460963643507226767402 50\epsilon^{14} \\
&- 0.12500064416995550194407673358956370468093632690 27\epsilon^{15} \\
&+ 0.12500032201148774569229497188287498969172022771 76\epsilon^{16} \\
&- 0.12500016098129529050962724112320349722656038980 97\epsilon^{17} \\
&+ 0.12500008048251006422266520971829689026319297303 29\epsilon^{18} \\
&- 0.12500004023854547687794135751413365565301830759 37\epsilon^{19} \\
&+ \mathcal{O}\left(\epsilon^{20}\right)
\end{aligned}
\tag{E.1}
$$

$$
\begin{aligned}
&S(3, 3-2\epsilon, 1;\ s_{\max}=4000, x_{\max}=800;\ \gtrsim 170 \text{ correct digits}) = \\
&- 7.99999999999999999999999999999999999999999999999999\epsilon^{-1} \\
&- 41.81929022208175009864857211333834982158399570047 1 \\
&- 306.56670836117969234565314308183288372305605689341\epsilon \\
&- 1505.20074947370013610754655745722813169702299900 20\epsilon^2 \\
&- 11039.36110002923400779238245952942820907992869300 2\epsilon^3 \\
&- 54185.44451812645201504519002336449199434129380784 3\epsilon^4 \\
&- 397417.99759794782308439780280919214801222373305393\epsilon^5 \\
&- 1.95067602631174421943904139863356354181159702058 17 \cdot 10^6\epsilon^6 \\
&- 1.43070466492328874812059541864040610184499919073 90 \cdot 10^7\epsilon^7 \\
&- 7.02243397233242255813994075289382085925938065546 33 \cdot 10^7\epsilon^8 \\
&- 5.15053674760655468480795699725902906094907303961 49 \cdot 10^8\epsilon^9 \\
&- 2.52807623687357405404667345806693272289737566872 44 \cdot 10^9\epsilon^{10} \\
&- 1.85419322818659802477353655937423270226178141533 79 \cdot 10^{10}\epsilon^{11} \\
&- 9.10107445402016147882404481967737288947288735693 11 \cdot 10^{10}\epsilon^{12} \\
&- 6.67509562130527096074304306576886469306581080672 15 \cdot 10^{11}\epsilon^{13} \\
&- 3.27638680346859167058840007830960605238689743219 69 \cdot 10^{12}\epsilon^{14} \\
&- 2.40303442366720100143147047893426869169292105155 83 \cdot 10^{13}\epsilon^{15} \\
&- 1.17949924924903032016016169065882556480327665108 87 \cdot 10^{14}\epsilon^{16} \\
&- 8.65092392520150501941396734325812295966962585980 50 \cdot 10^{14}\epsilon^{17} \\
&- 4.24619729729656076917530738963959903726446807415 39 \cdot 10^{15}\epsilon^{18} \\
&+ \mathcal{O}\left(\epsilon^{19}\right)
\end{aligned}
\tag{E.2}
$$

$$
\begin{aligned}
&S(4, 3-2\epsilon, 1;\ s_{\max}=4000, x_{\max}=400;\ \gtrsim 70 \text{ correct digits}) = \\
&+ 44.999999999999999999999999999999999999999999999999\epsilon^{-1} \\
&+ 356.741853625168986963294557646397785709979756018 34 \\
&+ 3163.22798085456290614488030215828823053816049961 63\epsilon \\
&+ 18912.37505091413420109568071678952746808688235278 6\epsilon^2 \\
&+ 138631.68341208858694544411836368879758049566502014\epsilon^3 \\
&+ 777993.92660042526612420897733035769523866301956529\epsilon^4 \\
&+ 5.38681904643147426848665932265169394591874600321 85 \cdot 10^6\epsilon^5 \\
&+ 2.95621624058367288589242850156276354730878808111 61 \cdot 10^7\epsilon^6 \\
&+ 2.00262741192321761200535703605034683149942201256 66 \cdot 10^8\epsilon^7 \\
&+ 1.08910793633534940939932149900268799872110893533 32 \cdot 10^9\epsilon^8 \\
&+ 7.31085478493024873673505001939410438578134839153 07 \cdot 10^9\epsilon^9 \\
&+ 3.96058071240494084892202573499909608420837686318 00 \cdot 10^{10}\epsilon^{10} \\
&+ 2.64813109913537533878679882870126173175591875248 17 \cdot 10^{11}\epsilon^{11} \\
&+ 1.43217579909621366121850891763009056976568294261 37 \cdot 10^{12}\epsilon^{12} \\
&+ 9.55922935940545328176806563711421675473773465802 72 \cdot 10^{12}\epsilon^{13} \\
&+ 5.16601966495412545698365871016485571027206328201 82 \cdot 10^{13}\epsilon^{14} \\
&+ 3.44547575378871214320360907918946271765036286104 15 \cdot 10^{14}\epsilon^{15} \\
&+ 1.86139696549678305064475949923872771639029112958 68 \cdot 10^{15}\epsilon^{16} \\
&+ \mathcal{O}\left(\epsilon^{17}\right)
\end{aligned}
\tag{E.3}
$$

$$
\begin{aligned}
&S(5, 3-2\epsilon, 1;\ s_{\max}=4000, x_{\max}=200;\ \gtrsim 50 \text{ correct digits}) = \\
&- 224.00000000000000000000000000000000000000000000000000\epsilon^{-1} \\
&- 2265.06531012100430217934415373191705491275754405 48 \\
&- 23860.04975481398835087971054152280511750744913149 9\epsilon \\
&- 169712.34196716622558061879130824537096449366502149\epsilon^2 \\
&- 1.44906463071989054796617061178909965491663030091 31 \cdot 10^6\epsilon^3 \\
&- 9.63530638522976951749938909366540083198279284870 15 \cdot 10^6\epsilon^4 \\
&- 8.50281123318072788204472066022595864852339254337 86 \cdot 10^7\epsilon^5 \\
&- 5.80430128136530657464447760041975101858067201710 13 \cdot 10^8\epsilon^6 \\
&- 5.81415170023515070584206654041265206603510869793 47 \cdot 10^9\epsilon^7 \\
&- 4.19656588057563500437292118506417945992627882278 71 \cdot 10^{10}\epsilon^8 \\
&- 4.74820764752723335402833428301499107312599502549 50 \cdot 10^{11}\epsilon^9 \\
&- 3.57696913184687901514066640076218223077847154480 44 \cdot 10^{12}\epsilon^{10} \\
&- 4.34736792849188239487012498815593988364904363668 25 \cdot 10^{13}\epsilon^{11} \\
&- 3.34691324458902282548518307016729499321569998055 15 \cdot 10^{14}\epsilon^{12} \\
&+ \mathcal{O}\left(\epsilon^{13}\right)
\end{aligned}
\tag{E.4}
$$

Bibliography

[1] CERN, *New results indicate that new particle is a Higgs boson* [http://home.web.cern.ch/about/updates/2013/03/new-results-indicate-new-particle-higgs-boson].

[2] D. Bieletzki, K. Lessmeier, O. Philipsen and Y. Schröder, JHEP **1205** (2012) 058 [arXiv:1203.6538 [hep-ph]].

[3] M. E. Peskin and D. V. Schroeder, Reading, USA: Addison-Wesley (1995) 842 p

[4] H. F. Jones, Bristol, UK: Hilger (1990) 287 p

[5] A. D. Linde, Rept. Prog. Phys. **42** (1979) 389.

[6] J. I. Kapusta and C. Gale, Cambridge, UK: Univ. Pr. (2006) 428

[7] E. Braaten, Phys. Rev. Lett. **74** (1995) 2164 [hep-ph/9409434].

[8] A. Cucchieri, D. Dudal, T. Mendes and N. Vandersickel, arXiv:1202.0639 [hep-lat].

[9] V. P. Nair, arXiv:1201.0977 [hep-th].

[10] C. -N. Yang and R. L. Mills, Phys. Rev. **96** (1954) 191.

[11] G. 't Hooft and M. J. G. Veltman, Nucl. Phys. B **44** (1972) 189.

[12] H. D. Politzer, Phys. Rev. Lett. **30** (1973) 1346.

[13] D. J. Gross and F. Wilczek, Phys. Rev. Lett. **30** (1973) 1343.

[14] Y. Schröder, Lectures on Quantum Chromodynamics [http://www.physik.uni-bielefeld.de/~yorks/qcd13/].

[15] L. D. Faddeev and V. N. Popov, Phys. Lett. B **25** (1967) 29.

[16] C. Becchi, A. Rouet and R. Stora, Annals Phys. **98** (1976) 287.

[17] K. Kajantie, M. Laine, K. Rummukainen and M. E. Shaposhnikov, Nucl. Phys. B **458** (1996) 90 [hep-ph/9508379].

[18] M. Laine, Lectures on Thermal Field Theoriy [http://www.physik.uni-bielefeld.de/~laine/thermal/].

[19] A. Gynther, M. Laine, Y. Schröder, C. Torrero and A. Vuorinen, JHEP **0704** (2007) 094 [hep-ph/0703307 [HEP-PH]].

[20] M. Gell-Mann and MLevy, Nuovo Cim. **16** (1960) 705.

[21] S. A. Larin, arXiv:1304.8107 [hep-ph].

[22] R. Jackiw and S. -Y. Pi, Phys. Lett. B **403** (1997) 297 [hep-th/9703226].

[23] J. Zinn-Justin, Int. Ser. Monogr. Phys. **113** (2002) 1.

[24] A. V. Smirnov and A. V. Petukhov, Lett. Math. Phys. **97** (2011) 37 [arXiv:1004.4199 [hep-th]].

[25] S. Laporta, Int. J. Mod. Phys. A **15** (2000) 5087 [hep-ph/0102033].

[26] K. G. Chetyrkin and F. V. Tkachov, Nucl. Phys. B **192** (1981) 159.

[27] T. Gehrmann and E. Remiddi, Nucl. Phys. B **580** (2000) 485 [hep-ph/9912329].

[28] R. N. Lee, JHEP **0807** (2008) 031 [arXiv:0804.3008 [hep-ph]].

[29] A. V. Smirnov, JHEP **0810** (2008) 107 [arXiv:0807.3243 [hep-ph]].

[30] A. von Manteuffel and C. Studerus, arXiv:1201.4330 [hep-ph].

[31] L. M. Milne-Thomson, *The calculus of finite differences* (Macmillan, London, 1951).

[32] S. Laporta, Acta Phys. Polon. B **34** (2003) 5323 [hep-ph/0311065].

[33] M. Veltman, *Schoonship* (CERN preprint, 1967).

[34] A. C. Hearn, C670826-1.

[35] S. Wolfram, *Mathematica: A system for mathematics by computer* (Addison-Wesley, New-York, 1988).

[36] J. A. M. Vermaseren, KEK-TH-326.

[37] P. Nogueira, Journal of Computational Physics 105 (1993) 279-289.

[38] C. Anastasiou and A. Lazopoulos, JHEP **0407** (2004) 046 [hep-ph/0404258].

[39] A. V. Smirnov, JHEP **0604** (2006) 026 [hep-ph/0602078].

[40] H. Hirabayashi and M. Hirabayashi, *Quick Database Manager* [`http://fallabs.com/qdbm/`].

[41] R. H. Lewis, *Computer Algebra System* [`http://home.bway.net/lewis/`].

[42] A. V. Smirnov and V. A. Smirnov, arXiv:1302.5885 [hep-ph].

[43] R. N. Lee, arXiv:1212.2685 [hep-ph].

[44] O. V. Tarasov, Phys. Rev. D **54** (1996) 6479 [hep-th/9606018].

[45] S. G. Gorishnii, S. A. Larin, L. R. Surguladze and F. V. Tkachov, Comput. Phys. Commun. **55** (1989) 381.

[46] M. Steinhauser, Comput. Phys. Commun. **134** (2001) 335 [hep-ph/0009029].

[47] M. Steinhauser, *Loop integrals, integration-by-parts and MATAD* (Computer Algebra and Particle Physics 2009, DESY, Zeuthen) [`http://www.ttp.kit.edu/~ms/capp09.pdf`].

[48] R. Mertig and R. Scharf, Comput. Phys. Commun. **111** (1998) 265 [hep-ph/9801383].

[49] R. Mertig and R. Scharf, *FeynCalc* [`http://www.feyncalc.org/`]

[50] O. V. Tarasov, Nucl. Phys. B **502** (1997) 455 [hep-ph/9703319].

[51] C. W. Bauer, A. Frink and R. Kreckel, cs/0004015 [cs-sc].

[52] *Open MPI*, [`http://www.open-mpi.org/`].

[53] Oracle, *Berkeley DB*, [`http://www.oracle.com/technetwork/products/berkeleydb/overview/index.html`].

[54] *YAML: YAML Ain't Markup Language*, [`http://www.yaml.org/`].

[55] S. de Boer, [`http://www2.physik.uni-bielefeld.de/fileadmin/user_upload/theory_e6/Master_Theses/MT-SdB.html`]

[56] A. S. Kronfeld, Phys. Rev. D **58** (1998) 051501 [hep-ph/9805215].

[57] R. N. Lee and A. A. Pomeransky, arXiv:1308.6676 [hep-ph].

[58] S. Groote, J. G. Korner and A. A. Pivovarov, Annals Phys. **322** (2007) 2374 [hep-ph/0506286].

[59] J. Möller and Y. Schröder, unpublished.

[60] J. Kuipers, T. Ueda, J. A. M. Vermaseren and J. Vollinga, Comput. Phys. Commun. **184** (2013) 1453 [arXiv:1203.6543 [cs.SC]].

[61] Wolfram Research, Inc., `Mathematica`, Version 9.0, Champaign, IL (2012).

[62] Y. Schröder and A. Vuorinen, JHEP **0506** (2005) 051 [hep-ph/0503209].

[63] Y. Schröder and A. Vuorinen, hep-ph/0311323.

[64] O. Philipsen, D. Bieletzki and Y. Schröder, PoS QCD **-TNT09** (2009) 052 [arXiv:0911.3595 [hep-ph]].

[65] M. Sangel, Master thesis, *Three-loop gap equation for a spontaneously broken 3d Yang-Mills* [`http://www2.physik.uni-bielefeld.de/fileadmin/user_upload/theory_e6/Master_Theses/Masterarbeit_MarcSangel.pdf`].

Acknowledgements

I would like to give my special thanks to York Schröder for providing me the opportunity to write this thesis, his excellent supervision on and beyond this work and many interesting talks. Furthermore, I would like to thank Nicolas Borghini for examining this thesis. Cordial thanks to Ioan Ghisoiu proof-reading and to Sayantan Sharma for proof-reading and instructive talks. Many thanks to Marc Sangel for the cooperative work and many interesting conversations. In addition, I would like to thank all members of the working group E6/D6 for a friendly atmosphere, and especially Gudrun Eickmeyer and Susi Reder for the organization.
I convey my deep gratitude to my family, in particular to my parents, for their continuous support. Cordial thanks to Julieta Kröhnert for proof-reading. Moreover, warm thanks to my friends who accompanied me all the time, especially to Christian Bartelheimer, Tomasz Checinski, Nick Diederich, Tatiana Esau, Laura Korfmacher, Sarah Reschke and Gregor Sures.

Declaration

I hereby affirm that this master thesis represents my own work, has not been previously submitted to any examination office and all resources used have been referenced.

September 18, 2013